Movement in the Dark: Gravitational Probes of Dark Matter Models

BY

ISABELLE S. GOLDSTEIN

B.S. IN PHYSICS, CARNEGIE MELLON UNIVERSITY, 2018

M.S. IN PHYSICS, BROWN UNIVERSITY, 2020

A dissertation submitted in partial fulfillment of the requirements for the Degree of Doctor of Philosophy in the

DEPARTMENT OF PHYSICS AT BROWN UNIVERSITY

BROWN

Providence, Rhode Island

May 2023

This dissertation by Isabelle S. Goldstein is accepted in its present form
by the Department of Physics as satisfying the
dissertation requirement for the degree of Doctor of Philosophy.

Date _____ _____

Savvas Koushiappas, Advisor

Recommended to the Graduate Council

Date _____ _____

Ian Dell'Antonio, Reader

Date _____ _____

Stephon Alexander, Reader

Approved by the Graduate Council

Date _____ _____

Thomas A. Lewis,

Dean of the Graduate School

Curriculum vitae

Isabelle Goldstein, Sc.M

ORCID: 0000-0001-9247-9474

Email: isabelle_goldstein@brown.edu

Education

Brown University Providence, RI USA

Doctor of Philosophy, Physics 2018–Present

Master of Science, Physics 2020

– Advisor: Savvas Koushiappas, PhD

Carnegie Mellon University Pittsburgh, PA USA

Bachelor of Science, Physics 2014–2018

Publications

1. "Viability of ultralight bosonic dark matter in dwarf galaxies"
   Isabelle S. Goldstein, Savvas M. Koushiappas, and Matthew G. Walker
   Phys. Rev. D 106, 063010 (2022)

2. "Could the 2.6 $M_\odot$ object in GW190814 be a primordial black hole?"
   Kyriakos Vattis, Isabelle S. Goldstein, and Savvas M. Koushiappas
   Phys. Rev. D 102, 061301(R) (2020)

Research Experience

Brown University 2018–Present

Graduate Student Research Assistant

– Experience in cosmology, astroparticle physics, axion-like dark matter, dwarf galaxy dynamics and primordial black holes.

– Coding fluency in Python, Fortran 90, C++, and Cluster high performance computing.

Carnegie Mellon University 2017–2018

Undergraduate Research Assistant with Dr. Matthew Walker

– Examined the strength of standard dwarf galaxy detection methods using gamma ray data with stellar data from the Sloan Digital Sky Survey and Pan-STARRS.

Lawrence Berkeley National Labs Summer 2016

Assistant Researcher with the DESI and BOSS collaborations

– Tested ultra faint spectra sky subtraction by integrating the Spectroperfectionism method into DESI and BOSS analysis pipelines.

Carnegie Mellon University 2015–2016

Undergraduate Research Assistant with Dr. Shirley Ho

– Dark matter and galaxy cross correlation bias for redshift dependance.

Research Interests

My research interests lie in astrophysics and cosmology, particularly in the intersection between theory and observation. My previous work has focused on dark matter searches, as well as the large scale structure of dark matter in contrast to baryonic matter. I am interested in studying local group astrophysics to learn about the dark and light sector.

Teaching Experience

Brown University

Lab Instructor, PHYS 0470 Electricity and Magnetism Fall 2018, 2019, 2020

– Course Instructor: Dr. Savvas Koushiappas
Number supervised: 22, 24, 32

Lab Instructor, PHYS 0060 & 0160 Spring 2019

Foundations of Electromagnetism and Modern Physics

Introduction to Relativity and Quantum Physics

– Course Instructor: Dr. Meenakshi Narain

Number supervised: 15

Lab Instructor, PHYS 0220 Astronomy — Spring 2020

– Course Instructor: Dr. Jonathan Pober

Number of students: 200

Course Teaching Assistant and Zoom coordinator, PHYS 0070 — Spring 2021

Analytical Mechanics

– Course Instructor: Dr. James Valles

Number of students: 85

Scholarships and Awards

- Physics Merit Fellowship — 2022-2023

  Brown University Department of Physics

- Award of Excellence as a Graduate Teaching Assistant — 2021

  Brown University Department of Physics, PHYS 0070

- RI Space Grant Graduate Fellow with the NASA RI — 2021

  Space Grant Consortium

- National Science Foundation Graduate Research Fellowship — 2020

  Program Honorable Mention

- Associate Member of Sigma Xi Scientific Research Honors Society — 2020

  Brown University Chapter, Elected to Membership

- Award of Excellence as a Graduate Teaching Assistant — 2018

  Brown University Department of Physics, PHYS 0470

- Senior Leadership Recognition Award — 2018

  Carnegie Mellon University Department of Physics

- NASA Pennsylvania Space Grant 2015
- H. Joseph Gerber Medal of Excellence 2014
  Connecticut Academy of Science and Engineering
- CERN Special Award at the Intel International Science 2014
  and Engineering Fair European Organization for Nuclear Research

Conference Presentations

Workshop Papers or Presentations

- Title: *The Viability Of Ultralight Bosonic Dark Matter In Dwarf Galaxies*
  - Presented at the Workshop on Very Light Dark Matter, 2023
    Mario Royal Kaikan (Chino, Nagano) + Online
  - Presented at the Carnegie Mellon University Astrolunch 2023
  - Presented at the Mitchell Conference on Collider, Dark Matter, 2022
    and Neutrino Physics at Texas A&M University
- Title: *Cross correlations of the CMB lensing potential and Sloan Digital* 2016
  Sky Survey galaxies
  - Presented at Essential Cosmology for the Next Generation

Conferences Organized

- Local committee graduate student organizer for the Conference for 2022
  Undergraduate Women in Physics
  - Cancelled due to Covid-19

Conferences Attended

- LSST Dark Matter Workshop, Kavli Institute for Cosmological Physics 2019
  at the University of Chicago

– Summer School on Cosmology, International Centre for Theoretical Physics

Additional Experience

Community Outreach

- Guest speaker at the Urban Assembly School for Emergency Management (NYC, NY) 2022
  Pursuing STEM in undergraduate and graduate level education
- Pittsburgh Glass Center teaching assistant for community glassblowing classes and demonstrations 2015–2018

Additional Scholarships

- Pittsburgh Glass Center scholarship for advanced summer intensive 2018
  Fictional Sculpting with Danny White
- Corning Museum of Glass scholarship for advanced summer intensive 2020
  Finding Your Voice: Glass Sculpting with Shelley Muzylowski Allen
  Cancelled due to Covid-19

Covid Impact

The Covid-19 pandemic had a significant impact on the progression of my graduate career. The pandemic began right at the time I was finishing courses and would have begun attending conferences with regularity while commencing research. Additionally, strain from the pandemic delayed the completion of ongoing research.

Acknowledgments

The road taken to this thesis was a long and winding one, and I could not have walked it without help from many people in my life. First and foremost, I'd like to thank my advisor Savvas Koushiappas for his support and guidance throughout my graduate career. I am immensely grateful for every meeting, question, and challenge that helped me grow into the physicist I am today. His belief in my potential and genuine recognition of my achievements were invaluable in building my confidence and sense of belonging in the physics community. I am also incredibly grateful for the discussions and support from the professors of my prelim and thesis committees: Ian Dell'Antonio, Stephon Alexander, and JiJi Fan.

I would also like to thank the friends who have made all the difference in my time here. Aaron Baumgart, Akshay Nagar, Ben Plaut, Calvin Bales, Jae Jong Oh, Janie Levin, Khing Klangboonkrong, Nicole Ozdowski, and Shelby Zasacky: you have kept me sane– and more importantly– happy. Inextricable from my friends are the other students I have shared an office with: Alexis Ortega, Anders Schreiber (honorary office member), Jatan Buch, John Leung, Kyriakos Vattis, Leah Jenks, and Mike Toomey. Thank you for every physics debate or tangent, and for your collaboration and commiseration in equal measure.

I would be remiss not to thank some of the people who set me on this path through foresight or luck years ago. Patrick Hughes' and Michael Yagid's encouragement to join the Ridgefield High School Science Research program changed the course of my life to an unknowable degree, and I will always appreciate their help in those early stumbling steps. It is also not an exaggeration to say that James Robey and Amy Piantaggini, my dance teachers for years, helped to raise me and shape me into the person I am today. I would also like to thank Dr. Gillian Morris for her aid. I cannot imagine how much more difficult it

would've been to complete this trial without a doctor as fiercely competent and caring.

Lastly, but most importantly, a simple thanks is not enough for my family. To my parents Joan and Michael Goldstein: your unwavering support and love is the bedrock of my life. And to my sister Alexa Goldstein: you are my best friend, and first and last editor in all important things. To my cat Ozymandias (King of Kings, Cat of Cats): thank you for the constant supervision while writing this thesis, it was very helpful.

There are many other people and twists of fate indispensable to my journey here. I hope they know the depth of my appreciation. I could say much more to thank them– but while the woods are lovely, dark and deep, I have promises to keep. And miles to go before I sleep.[1]

[1] Stopping by Woods on a Snowy Evening, by Robert Frost

Contents

List of Figures

List of Tables

CHAPTER 1

Introduction to cosmology

> *"The story so far: In the beginning the Universe was created. This has made a lot of people very angry and been widely regarded as a bad move. "*
>
> — Douglas Adams,
> *The Restaurant at the End of the Universe*

1.1 A Brief History

There is something foundational to humanity in looking at the stars. Evidence from cave paintings suggests humans observed Aldebaran and the Pleiades as long ago as ∼20,000 BC [4]– and while it's impossible to know how ancient people imagined the architecture of the universe, that blueprint has changed dramatically with time.

Insofar as it is possible to construct a narrative towards modern cosmology, we begin with the Copernican Principle [5]: that the Earth is no privileged observer. Although it is difficult to trace historically, the idea that the Earth is not the center of the universe was massively influential and a less precise version of the foundational Cosmological Principle. The Cosmological Principle, which is being tested continuously by modern cosmology experiments, states that the universe is approximately the same everywhere (homogeneous) and looking in any direction (isotropic). Isaac Newton's *Philosophiae Naturalis Principia Mathematica* assumes a version of the Copernican principle as well, by studying laws that govern the motions of the spheres as the same laws that govern the motion of objects on Earth, in a time period when the heavens were considered to have a separate celestial mechanics to Earthly laws. [6]

But the theoretical foundation of cosmology calculations is Einstein's special [7] and general relativity. [8, 9] As shown in Section 1.2.1, relativity is the base for understanding the growth of the universe and how Alexander Friedmann derived the expansion of the universe [10]. It is essential for understanding redshift, the Cosmic Microwave Background, dark matter, structure formation, and far more.

For an observational beginning of modern cosmology, measurements of astronomical objects have been made with varying degrees of depth and understanding for all of human history. But the Shapley–Curtis Debate [11] was a turning point in understanding structures of the universe; in 1920 Harlow Shapely and supporters argued that the Milky Way was the sole universe while Heber Curtis and supporters believed that "spiral nebulae" were in fact other galaxies similar to our Milky Way. The work of Henrietta Swan Leavitt identifying the period-luminosity relationship in Cepheid variable stars [12] made possible Edwin Hubble's measurement of the distance to the Andromeda galaxy [13], proving that it was extragalactic. This was the beginning of modern understanding of structure hierarchy in the universe, proving our place as one solar system in one of many galaxies. Note that although many discoveries of this period were attributed to men leading observational teams, teams of women "computers" were often behind the measurements and development of the necessary techniques while being segregated into lower paying and less respected positions. [14]

The 20^{th} century was a period of rapid development in humanity's observationally proven understanding of the universe. There is too much history to include here, but we can sketch some of the important developments. Hubble's measurements of distances to nearby galaxies and their velocities [15] along with the Friedmann equations [10] showed that the universe is expanding rather than static. The Big Bang theory was developed by many people in the time including those working on elemental abundances [16–19, 19–21]; although the measurements showing that this expansion is accelerating leading to the discovery of dark energy by Riess et al. [22] and Perlmutter et al. [23] wouldn't occur until the 1990s. The Big Bang theory lead naturally to the prediction of the Cosmic Microwave Background by Dicke et al. [24], and then its discovery by Penzias and Wilson [25] in 1965. Building off the Cosmic Microwave Background, inflation was proposed in 1980 and 1981 by Starobinsky [26] and Guth [27]. In 1933 Fritz Zwicky's measurements of the Coma cluster, while not

quite correct, was the first evidence for dark matter [28] that was later supported by other measurements of galaxy rotation curves such as the influential work by Vera Rubin and collaborators in the late 1970s and early 1980s [29, 30].

1.2 State of current cosmology

Modern cosmology has developed a set of very successful models for explaining the majority of observations including the expansion of the universe, primordial element abundances, the Cosmic Microwave Background's existence and its features, and the statistics of large scale structure. The two main models we will consider here are Λ Cold Dark Matter (ΛCDM), the Big Bang, and inflation. ΛCDM is characterized by a cold, non-interacting dark matter in a flat universe currently dominated by dark energy. It is parameterized by the Hubble constant H_0, the energy density parameters for matter Ω_m, baryons Ω_b, and dark energy Ω_Λ, the angular scale of the sound horizon at last scattering θ_{MC}, spectral index n_s, optical depth τ, and amplitude of perturbations at a given scale (0.05 Mpc^{-1} for Planck) $\Delta^2_{\mathcal{R}}$.

In this chapter we will describe these models in more detail, and in Section 1.2.6 will discuss the main problems in ΛCDM.

1.2.1 Formalism

We begin with Einstein's general relativity. A geometry is encoded by the metric $g_{\mu\nu}(x)$, defined such that in locally inertial and Cartesian coordinates the metric is $\eta_{\alpha\beta} = \text{diag}(-1, 1, 1, 1)$ and that coordinate transformations $x \to x'$ change the metric in the following way:

$$g'_{\rho\sigma}(x') = g_{\mu\nu}(x)\frac{\partial x^\mu}{\partial x'^\rho}\frac{\partial x^\nu}{\partial x'^\sigma}. \tag{1.1}$$

In an expanding universe, the proper distance $d(t)$ between two points in space will change over time. We can describe this change from proper time t_0 to t by the scale factor $a(t)$:

$$a(t) \equiv \frac{d(t)}{d(t_0)}. \tag{1.2}$$

And by convention, $a(\text{today}) = 1$. Note also that scale factor relates to redshift z like $a^{-1} = 1 + z$. Then the metric in a flat, expanding universe is given by $g_{\mu\nu} =$

diag$(-1, a^2, a^2, a^2)$. This can be generalized to an expanding universe of any curvature with the Friedmann–Lemaître–Robertson–Walker metric, easiest written in spherical polar coordinates [31]

$$ds^2 = dt^2 - a^2(t)\left[\frac{dr^2}{1-Kr^2} + r^2(d\theta^2 + \sin^2\theta d\phi^2)\right]. \tag{1.3}$$

Where K is the curvature,

$$K = \begin{cases} -1, & \text{closed, elliptical} \\ 0, & \text{flat, Euclidean} \\ 1, & \text{open, hyperbolic} \end{cases} \tag{1.4}$$

The expanding universe's evolution is governed by the Einstein equations [9]

$$G_{\mu\nu} + \Lambda g_{\mu\nu} = 8\pi G T_{\mu\nu}. \tag{1.5}$$

Where $G_{\mu\nu}$ is the Einstein tensor describing curvature, $T_{\mu\nu}$ is the stress-energy-momentum tensor, Λ is the cosmological constant, and G is Newton's gravitational constant. Notice that this equation is relating terms describing spacetime geometry to the density and flux of energy and momentum; thus the Einstein equations can be interpreted as the stress energy momentum tensor determining curvature. The choice to write $\Lambda g_{\mu\nu}$ on the left side of the equation is a choice made for convenience here, but in reality it's not clear. If $\Lambda g_{\mu\nu}$ belongs on the left, that implies dark energy is a property of spacetime geometry. If it belongs on the right, that implies dark energy is dynamical and a source for energy density.

If we assume $T_{\mu\nu} = \text{diag}(-\rho, P, P, P)$ is describing a perfect fluid with energy density ρ and pressure p, then together with the FLRW metric the Einstein equations can be simplified to find the Friedmann equations

$$\begin{aligned} \left(\frac{\dot{a}}{a}\right)^2 &= \frac{8\pi G}{3}\rho - \frac{K}{a^2} \\ &= H^2(a) = H_0^2\left(\sum_i \rho_i\right) - \frac{k}{a^2} \end{aligned} \tag{1.6}$$

and

$$\frac{\ddot{a}}{a} = -\frac{4\pi G}{3}(\rho + 3P), \tag{1.7}$$

where Equation 1.6 is the 00 component of the Einstein equations and Equation 1.7 is the ij components. The pressure as a function of density $P(\rho)$ is called an equation of state; together with Equations 1.6 and 1.7 the equation of state completely determines the dynamics of a. Notice that $\frac{\dot{a}}{a}$, a measure of how quickly the scale factor changes, is what Edwin Hubble was measuring locally in 1929 [15]. Thus we define $H \equiv \frac{\dot{a}}{a}$ to be the Hubble parameter, with H_0 being its value today.

By differentiating Equation 1.6 with respect to time, doing a little algebraic manipulation with Equation 1.7, and assuming that the curvature K does not evolve over time, you can arrive at the conservation law

$$\dot{\rho} = -\frac{3}{a}(\rho + P). \tag{1.8}$$

And for a perfect fluid, the density and pressure can be related through an equation of state [31]

$$P = w\rho \tag{1.9}$$

where w is a constant that takes different values depending on the fluid in question. Equations 1.8 and 1.9 together give the scaling relation

$$\rho \sim a^{-3(w+1)}, \tag{1.10}$$

showing how a fluid's density evolves with scale factor. For nonrelativistic matter like gas and dust, $w = 0$ and the fluid's energy density decreases proportional to the volume expanding. For radiation $w = 1/3$, and thus $\rho_\gamma \sim a^{-4}$; this is indicative of the energy density lost through the volume expanding and through cosmological redshift. For vacuum energy $w = -1$ so that energy density remains constant.

It is also useful to define the critical density $\rho_{\text{crit}} \equiv 2H_0^2/8\pi G$ at which the universe is flat, and a dimensionless density parameter $\Omega = \rho/\rho_{\text{crit}}$. We can now write down Equation 1.6 in a form widely used in cosmology:

$$H^2(a) = H_0^2\left[\Omega_M a^{-3} + \Omega_R a^{-4} + \Omega_\Lambda\right] - \frac{K}{a^2}. \tag{1.11}$$

Where the dimensionless density parameters are Ω_M for nonrelativistic matter, Ω_R for relativistic matter (i.e. radiation, neutrinos), and Ω_Λ is for vacuum energy. Note that Ω_M is

the sum of the dimensionless density parameters for baryons and dark matter. This is not always the case for more exotic theories of dark matter, and in fact the calculation of several cosmological parameters can be adjusted by proposing different a dependencies for theories like exotic dark matter or dark radiation.

Note that for different values of a, the universe will be dominated by different components. At very small a, early in the universe, radiation will be the dominant component. This gives way to matter domination and then at late times, cosmological constant domination [32]. One important time to note is the epoch of matter-radiation equality, since perturbations in the early universe will develop differently in matter domination than radiation domination.

1.2.2 Initial Conditions

One of the earliest parts of the universe's history we can hope to understand is inflation. Inflation proposes that the very early universe, at energies of $\gtrsim 10^{15}$ GeV, had a period of extremely rapid growth where the scale factor increased by a factor of $\sim 10^{28}$ [31]. Originally proposed by Starobinsky [26] and Guth [27] in the 1980s, it solves several problems with the standard cosmology at the time. One of which is the horizon problem: the early universe is essentially homogeneous in all directions as will be shown in more detail in Section 1.2.4, including those that could not be causally connected with standard Hubble expansion. The comoving horizon is the total comoving distance light can travel,

$$\eta \equiv \int_0^t \frac{dt'}{a(t')}. \tag{1.12}$$

Without inflation, at the time of matter radiation decoupling regions of space separated by distances farther than the comoving horizon at decoupling would have no way to homogenize. In present day observations of primordial radiation, that works out to be regions separated by $\sim 1.6°$ in the sky [33]. The fact that observations are homogenized over the full sky excluding small anisotropies at the scale $\Delta T/T \sim 10^{-5}$ is the horizon problem. With inflation, the entire sky could be in causal contact at very early times.

Inflation is also essential in seeding perturbations in the early universe. There is no reason to expect perturbations in the density field to exist from just the Big Bang other than those generated by quantum fluctuations. However a period of rapid expansion would

cause quantum fluctuations in the existing fields to enter the classical regime. There are two main types of perturbations: adiabatic and isocurvature.

Primordial perturbations are usually taken to be in the radiation epoch, and after nucleosynthesis so we only need to consider the photon, dark matter, baryon, and neutrino components of the universe. The adiabatic mode is defined to be perturbations that leave the ratios of species' number density the same [34],

$$\delta\left(\frac{n_X}{n_Y}\right) = 0. \tag{1.13}$$

From the equations of state for each species, this implies for adiabatic perturbations that

$$\frac{1}{4}\delta_\gamma = \frac{1}{4}\delta_\nu = \frac{1}{3}\delta_b = \frac{1}{3}\delta_{DM}. \tag{1.14}$$

The isocurvature mode is defined as perturbations that do not change the curvature, instead changing the relative number density ratios. These are orthogonal modes to adiabatic ones, although in theory there could be a mixing of both types. Pure isocurvature modes are quantified by the entropy perturbation

$$\begin{aligned} S_{X,Y} &\equiv \frac{\delta n_X}{n_X} - \frac{\delta n_Y}{n_Y} \\ &= \frac{\delta_X}{1+w_X} - \frac{\delta_Y}{1+w_Y} \end{aligned} \tag{1.15}$$

where $w_X = p_X/\rho_X$ is the equation of state parameter for species X. Typically photons are chosen as a reference point, and the baryon isocurvature mode, cold dark matter isocurvature mode, and neutrino isocurvature mode are defined from it:

$$S_b \equiv \delta_b - \frac{3}{4}\delta_\gamma \tag{1.16}$$

$$S_{DM} \equiv \delta_{DM} - \frac{3}{4}\delta_\gamma \tag{1.17}$$

$$S_\nu \equiv \frac{3}{4}\delta_\nu - \frac{3}{4}\delta_\gamma. \tag{1.18}$$

Note that for the adiabatic case, these parameters are clearly equal to zero. The fourth non-decaying mode, neutrino isocurvature velocity perturbations, arises from the additional constraint that perturbations don't diverge when going further back in time. However there are currently no known mechanisms to excite this type of perturbation [35].

1.2.3 First Observables

If we rewind time in an expanding and cooling universe, the starting point must have been localized, dense, and hot. This extremely hot soup of particles smashing into each other was an effective nuclear reactor; but as the universe expands and cools, baryons lost enough energy to stop forming heavy nuclei. This process and its predicted abundances are called Big Bang Nucleosynthesis (BBN). In fact in standard cosmology the primordial abundances of the most formed nuclei (D, ^{3}He, ^{4}He, and ^{7}Li) will depend only on the baryon to photon ratio η. Historically this was a cogent test of the Big Bang theory [36, 33], first done roughly in the late 1940s [19, 18], but today more precise measurements of primordial abundances are a way to test for mixing with nonstandard particle models.

The abundance of different species is described with a distribution function, the probability of finding a particle in some volume of phase space at a given time. Assuming the cosmological principle, we can write this as

$$f(\mathbf{p},t) = \frac{g}{(2\pi)^3}\frac{1}{e^{(E(\mathbf{p})-\mu)/T(t)} \pm 1}, \tag{1.19}$$

where g is the species' degeneracy, $E = \sqrt{p^2c^2 + m^2c^4}$ is the energy, m is the mass, μ is the chemical potential, $T(t)$ is the temperature at time t, and the $+/-$ of the denominator corresponds to fermions/bosons respectively. We can then calculate the number density by integrating over all momenta, finding in the $T << m$ limit a Maxwell Boltzmann distribution

$$n = g\left(\frac{mT}{2\pi}\right)^{3/2} e^{-(m-\mu)/T}. \tag{1.20}$$

For a nucleus of mass A and charge Z, the chemical potential will be conserved in producing $^A\mathrm{N}_Z$ from A neutrons and protons,

$$\mu_A = Z\mu_p + (A-Z)\mu_n \tag{1.21}$$

and we can therefore write down the number density [33]

$$\begin{aligned} n_A &= g_A\left(\frac{m_A T}{2\pi}\right)^{3/2} e^{-(m_A-\mu_A)/T} \\ &= g_A 2^{-A} A^{3/2}\left(\frac{m_B T}{2\pi}\right)^{3(A-1)/2} n_p^Z n_n^{(A-Z)} e^{B_A/T} \end{aligned} \tag{1.22}$$

where $m_N = m_n \approx m_p$ is the nucleon masses that are approximately equal and $B_A \equiv Zm_p + (A_Z m_n) - m_Z$ is the binding energy. This allows us to calculate the abundance fraction of a species

$$\begin{aligned} X_A &\equiv A n_A / n_N \\ &= g_A 2^{-A} A^{1/2} \left(\frac{m_N T}{2\pi}\right)^{3(A-1)/2} \eta^{A-1} n_\gamma^{A-1} X_p^Z X_n^{A-Z} e^{B_A/T}. \end{aligned} \tag{1.23}$$

The neutron and proton abundances will freeze out when the rate of the following weak interactions is lower than the Hubble rate, i.e. when they fall out of equilibrium:

$$\begin{aligned} n + \nu_e &\rightleftharpoons p + e^-, \\ n + e^+ &\rightleftharpoons p + \overline{\nu}_e, \\ n &\rightleftharpoons p + e^- + \overline{\nu}_e. \end{aligned} \tag{1.24}$$

This sets the nucleon abundance available to form heavier elements at the time of their decoupling (1 MeV). The universe is then limited by the neutron decay half life, and as such has ∼15 minutes to form heavy elements [37]. Conservation of chemical potential from these reactions tells us that $\mu_n = \mu_p$, so the relative abundance of neutrons to protons is simply given by the Boltzmann term

$$\frac{n_n}{n_p} = e^{-(m_n - m_p)/T_\mathrm{D}} \approx \frac{1}{6} \tag{1.25}$$

where the decoupling temperature for the reactions of Equation 1.24 is $T_D \approx (0.7 - 0.8)$MeV. Therefore $X_n = 1/7, X_p = 6/7$ at that temperature, and X_n (X_p) decreases (increases) as dictated by neutron decay. But as the temperature decreases, it is not as simple as 2p+2n to make ^{4}He. Instead you need to first create deuterium with neutron capture $p + n \to d + \gamma$. We can write down the abundance of deuterium using Equation 1.23,

$$X_\mathrm{D} = \frac{3}{2^{3/2}} \left(\frac{(m_p + m_n)T}{2\pi}\right)^{3/2} \eta n_\gamma X_p X_n e^{B_\mathrm{D}/T} \tag{1.26}$$

This is not a rare interaction but the binding energy of deuterium, 2.22 MeV, is relatively low. This means that there are enough photons at the high energy tail of the distribution to keep deuterium rare until 0.07 MeV. After cooling to the formation temperature of deuterium, the next step processes in forming heavier nuclei, D+$n \to {}^3\mathrm{H} + \gamma$, D + D$\to {}^3\mathrm{H} + p$, and

D + D $\rightarrow$ ^{3}He + n can happen fairly quickly. Figure 1.1 shows the calculated primordial abundance of D. Note that deuterium is the more accurate prediction in comparison to ^{4}He and ^{7}Li, which are produced in stars.

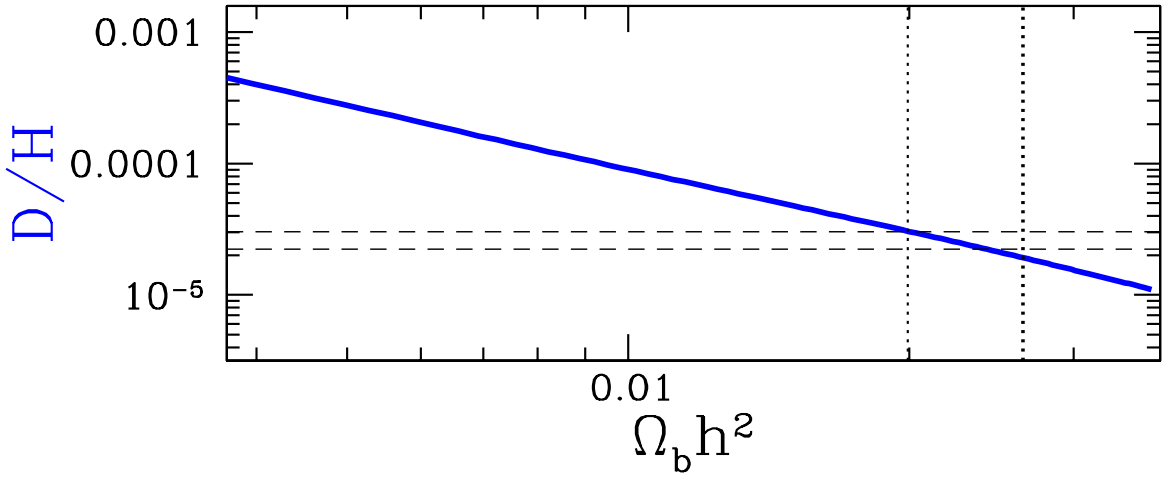

Figure 1.1: Calculated abundance of deuterium relative to hydrogen n as a function of $\Omega_b h^2$. The vertical dotted lines represent present day $\Omega_b h^2$ and the horizontal dotted lines represent observations of deuterium abundance [1].

Deuterium is a particularly important element to calculate abundances for; we see here that it is produced and then depleted as part of BBN, but once nucleosynthesis is over there are only stellar processes to deplete deuterium and none to create it. Any measurement made of deuterium abundance will be a lower bound on the primordial abundance, but it can provide information on baryon density and the number of neutrino species. [38–41] ^{3}He and ^{4}He can both be probed through measurements of hot ionized gas (HII regions), but ^{7}Li is studied in the surface abundances of Population II halo stars. These extremely metal-poor stars are thought to be made of nearly primordial material, but their age means their surface abundances may have been modified in ways that are difficult to estimate. [38]

1.2.4 Recombination and the Cosmic Microwave Background

All of the elements formed in BBN ionized. The naive assumption would be to expect neutral hydrogen to form at temperatures around the binding energy of hydrogen, 13.6eV; but as with deuterium the low baryon to photon ratio means that even at lower temperatures

there will be enough high energy photons to keep the hydrogen ionized. As the temperature drops below $\sim$ 1eV, electrons and protons begin to form neutral hydrogen for the first time, in an epoch somewhat misleadingly known as Recombination. This is also approximately the same time as radiation decoupling[1] from matter when the universe becomes "transparent" to photons, i.e. when a photon's mean free path is the size of the universe. This is known as the surface of last scattering.

When the reaction rate for $e^- + p \rightleftharpoons H + \gamma$ is much larger than the Hubble rate, the Boltzmann equation can be written as

$$\frac{n_e n_p}{n_H} = \left(\frac{m_e T}{2\pi}\right)^{3/2} e^{-(m_e+m_p-m_H)/T}. \tag{1.27}$$

If we define the fraction of ionized electrons $\chi_e \equiv \frac{n_e}{n_e+n_H}$, we can rewrite in a form known as the Saha equation [42, 43]

$$\frac{\chi_e^2}{1-\chi_e} = \frac{1}{n_e+n_H}\left[\left(\frac{m_e T}{2\pi}\right)^{3/2} e^{-(m_e+m_p-m_H)/T}\right]. \tag{1.28}$$

This approximation holds for equilibrium and as such is good at identifying the redshift of recombination, but not the evolution of the ionized electron fraction. Regardless, the Saha approximation gives us that recombination for $\chi = 0.5$ occurs at $T \sim 0.4$eV ($z \sim 1350$). The reality of recombination is more complex, as originally outlined by Peebles [44]. A photon emitted when an electron is captured into the ground state for hydrogen is energetic enough to ionize another hydrogen atom; instead excited states must be formed with subsequent radiative decays bringing the electron down to a $2p$ state. The fall from $2p$ to $1s$ emits a Lyman α photon that can be cosmologically redshifted so that it can no longer ionize hydrogen.

Alternatively, we can think about the surface of last scattering[2] : the redshift at which a photon last scattered before being able to free stream through the universe. Define the optical depth τ,

$$\tau \equiv \int_0^z n_e(z)\chi_e(z)\sigma_T \frac{dt}{dz} dz \tag{1.29}$$

[1] Photons largely stop scattering off electrons at $z \sim 1000$, but electrons continue to scatter off of photons for longer due to the low baryon to photon ratio, making the term "decoupling" an incomplete picture.[31]

[2] Despite the name, there is of course some spread for the probability distribution of a photon's point of last scattering. The "surface" has some width Δz.

where $n_e(z)\chi_e(z)$, the number density of electrons times the ionized electron fraction, gives the number of free electrons at redshift z and σ_T is the Thomson scattering cross section. Then we can solve for $\tau(z_{LS}) = 1$ to find the redshift of last scattering, $z_{LS} \sim 1080$.

The photons free streaming from last scattering are cosmologically redshifted until, from the first three minutes of the universe, they can be observed on Earth. These are known as the Cosmic Microwave Background (CMB). The CMB was originally predicted in conjunction with work on Big Bang Nucleosynthesis by Alpher, Bethe, and Gamow [21] [20], but first observed by Penzias and Wilson [25]. Figure 1.2 shows the high resolution temperature map measure by Planck in 2013 [45].

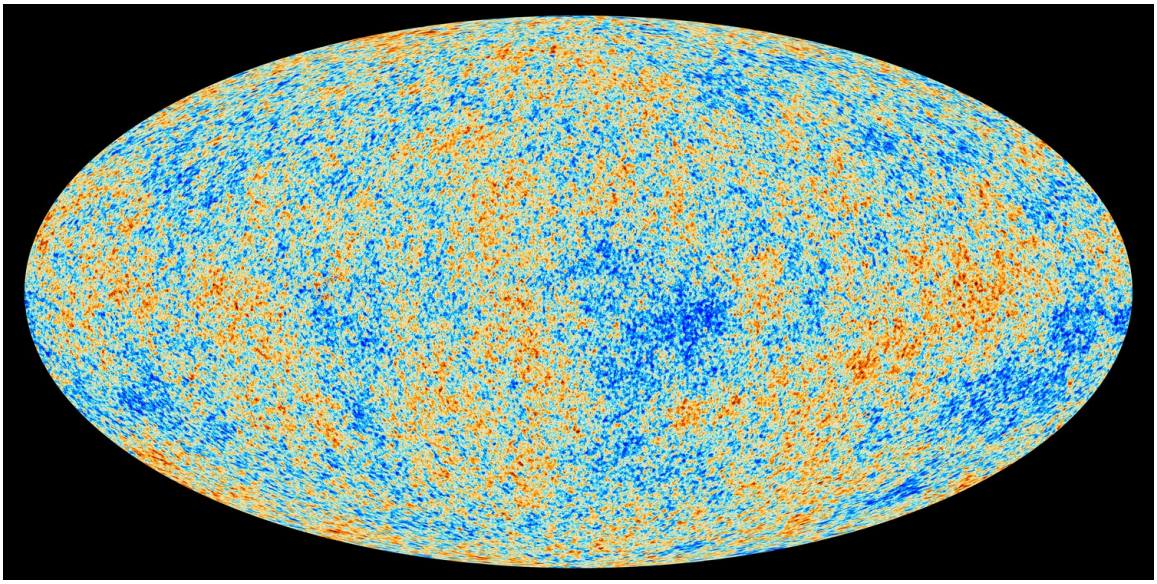

Figure 1.2: Planck 2013 map of the CMB temperature anisotropies. Courtesy NASA/JPL–Caltech.

The temperature is extremely uniform– a black body spectrum with average temperature $T_0^{CMB} = 2.7255 \pm 0.0006\text{K}$ [46] across the sky– but not without anisotropies at the scale $\Delta T/T \sim 10^{-5}$ [2]. The dipole moment was the easiest and first anisotropy to be measured, caused by redshifting of the radiation from Earth's motion with respect to the CMB [47]. Late time contributions to the observed anisotropies can be considered by relaxing the assumption that photons would have no interactions since the surface of last scattering. Some of these interactions include the Sunyaev-Zel'dovich effect (from inverse Compton

scattering with electrons in galaxy clusters) [48–50] and the Integrated Sachs-Wolfe effect (from gravitational redshifting in a radiation or dark energy dominated universe) [51]. However, not all anisotropies arise from late time physics. Under the theory of inflation, primordial fluctuations were sourced from quantum fluctuations that after inflation became over or under densities [52]. See Section 1.2.2 for details on seeding perturbations. Prior to matter-radiation decoupling, these perturbations would continue to evolve as governed by their Boltzmann equations, with gravity growing matter perturbations and radiation pressure opposing collapse. These are called baryonic acoustic oscillations [53, 52, 54, 55], and we'll see that their imprint on the CMB can be used as a standard ruler to measure cosmological parameters.

In the era of precision CMB measurements, this tie-dye of a map actually holds a great deal of cosmological information that can be understood by looking at its statistics. To see this, define the temperature anisotropies in the $\hat{n}$ direction as $\Delta T(\hat{n}) \equiv T(\hat{n}) - T_0$. This full sky map can be decomposed into spherical harmonics $Y_l^m(\hat{n})$:

$$\Delta T(\hat{n}) = \sum_{lm} a_{lm} Y_l^m(\hat{n}). \tag{1.30}$$

If ΔT is a Gaussian distribution, then its multipole coefficients are Gaussian random variables. It is possible for non Gaussianities to exist, particularly sourced by some theories of inflation [56], but no evidence has been found for it to date [57]. The coefficients a_{lm} encode information both about the CMB and about the Earth's position so to extract cosmologically relevant information we must take averages over possible positions, or equivalently over possible universes [33]. The average $\langle a_{lm} \rangle = 0$, with the simplest non trivial average being:

$$\langle a_{lm} a^*_{l'm'} \rangle = \delta_{ll'} \delta_{mm'} C_l \tag{1.31}$$

where δ_{ij} is the Kronecker delta function. We can write down the C_ls by inverting a Legendre transformation, and then what is actually observed is the coefficient C_l averaged over m:

$$C_l^{\text{obs}} \equiv \frac{1}{2l+1} \sum_m a_{lm} a_{l,-m} = \frac{1}{4\pi} \int d^2\hat{n}\, d^2\hat{n}' \mathcal{P}_l(\hat{n} \cdot \hat{n}') \Delta T(\hat{n}) \Delta T(\hat{n}') \tag{1.32}$$

where $\mathcal{P}_l$ are the Legendre polynomials. Because we cannot observationally average over different positions to observe from, or different universes, there is an inherent limit to the

accuracy we can measure a C_l. This cosmic variance is given by

$$\left\langle \left(\frac{C_l - C_l^{\rm obs}}{C_l} \right)^2 \right\rangle = \frac{2}{2l+1}, \tag{1.33}$$

implying that low l measurements of C_l have a high cosmic variance and should be taken with a grain of salt. High l measurements have low cosmic variance, but are limited by instrumentation and our understanding of the astrophysical foreground. Figure 1.3 shows the 2013 Planck measurement of the power spectrum, plotting temperature fluctuations squared as a function of angular scale [45].

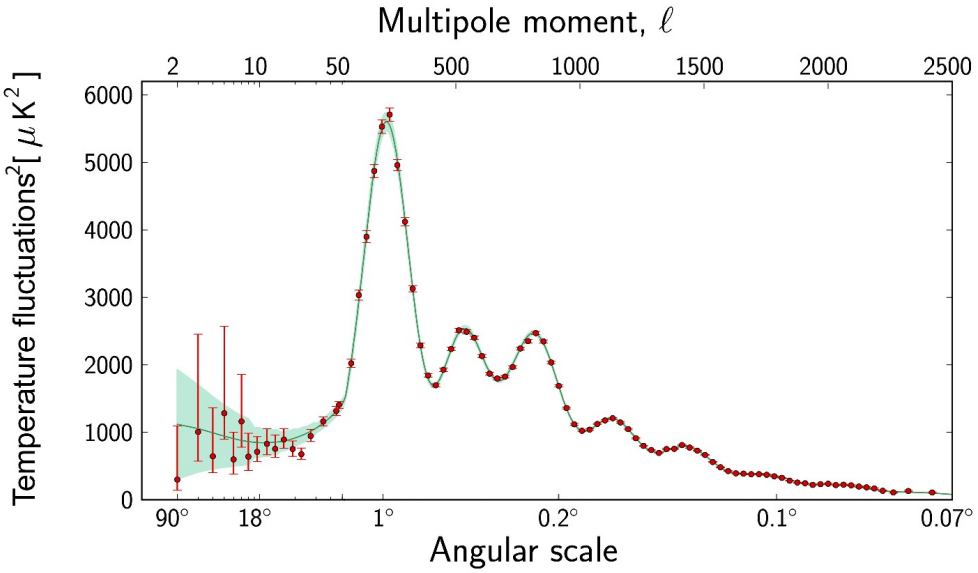

Figure 1.3: Planck 2013 CMB power spectrum (red data points), with the best fit ΛCDM calculations plotted as a solid green line. Error bars are $\pm 1\sigma$ uncertainties including cosmic variance but not including foreground uncertainties. Courtesy NASA/JPL–Caltech.

The "wiggles" in the power spectrum are due to an effect called Baryonic Acoustic oscillations (BAO). These are effectively a harmonic oscillator formed in the early universe photon-baryon fluid. Once an overdensity enters the horizon in the radiation dominated

epoch, radiation pressure will work to disperse baryon overdensities while gravity will work to collapse them. But because baryons and radiation are tightly coupled, gravitational fluctuations are sourced by dark matter overdensities. The photon baryon fluid will oscillate in dark matter potential wells until decoupling, when photons are able to free stream away and the matter overdensities are frozen in to their positions at decoupling. This increases power at scales corresponding to the oscillations' compression and rarefaction, and is dependent on the sound horizon at recombination.

The precise shape of the power spectrum allows us to measure several cosmological parameters. The first BAO peak corresponds to the scale of the horizon at recombination, which is a calculable quantity dependent on a value of H_0 at early times. However, the location of the peak we actually observe is affected by the curvature of the universe. In fact all of the peaks would shift for nonzero curvature, as photons that are initially parallel diverge or converge depending on positive or negative K. This allows for a measurement of curvature with the assumption of a value of the Hubble constant. Current measurements are consistent with zero curvature [58]. The heights of the first and second peak give a measure of the baryon energy density and total matter energy density. Figure 1.4 shows a comparison of the theoretical CMB power spectrum with best fit ΛCDM parameters versus a flat universe with no dark matter, computed using `CAMB` [59]. The power spectrum for a universe without dark matter uses a baryonic matter abundance predicted by BBN ($\Omega_b h^2 \sim 0.02$, shown in Figure 1.1). You can see that the CMB power spectrum is very convincing evidence for the existence of dark matter, since if all of the matter is baryonic, the resulting power spectrum is a very bad fit to the Planck 2018 data [2].

While matter and radiation are still coupled, a photon will travel some finite distance before its next collision. Therefore it can travel a distance governed by random walk statistics depending on the density of free electrons available for scattering, and perturbations smaller than an average random walk distance $\lambda_D \sim (n_e \sigma_T H)^{-1/2}$ in a Hubble time H^{-1} are dampened. Specifically, very small scale perturbations are wiped out by this thermal conductivity. During decoupling the density of electrons available for scattering decreases and the photon's mean free path increases, dampening fluctuations smaller than the horizon in a process called Silk damping [60]. Smaller perturbations are more strongly affected,

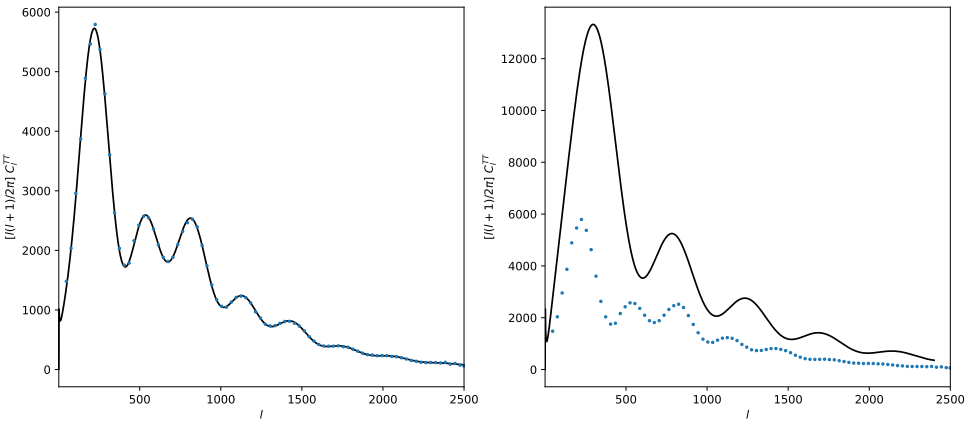

Figure 1.4: Left panel shows the theoretical CMB power spectrum with best fit ΛCDM parameters (black line) and Planck Collaboration et al. [2] measurements (blue points). Right panel shows the theoretical CMB power spectrum for a universe with no dark matter, and instead $\Omega_b h^2 = 0.02$ (black line) compared to Planck Collaboration et al. [2] measurements (blue points).

which is expressed in Figure 1.3 with peaks in the power spectrum after the third being significantly damped. Scales less than $\sim$ 10Mpc are effectively completely wiped out in the baryon distribution, and would not have had sufficient time to collapse in an entirely normal matter universe. Thus without dark matter present to provide small scale overdensities, galaxies would not have time to form [61].

1.2.5 Large Scale Structure

Present day cosmological structures– galaxies in galaxy clusters in superclusters– are significantly more complex than the simple overdensities we've discussed so far. To arrive at the present day universe, the matter overdensities are amplified by gravitational collapse and baryonic matter loses energy through radiative cooling. The dark matter remains in approximately spherical halos, but baryonic matter is able to form clouds of gas and dust that become the first stars and galaxies.

The evolution of the gravitational potential from primordial times can be described by a transfer function and a growth function, as schematically presented in Dodelson and Schmidt

[31]:

$$\Phi(\mathbf{k}, a) = \Phi_{\text{primordial}}(\mathbf{k}) \times \left\{\text{Transfer Function}(\mathbf{k})\right\} \times \left\{\text{Growth Function}(a)\right\} \tag{1.34}$$

where the transfer function describes perturbations evolving as k crosses the horizon and past the epoch of matter radiation equality, and the growth function describing late time evolution of structure independent of wavelength. The transfer function can be computed for a given cosmology by taking into account effects like Silk damping, gravitational collapse, free streaming of relativistic dark particles, etc. using codes like The Code for Anisotropies in the Microwave Background [CAMB] [3]. The growth function describes the growth of matter perturbations due to their gravitational pull. This holds in the linear regime where overdensities are small $\delta \equiv (\rho - \overline{\rho})/\overline{\rho} \ll 1$, but will break down as overdensities grow, and N-body simulations become necessary to study structure evolution precisely.

To quantify the statistics of structure we first define the angular overdensity map

$$\delta_2(\theta) = \int_0^\infty d\chi W(\chi)\delta(\mathbf{x}(\chi, \theta)) \tag{1.35}$$

where χ is the comoving distance, θ is the angle in the sky, $\delta(\mathbf{x}(\chi, \theta))$ is the three dimensional overdensity map at position $\mathbf{x}$ (given by a comoving distance and angular position), and $W(\chi)$ is a selection function. The selection function is the probability of observing a galaxy some comoving distance away, and depends both on the universe and instrumentation. We can then define a two dimensional two point correlation function,

$$\begin{aligned} \xi(r) &\equiv \langle \delta_2(\mathbf{r}) \delta_2^*(\mathbf{r}') \rangle \\ &= (2\pi)^2 \delta_{KR}^2(\mathbf{r} - \mathbf{r}') P_2(r), \end{aligned} \tag{1.36}$$

which is essentially a measure of how the overdensity field at one point one the sky is dependent on the density field at a projected distance r away. Typically the linear matter power spectrum is given in Fourier space as shown in Figure 1.5, and can be well explained by standard ΛCDM. The shape can be understood by thinking about when a given mode enters the horizon. Small scales (large k) will enter the horizon earlier– in the epoch of radiation domination. During radiation domination the gravitational potential will decay once it enters the horizon, so power at larger k values will be more strongly suppressed in the linear regime. In the non linear regime these smaller scales will be slightly enhanced due to

collapse, as we'll see in Chapter 2. The peak in $P_m(k)$ corresponds to k_{eq}, the scale entering the horizon at matter-radiation equality. In the matter dominated regime, at smaller k, the gravitational potential is constant and the power spectrum will be $\propto k$. The wiggles in the power spectrum at k slightly larger than k_{eq} correspond to BAO, similar to the CMB power spectrum, where power is amplified at scales corresponding to the overdensities created by BAO.

The power spectrum normalization isn't calculable with theory alone, and is characterized by the parameter σ_8, the expected RMS matter overdensity in a sphere of comoving radius $8h^{-1}$ Mpc

$$\begin{aligned}\sigma_8 &\equiv \langle \delta^2_{m,8}(\mathbf{x}) \rangle \\ &= \left\langle \int d^3x' \; \delta_m(\mathbf{x}') W_8(|\mathbf{x} - \mathbf{x}'|) \right\rangle\end{aligned} \tag{1.37}$$

where W_8 is the top hat window function smoothing over a scale of $8h^{-1}$ Mpc. The scale of $8h^{-1}$ Mpc is largely used for historical reasons, but is also contains approximately the right amount of matter to form galaxy clusters.

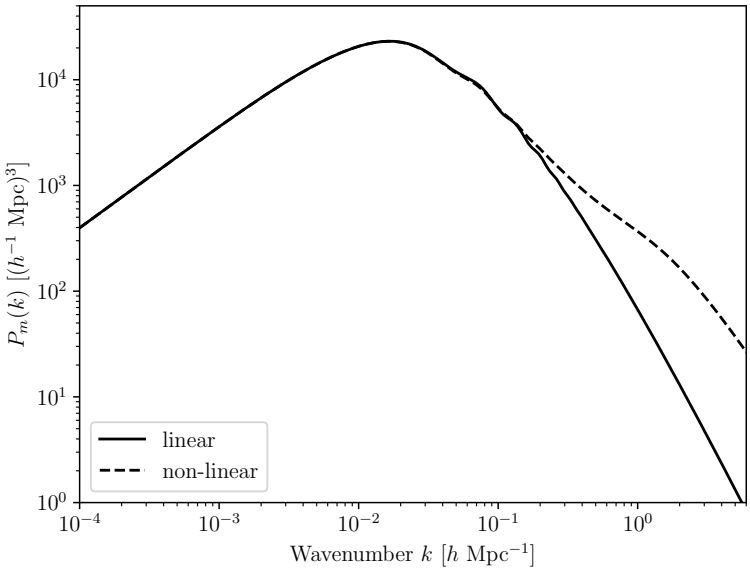

Figure 1.5: Matter power spectrum at $z = 0$ computed using `CAMB` [3]. The solid black line is the ΛCDM prediction for the linear regime, and the dotted black line includes non-linear effects.

An important error introduced into measuring galactic redshifts is their peculiar velocities– galaxies are moving not only in accordance to their cosmological expansion but also with respect to their comoving coordinates. This motion is called an object's peculiar velocity. Peculiar velocity along the line of sight causes redshift space distortions [62], which introduce error in the selection function $W(\chi)$, local distance measurements based on redshift, and other methods proposed to study local expansion like the Alcock-Paczyński test [63].

1.2.6 Problems in ΛCDM

As you can see from this chapter, the current standard model of cosmology is extremely powerful in its predictive and explanatory power. But it is far from complete. Both direct searches [64, 65] and indirect searches [66, 67] for particle dark matter have remained inconclusive, and there are several unsolved problems within the ΛCDM paradigm [68]. Once such problem is the Hubble tension at $> 4\sigma$; local measurements of the Hubble constant H_0 based on Cepheids and Type 1a supernovae in the late universe measure $H_0 = 73.04 \pm 1.04$ km s^{-1} Mpc^{-1} [69] while early universe measurements such as the Planck mission find $H_0 = 67.4 \pm 0.5$ km s^{-1} Mpc^{-1} [58]. It is still possible that this discrepancy is still due to systematics [70]. Another related problem is the growth tension σ_8, which is dependent on changes in H_0 and as such has a $(2-3\sigma)$ tension. Measurements from weak lensing and galaxy clustering [71] are lower than values derived from CMB measurements [58]. There are also a number of small scale structure problems, although it is not clear if they are actual problems or a lack of data. The core-cusp problem refers to cold dark matter simulations predicting a density profile with approximately $\rho \propto r^{-1}$ at low radii [72, 73], while velocity measurements indicate an approximately flat inner density profile [74–77]. The missing satellites problem is the discrepancy between the number of low mass subhalos in the Milky Way and the relatively low number of them seen in observations [78–81]. The too big to fail problem is the prediction that there should be more high mass subhalos with visible matter than observed [82–87]. This is a very abbreviated description of these problems, and are far from the only ones remaining with ΛCDM particularly at small scales, but are the most significant motivators for the non CDM dark matter model considered in Chapter 3.

CHAPTER 2

Foundations of Galaxy Formation

"These learned fields. Dark and ignorant,
Unable to see here what our forebears saw,
We keep some fear of random firmament
Vestigial in us. And we think, Ah,
If I had lived then, when these stories were made up, I
Could have found more likely pictures in haphazard sky."

— William Meredith, *Starlight*

2.1 Spherical Collapse

How would a matter overdensity in the early universe evolve into galaxies embedded in dark matter halos like we see today? We call early times the "linear regime," when overdensities are $|\delta(\mathbf{x})| << 1$ everywhere. In this regime, matter overdensities in Fourier space evolve like a linear combination of growing and decaying modes [61]

$$\delta_{\mathbf{k}} \sim t^{2/3}, \qquad \delta_{\mathbf{k}} \sim t^{-1} \tag{2.1}$$

when in the matter dominated epoch. The decaying mode will quickly become negligible, so perturbations grow like $t^{2/3}$ until that growth freezes in the cosmological constant dominated era at $z_{m\Lambda \text{ equality}} \sim 0.5$. This is an approximation for a matter only universe, which is not exactly true even within matter domination. The deviation of this approximation from the full solution can be seen in the growth factor $g_i \equiv \delta_{|k|=0}(t)/\delta_{|k|=0}(t_i)$, comparing the growth in long wavelength perturbations from time t_i to t. If t_i is the time of matter radiation decoupling and t is present day, the growth factor is 10% lower in the full solution than the approximation [61].

To see how these overdensities might evolve in the nonlinear regime, consider the simple example of spherical collapse. In a flat, matter dominated universe the density is

$$\rho_m(t) = \frac{1}{6\pi G t^2}, \tag{2.2}$$

so the total mass within a sphere radius r_i centered on some overdensity δ_i at time t_i is

$$M = \frac{4}{3}\pi(1+\delta_i)\rho_m(t_i)r_i^3. \tag{2.3}$$

The equations of motion for a test mass at radius r_i is determined by Newton's laws and this mass M. If this overdensity is to evolve into a galaxy we can assume the test mass has too little energy to escape, and the solution is given by

$$r = b(1-\cos\eta); \qquad t = \sqrt{\frac{a^3}{GM}}(\eta - \sin\eta) \tag{2.4}$$

where b is a constant and the maximum radius the test mass reaches before collapse, $r_{\max} = 2b$ at $\eta = \pi$, is the turnaround radius. Therefore the average overdensity is

$$\begin{aligned}\delta(t) &= \frac{M/\frac{4}{3}\pi r^3}{\rho_m(t)} - 1 \\ &= \frac{9}{2}\frac{(\eta-\sin\eta)^2}{(1-\cos\eta)^3} - 1\end{aligned} \tag{2.5}$$

corresponding to an overdensity at turnaround of

$$\delta(\eta = 0.5) = \frac{9\pi^2}{16} - 1 \approx 4.55. \tag{2.6}$$

By Taylor expanding Equations 2.5 and 2.4, we can find an approximate solution by for the turnaround radius and time

$$r_{\text{turn}} \approx \left(\frac{243}{250}\right)^{1/3} \frac{(GMt_i^2)^{1/3}}{\delta_i}, \tag{2.7}$$

$$t_{\text{turn}} \approx \pi \left(\frac{243}{2000}\right)^{1/2} \frac{t_i}{\delta_i^{3/2}}. \tag{2.8}$$

And so the larger overdensities will collapse first. This is however a highly idealized model, assuming a spherical symmetric and isolated system. In reality the dark matter will go through virialization before forming a halo. Virialization is the process of phase mixing and violent relaxation, after which the halo will satisfy the virial theorem. In brief, phase mixing

is the course grained distribution appearing to cover a greater volume of phase space by incorporating empty shells of phase space [88, 89]. Violent relaxation broadens the range of the stars' energies (independent of their mass) due to a time dependent potential, in a way analogous to collisions in a gas [90]. The potential energy at turnaround is given by $W_{\rm turn} = -\frac{3}{5}GM^2/r_{\rm turn}$, and assuming all of the energy is potential at turnaround we can approximate the radius containing half of the system's mass as $r_{HM} \simeq 0.375 r_{\rm max}$. The average density inside the half mass radius is $\rho_{HM} = \frac{1}{2}M/(\frac{4}{3}\pi r_{HM}^3)$. Assuming that the halo virializes by two times the time of maximum density in our simple spherical collapse model (when $\eta = \pi$ in Equation 2.4), we can compute the overdensity

$$\Delta = \frac{\rho_{HM}}{\rho_m(2t(\eta = \pi))} \simeq 200. \tag{2.9}$$

This calculation is not precise, but $\Delta \simeq 200$ has historically been used as a benchmark overdensity value to define the radius of halos.

2.2 Jeans Length and Collapse

An overdensity collapsing is no guarantee that it will form into a galaxy. In fact, the self gravity of a system can cause perturbations significant enough to become unstable. A tool often used to contextualize the stability and collapse of gas clouds is the Jeans length. Very roughly, it is possible to estimate that perturbations with a scale longer than some Jeans length are unstable if the inward force of gravity can overcome the outward force of pressure. This is called a Jeans instability, and can be calculated for a self gravitating fluid with a pressure term, or equivalently for a stellar system supported by gradients in the stress tensor $-\nu\sigma_{ij}^2$ (where ν is stellar density and σ_{ij} is the velocity dispersion tensor).

Let us first consider a homogeneous fluid system, and compute its linearized fluid equations. Suppose an isolated equilibrium system has the time independent potential $\Phi_0(\mathbf{x})$. Now introduce a weak gravitational force due to an external potential $\epsilon\Phi_e(\mathbf{x}, t)$ where $\epsilon << 1$ and $|\Phi_e(\mathbf{x}, t)|$ is of order $|\Phi_0(\mathbf{x})|$. If the perturbation is weak, the system's response to it will be linear and generate a density perturbation $\epsilon\rho_{s1}(\mathbf{x}, t)$, where

$$\rho_{s1}(\mathbf{x}, t) = \int d^3\mathbf{x}'\, dt' R(\mathbf{x}, \mathbf{x}', t - t')\rho_e(\mathbf{x}', t'), \tag{2.10}$$

and the response density is related to the forcing density $\rho_e(\mathbf{x}', t')$ by the response function $R(\mathbf{x}, \mathbf{x}', t - t')$. An enlightening analogy made by Binney and Tremaine [61] makes use of the polarization function $P(\mathbf{x}, \mathbf{x}', t - t')$ that connects the response density ρ_{s1} to total density ρ_1

$$\rho_{s1}(\mathbf{x}, t) = \int d^3\mathbf{x}' dt' P(\mathbf{x}, \mathbf{x}', t - t')\rho_1(\mathbf{x}', t'). \tag{2.11}$$

It is then possible to draw a parallel between this gravitational scenario and electrostatics in macroscopic media, with the analogous electrostatic polarization and displacement field [91]. Recall from electrostatics

$$\nabla \cdot \mathbf{D} = \rho; \qquad \mathbf{P} = \epsilon_0 \chi_e \mathbf{E}; \qquad \mathbf{D} = \epsilon_0 \mathbf{E} + \mathbf{P} = \epsilon \mathbf{E}; \qquad \frac{\epsilon}{\epsilon_0} = 1 + \chi_e; \tag{2.12}$$

where ϵ_0 is the electric permittivity of free space, ϵ is the electric permittivity of the material, and χ_e is the electric susceptibility of the material. The displacement field $\mathbf{D}$ resulting from unbound charges is similar to the forcing density ρ_e, and $\epsilon_0 \mathbf{E} - \mathbf{D} = -\mathbf{P}$ is the field resulting from the media's response, analogous to ρ_{s1}. Thus the gravitational polarization function of Equation 2.11 is analogous to $-\chi_e$. The negative sign implies a significant difference between the electrostatic case and the gravitational case: while bound charges can move to cancel out the displacement field imposed on the system, a gravitational response will augment the field and can aid in collapse.

Using the definitions for response density, we can write the gravitational potential from the stellar system

$$\Phi_s(\mathbf{x}, t) = \Phi_0(\mathbf{x}) + \epsilon \Phi_{s1}(\mathbf{x}, t) \tag{2.13}$$

and the total potential becomes

$$\Phi(\mathbf{x}, t) = \Phi_0(\mathbf{x}) + \epsilon \Phi_1(\mathbf{x}, t). \tag{2.14}$$

Then with Euler's equation, Poisson's equations, and some algebra, we arrive at the linearized

fluid equations

$$\begin{aligned} \frac{\partial \rho_{s1}}{\partial t} + \nabla \cdot (\rho_0 \mathbf{v}_1) + \nabla \cdot (\rho_{s1} \mathbf{v}_0) &= 0 \\ \frac{\partial \mathbf{v_1}}{\partial t} + (\mathbf{v}_0 \cdot \nabla)\mathbf{v}_1 + (\mathbf{v}_1 \cdot \nabla)\mathbf{v}_0 &= -\nabla(h_1 + \Phi_{s1} + \Phi_e) \\ \nabla^2 \Phi_{s1} &= 4\pi G \rho_{s1} \\ h_1 = \frac{p_1}{\rho_0} = \left(\frac{dp}{d\rho}\right)_{\rho_0} \frac{\rho_{s1}}{\rho_0} &= v_s^2 \frac{\rho_{s1}}{\rho_0} \end{aligned} \tag{2.15}$$

where h_1 is the linear perturbation term $h(\mathbf{x}, t) = h_0(\mathbf{x}) + \epsilon h_1(\mathbf{x}, t)$ of specific enthalpy h defined as

$$h(\rho(\mathbf{x}, t)) \equiv \int_0^\rho \frac{dp(\rho')}{\rho'}. \tag{2.16}$$

If we consider the equilibrium state to have constant density ρ_0, constant pressure p_0, and no internal motions so $\mathbf{v}_0 = 0$, then Euler's equation implies that $\nabla \Phi_0 = 0$. However, Poisson's equation states that $\nabla^2 \Phi_0 = 4\pi G \rho_0$. This inconsistency for $\rho_0 \neq 0$ is solved in Binney and Tremaine [61] by the Jeans swindle, which is the assumption that Poisson's equation only applies to the perturbed density and perturbed potential. [1] The Jeans swindle and taking the unperturbed state to have to have constant density ρ_0, constant pressure p_0, and $\mathbf{v}_0 = 0$, allows us to write Equations 2.15 as

$$\begin{aligned} \frac{\partial \rho_{s1}}{\partial t} + \rho_0 \nabla \cdot \mathbf{v}_1 &= 0, \\ \frac{\partial \mathbf{v}_1}{\partial t} &= -\nabla(h_1 + \Phi_{s1} + \Phi_e), \\ \nabla^2 \Phi_{s1} &= 4\pi G \rho_{s1}, \\ h_1 &= v_s^2 \rho_{s1} / \rho_0. \end{aligned} \tag{2.17}$$

With some manipulation, Equations 2.17 can be written as one equation in Fourier space

$$\frac{\partial^2 \overline{\rho}_{s1}}{\partial t^2} + v_s^2 k^2 \overline{\rho}_{s1}(\mathbf{k}, t) - 4\pi G \rho_0 \overline{\rho}_{s1}(\mathbf{k}, t) = 4\pi G \rho_0 \overline{\rho}_e(\mathbf{k}, t). \tag{2.18}$$

To find a mode, a sustained perturbation requiring no external forces, set $\overline{\rho}_e(\mathbf{k}, t) = 0$ and $\overline{\rho}_{s1}(\mathbf{k}, t) \sim e^{-i\omega t}$ in Equation 2.18. Then we see a mode must satisfy

$$\omega^2 = \omega_0^2(k) \equiv v_s^2 k^2 - 4\pi G \rho_0 = v_s^2 (k^2 - k_J^2) \tag{2.19}$$

[1] The generalized version of a Jeans analysis for a relativistic fluid in an expanding universe do not require the Jeans swindle to function [61].

where k_J is the Jeans wavenumber corresponding to a Jeans wavelength λ_J,

$$k_J^2 \equiv \frac{4\pi G\rho_0}{v_s^2} \tag{2.20}$$

$$\lambda_J^2 = \frac{\pi v_s^2}{G\rho_0}. \tag{2.21}$$

Short wavelength $k > k_J$ perturbations give oscillatory solutions ($\omega^2 > 0$), while long wavelength perturbations $k < k_J$ will exponentially grow or decay. A perturbation will be unstable and collapse if its λ is greater than the Jeans wavelength. This is also often discussed in terms of a Jeans mass, the mass contained within a sphere of Jeans length diameter.

$$M_J = \frac{\pi^{5/2}}{6}\frac{v_s^3}{G^{3/2}\rho^{1/2}} \tag{2.22}$$

A mass greater than the Jeans mass within a sphere of that size will collapse under the assumptions of an infinite and homogeneous system and the Jeans swindle.

2.3 Hierarchical Structure Formation and Extended Press–Schechter Formalism

Imagine a region of the universe containing two nearby underdensities in the matter dominated regime. The expansion rate of test particles in those regions will be slowed less by gravity than in the adjacent denser regions of space. In other words, the local expansion rate will be dominated by cosmological constant, as opposed to the matter dominated expansion rate $\propto a^{-3}$. Thus the adjacent low density regions, called voids, will expand until colliding and merging with each other. The result is that two adjacent voids will be separated by an overdense sheet of matter, and three adjacent voids would create a filament. [92] Since the universe is populated by early universe fluctuations, randomly distributing over and underdensities, large scale structure will form into a three dimensional web of matter filaments connected by overdense nodes. This sketched prediction has been borne out by many hydrodynamic simulations with Cold Dark Matter and baryons, such as the recent IllustrisTNG simulation [93], and agrees with observations of a filament structure in the present day galaxy distribution [94–97]. The first objects will form at the nodes of

this cosmic web, where matter is the most dense, and in general galaxies are more likely to form along a filament than in void [61]. This is hierarchical structure formation, in that smaller structures will form before large ones. This is described statistically by extended Press–Schechter formalism, originally proposed by Press and Schechter [98] and elaborated on by Bond et al. [99] and Lacey and Cole [100].

From the discussion on spherical collapse in Section 2.1, we can track overdensities before collapse as any region exceeding a critical density. Assuming virialization by $t = 2t_{\text{turn}}$, we can use Equation 2.8 to write the critical density

$$\delta_c = \left(2\pi\sqrt{\frac{243}{2000}}\frac{t_i}{t}\right)^{2/3} \approx \left(2.19\frac{t_i}{t}\right)^{2/3} \tag{2.23}$$

For a particular overdensity at location $\mathbf{x}$ in the sky, we can write the overdensity as Fourier sum

$$\delta(\mathbf{x}) = \frac{1}{V}\sum_{\mathbf{k}} \delta_{\mathbf{k}} e^{i\mathbf{k}\cdot\mathbf{x}} \tag{2.24}$$

for the large but finite volume V, and consider "building" the overdensity in increments of Δ_K with increasing $K \equiv |\mathbf{k}|$

$$\Delta_K = \frac{1}{V}\sum_{K\leq|\mathbf{k}|<K+dK} \delta_{\mathbf{k}} e^{i\mathbf{k}\cdot\mathbf{x}} \quad . \tag{2.25}$$

The variance σ_K^2 of $\delta(\mathbf{x})$ when including only wavelengths of $|\mathbf{k}| < K$ will be a monotonically increasing variable as K increases, and acts like the step number in a random walk of $\delta(\mathbf{x})$. The scale K at which $\delta(\mathbf{x})$ crosses the critical density threshold is the scale of the overdensity's collapse at a given time. As t increases, the critical density threshold will decrease and scales will enter the halo with some amount of associated mass. This can either be continuous in σ_K^2, associated with a steady infall of material, or discontinuous in σ_K^2 and associated with a merger event.

We can now ask what the probability $p_K(\delta)$ is that at a given step σ_K^2, an overdensity will have value between δ and $\delta + d\delta$. If we consider a large number N positions in the sky, the number of such overdensities is $Np_K(\delta)d\delta$. Since this is for a specific K, as we change the value of σ_K^2 the value of those overdensities will disperse according to a diffusion equation

$$\frac{\partial p_K}{\partial \sigma_K^2} = \frac{1}{2}\frac{\partial^2 p_K}{\partial \delta^2} \tag{2.26}$$

where the factor of 1/2 is a diffusion coefficient, which can be found with some manipulation from the definition of $\sigma_K^2 \equiv \langle \delta^2 \rangle = \int \delta \, \delta^2 p_K(\delta)$. The solutions to this equation that satisfy the boundary condition of $p_K(\delta) = 0$ when $\sigma_K^2(\delta \neq 0) = 0$ and the normalization of $\int d\delta \, p_K(\delta) = 1$ are

$$p_K(\delta) = \frac{1}{\sqrt{2\pi\sigma_K^2}} \exp\left(-\frac{\delta^2}{2\sigma_K^2}\right) \tag{2.27}$$

and

$$p_K(\delta) = \frac{1}{\sqrt{2\pi\sigma_K^2}} \left[\exp\left(-\frac{\delta^2}{2\sigma_K^2}\right) - \exp\left(-\frac{(\delta - 2\delta_c)^2}{2\sigma_K^2}\right)\right], \tag{2.28}$$

where one solution is for particles beginning at the origin and the other is for particles beginning at $\delta = 2\delta_c$. Extended Press-Schechter formalism is a powerful tool in its simplicity, enabling the calculation of a mass function (probability that the largest halo containing a given mass element has scale K^{-1} at time t) and a merger rate (probability that halo of mass M will undergo a merger increasing its mass to $M + dM$ at time t). The details of these calculations are beyond the scope of this brief overview, but follow from using the probability of Equation 2.28 to compute the probability that the largest halo, of a large number of overdensities $\delta(\mathbf{x})$, containing subhalo mass m has a mass in the interval $(M, M + dM)$.

2.4 Dependence on Dark Matter Properties

The presence of dark matter is essential for the formation of galaxies, as is touched on briefly in Section 1.2.4. But the effect of dark matter on structure formation doesn't end with its mere existence– the characteristics of the resulting structures are heavily dependent on the specific behavior of the dark matter model. One of the clearest places to see the effect of dark matter properties is on the prediction of a smallest possible length scale $K_{\max}^{-1}$ for halos. For a collisionless dark matter model, random particle velocities will disperse overdensities on scales $\leq \sigma t$ where σ is the velocity dispersion at time t. Prior to decoupling, when the dark matter is relativistic, this is simply the horizon scale $\sim ct$. After decoupling the velocity dispersion damping scale will become smaller than the horizon. This can also be thought of in terms of the virial theorem; a warm dark matter model with more kinetic energy requires a deeper potential well (and therefore more massive halo) to remain bound,

subsequently suppressing small scale structure for a warm dark matter model in comparison to a cold one. Current measurements are consistent with CDM hydrodynamic simulations over warm dark matter [101]. There are other theories that would have an effect as well, such as fuzzy dark matter [102, 103] suppressing small scale structures with quantum pressure, as described in greater detail in Chapter 3.

CHAPTER 3

The viability of ultralight bosonic dark matter in dwarf galaxies

> *"Where the telescope ends, the microscope begins. Which of the two possesses the larger field of vision? Choose. A bit of mould is a pleiad of flowers; a nebula is an ant-hill of stars."*
>
> — Victor Hugo, *Les Miserablés*

3.1 Introduction

In the last 20 years, Milky Way dwarf galaxies have provided a wealth of information regarding the nature of dark matter. As dark matter dominated systems with mass to light ratios in excess of $M/L \gtrsim 10$, and devoid of most baryonic astrophysical complexities, they are ideal hypothesis testing systems for some of the most fundamental properties of dark matter. Dwarf galaxies have been used to place the most robust to-date constraints on the annihilation [104, 105], decay [106–108], and self-interaction cross sections [109]. In addition, their mere existence places limits on whether the dark matter particle decoupled while relativistic.[110].

The distribution of dark matter in dwarfs is a subject of debate. Collision-less, cold dark matter gives rise to cusps, while alternative dark matter models, like self-interacting dark matter [112, 113] and warm dark matter (free streaming from non-zero velocities at decoupling) [114–116], predict central profiles that are cored. The formation and dark matter

The material in this chapter is published in Goldstein et al. [111].

distribution of these objects through complex baryonic galaxy formation arguments has been reproduced in simulations, and the underlying physics has been at the forefront of fundamental dark matter study.

The tool of choice in all the aforementioned studies is reconstructing the gravitational potential using stellar kinematics (e.g., [105, 117, 118]). Measurements of stellar velocities along the line of sight of bright red giants allows for the distribution of dark matter to be reverse engineered [119]. Such measurements are extremely powerful because under a set of reasonable dynamical assumptions they allow for robust potential reconstruction with well controlled errors, especially in the case of classical dwarf galaxies. Attempts to apply such methods to the faintest objects in the universe (ultra-faint dwarf galaxies discovered in the last few years) carry much larger uncertainties and thus are less constraining [106, 107].

In this chapter we use stellar kinematics to test the viability of ultralight bosonic dark matter in dwarf galaxies. Motivations for such dark matter candidates come from GUT-scale physics, originally introduced through the solution to the strong CP problem in quantum chromodynamics [120–122], and subsequently envisioned through cosmology and large scale structure [102, 123–138]. Qualitatively, such objects go by the name of "fuzzy dark matter", a term that denotes a fundamental characteristic property: the existence of a coherent quantum state (a Bose-Einstein condensate), described by the Schrödinger-Poisson equation and forming soliton cores instead of cusps [139, 140], for a thorough review please see Hui et al. [102].

The quantum pressure of fuzzy dark matter arises from ultralight bosons mass $\sim 10^{-22}$ eV or scalar field DM with de Broglie wavelength about the size of the dwarf galaxy stellar component ($\sim$ 1 kpc). The existence of a soliton core suppresses small scale structure [102, 141] (see [142, 143] for additional constraints from Milky Way satellites). Throughout the chapter we will be using the terms fuzzy dark matter and/or axion-like dark matter interchangeably to refer to dark matter that forms quantum pressure supported soliton cores.

We examine the viability of ultralight boson dark matter in dwarf galaxies using stellar kinematics in six classical dwarf galaxies: Fornax, Sculptor, Draco, Sextans, Ursa Minor, and Carina. We choose to use only classical dwarf galaxies because they contain enough stars and observations ($N_{\rm obs} \gtrsim 500$) to provide meaningful constraints on the dark matter

gravitational potential.

The primary goal of this work is to determine whether ultralight bosonic dark matter is consistent with velocity dispersion measurements, and if so, what range of parameters allow such consistency. We find that unless the Milky Way did not have a typical evolution, the mass of the ultralight dark matter particle must be at least $m > 10^{-20}\mathrm{e}V$.

The chapter is organized as follows: In Section 3.2 we outline the reconstruction of the mass distribution using stellar velocity dispersion measurements (Jeans analysis). In Section 3.3 we review a set of dark matter density profiles that have been proposed in the literature as soliton solutions to dark matter halos. Section 3.4 summarizes the observations used in the paper, and in Section 3.5 we present the results. We conclude in Section 3.6.

3.2 Stellar kinematics potential tracers

Line of sight stellar velocity measurements from dwarf galaxies can be used in the construction of a stellar velocity dispersion profile (velocity dispersion as a function of radius from the center of the dwarf). The velocity dispersion traces the underlying matter density distribution, and can be linked using the two Jeans equations, first applied to stellar kinematics in 1919 by Jeans [144].

Define the distribution function f so that $f(\mathbf{x}, \mathbf{v}, t)d^3xd^3v$ is the probability of finding a star in a volume element of phase space at time t, normalized to one over all of phase space. Probability is conserved in phase space just as mass is conserved in a fluid flow, so the continuity equation

$$\frac{\partial \rho}{\partial t} + \frac{\partial}{\partial \mathbf{x}}(\rho \dot{\mathbf{x}}) = 0 \tag{3.1}$$

can be written as

$$\frac{\partial f}{\partial t} + \frac{\partial}{\partial \mathbf{w}}(f \dot{\mathbf{w}}) = 0 \tag{3.2}$$

where $\mathbf{w} = (\mathbf{p}, \mathbf{q})$ are the canonical coordinates. This can be rewritten with Hamilton's equation's to derive the collisionless Boltzmann equation

$$\frac{\partial f}{\partial t} + \dot{\mathbf{q}}\frac{\partial f}{\partial \mathbf{q}} + \dot{\mathbf{p}}\frac{\partial f}{\partial \mathbf{p}} = 0. \tag{3.3}$$

When written in Cartesian coordinates and assuming a Hamiltonian with a gravitational potential Φ, Equation 3.3 becomes

$$\frac{\partial f}{\partial t} + \mathbf{v}\frac{\partial f}{\partial \mathbf{x}} - \frac{\partial \Phi}{\partial \mathbf{x}}\frac{\partial f}{\partial \mathbf{v}} = 0. \tag{3.4}$$

To relate this to observable quantities, define the stellar distribution function ν as the probability of finding a star at location $\mathbf{x}$ and time t

$$\nu(\mathbf{x}, t) \equiv \int d^3v f(\mathbf{x}, \mathbf{v}, t), \tag{3.5}$$

which when multiplied by the total number of stars would be the number density of stars. We can also define the observable velocity dispersion tensor,

$$\begin{aligned} \sigma_{ij}^2(\mathbf{x}) &\equiv \int d^3v (v_i - \overline{v}_i)(v_j - \overline{v}_j)\frac{f(\mathbf{x}, \mathbf{v}, t)}{\nu(\mathbf{x}, t)} \\ &= \overline{v_i v_j} - \overline{v_i}\,\overline{v_j}. \end{aligned} \tag{3.6}$$

Notice that f/ν is the probability distribution of stellar velocities. To find the first Jeans equation, integrate Equation 3.4 over all possible velocities,

$$\frac{\partial}{\partial t}\int d^3v f + \frac{\partial}{\partial x_i}\int d^3v\, v_i f - \frac{\partial \Phi}{\partial x_i}\int d^3v \frac{\partial f}{\partial v_i} = 0. \tag{3.7}$$

Where we have moved the time and position derivatives outside of the integrals, since velocity is not dependent on those variables. Because no stars move infinitely fast, $f(\mathbf{x}, \mathbf{v}, t) = 0$ for very large $|\mathbf{v}|$ and the last integral goes to zero with the divergence theorem. We can then identify the first integral as the definition of stellar distribution function ν. The second integral can be identified using the definition of mean velocity at position $\mathbf{x}$,

$$\overline{\mathbf{v}}(\mathbf{x}, t) \equiv \int d^3v\, \mathbf{v}\frac{f(\mathbf{x}, \mathbf{v}, t)}{\nu(\mathbf{x}, t)} = \frac{1}{\nu(\mathbf{x}, t)}\int d^3v\, \mathbf{v} f(\mathbf{x}, \mathbf{v}, t). \tag{3.8}$$

And as such Equation 3.7 can be simplified into the first Jeans equation:

$$\frac{\partial \nu}{\partial t} + \frac{\partial(\nu \overline{v}_i)}{\partial x_i} = 0. \tag{3.9}$$

This looks similar to the continuity equation, but conserving the flow of the stellar distribution instead of fluid flow. To obtain the second Jeans equation, we multiply Equation 3.4 by v_j and integrate over all velocities,

$$\frac{\partial}{\partial t}\int d^3v\, f v_j + \int d^3v\, v_i v_j \frac{\partial f}{\partial x_i} - \frac{\partial \Phi}{\partial x_i}\int d^3v\, v_j \frac{\partial f}{\partial v_i} = 0. \tag{3.10}$$

The last integral can be manipulated using integration by parts, then once again taking advantage of the divergence theorem and the fact that f disappears for large velocities,

$$\int d^3v\, v_j \frac{\partial f}{\partial v_i} = -\int d^3v \frac{\partial v_j}{\partial v_i} f = -\int d^3v \delta_{ij} f = -\delta_{ij}\nu \tag{3.11}$$

where δ_{ij} is the Kronecker delta function. The first and second integrals can be identified as average velocities, and then using Equation 3.9 and the definition for velocity dispersion σ_{ij}^2, Equation 3.10 can be simplified into the form of the second Jeans equation

$$\nu \frac{\partial \overline{v}_j}{\partial t} + \nu \overline{v}_i \frac{\partial \overline{v}_j}{\partial x_i} = -\nu \frac{\partial \Phi}{\partial x_j} - \frac{\partial (\nu \sigma_{ij}^2)}{\partial x_i}. \tag{3.12}$$

Notice that this is analogous to Euler's equation of fluid flow for a fluid with density ρ, pressure p, and under a gravitational potential Φ,

$$\rho \frac{\partial v_i}{\partial t} + \rho v_j \frac{\partial v_i}{\partial x_j} = -\rho \frac{\partial \Phi}{\partial x_j} - \frac{\partial p}{\partial x_i} \tag{3.13}$$

where in Equation 3.12 the stellar distribution ν takes the place of fluid density and the stress tensor $\nu\sigma_{ij}^2$ takes the place of an anisotropic pressure. This second Jeans equation is particularly useful in that it allows observable quantities like stellar position and line of sight velocities to be connected in a straightforward mathematical way to the underlying gravitational potential.

Under the assumption of a spherical and time independent system, Equation 3.12 can be written in the following form [61],

$$\begin{aligned} \frac{d\Phi}{dr} &= -\frac{GM(r)}{r^2} \\ &= -\frac{1}{\nu(r)} \frac{d}{dr} \left[\nu(r) \overline{u_r^2}(r) \right] - 2\frac{\beta_a(r) \overline{u_r^2}(r)}{r}. \end{aligned} \tag{3.14}$$

Here, β_a the orbital anisotropy is a measure of the difference between tangential and radial dispersions,

$$\beta_a(r) \equiv 1 - \frac{2\overline{u_\theta^2}(r)}{\overline{u_r^2}(r)}, \tag{3.15}$$

and $\overline{u_r^2}(r)$ is the radial stellar velocity dispersion profile,

$$\overline{u^2}(r) = \overline{u_r^2}(r) + \overline{u_\theta^2}(r) + \overline{u_\phi^2}(r). \tag{3.16}$$

The mass enclosed is $M(r)$ defined in the usual way,

$$M(r) = 4\pi \int_0^r s^2 \rho(s) ds. \tag{3.17}$$

Under the assumption of spherical symmetry and dynamical equilibrium, Equation (3.14) has the general solution:

$$\nu(r)\overline{u_r^2}(r) = \frac{1}{f(r)} \int_r^\infty f(s)\nu(s)\frac{GM(s)}{s^2} ds, \tag{3.18}$$

where $f(r)$ is

$$f(r) = 2\, f(r_1) \exp\left[\int_{r_1}^r \beta_a(s) s^{-1} ds\right]. \tag{3.19}$$

The assumption of dynamic equilibrium is implicit in the Jeans equation, but unlikely to hold precisely for all of the Milky Way satellites that we consider. Nevertheless, various studies have shown that violation of this assumption is unlikely to have dramatic effects on the inferred dynamical mass [145–147]. In any case, the dynamical crossing time of a typical Milky Way dwarf spheroidal is a small fraction of its orbital period, such that we can expect a state of near equilibrium to hold over most of the dwarf's orbit.

If we assume the orbital anisotropy is a constant within a given system, then the velocity dispersion projected along the line of sight is

$$\sigma^2(R)\Sigma(R) = 2\int_R^\infty \left(1 - \beta_a(r)\frac{R^2}{r^2}\right) \frac{\nu(r)\,\overline{u_r^2}(r)\, r}{\sqrt{r^2 - R^2}} dr, \tag{3.20}$$

where R is the projected radial distance from the center and $\Sigma(R)$ is the projected stellar density.

This formulation necessitates the use of a stellar profile. We assume a Plummer profile [148]

$$\nu(R) = \frac{3L}{4\pi R_e^3} \frac{1}{(1 + R^2/R_e^2)^{5/2}}, \tag{3.21}$$

for which the projected stellar distribution takes the form

$$\Sigma(R) = \frac{L}{\pi R_e^2} \frac{1}{(1 + R^2/R_e^2)^2}. \tag{3.22}$$

We use the Bayesian inference tool `MultiNest` [149] as implemented in the python package `PyMultiNest` [150]. `MultiNest` operates by sampling N points from the input prior space, then discarding the lowest likelihood L_0 point. It is replaced by a new point with likelihood

L_1 if $L_1 > L_0$, and the prior volume is reduced. Going from lowest to highest likelihoods in this way makes it easier to sum up the likelihood over the prior volume later to compute a model's evidence, making this tool well suited to comparing models for selection.

Following the analysis in Geringer-Sameth et al. [106], this is implemented with the unbinned Gaussian likelihood function[1]

$$L = \prod_{i=1}^{N} \frac{1}{\sqrt{2\pi}\sqrt{\delta_{u,i}^2 + \sigma^2(R_i)}} \exp\left[-\frac{1}{2}\frac{(u_i - \langle u \rangle)^2}{\delta_{u,i}^2 + \sigma^2(R_i)}\right]. \tag{3.23}$$

Here, u_i is the projected velocity, R_i is the projected position, and $\delta_{u,i}$ is the observational error in velocity of the ith star in the data set. $\langle u \rangle$ is the bulk velocity, which is marginalized over with a flat prior.

3.3 Halo profiles

A key ingredient in using stellar velocities to reconstruct the dark matter distribution in dwarf galaxies is the assumed functional form of the dark matter density profile. In order to explore the viability of ultralight bosonic dark matter in dwarf galaxies it is necessary to start from a basic description of the non-linear evolution of halos. This is a difficult problem where the only way to obtain such information is through numerical simulations.

Below we first summarize the distribution of cold dark matter in halos, namely the Navarro Frenk & White generalized profile (NFW hereafter) [151–153]. We then describe three different prescriptions of the distribution of dark matter in fuzzy dark matter halos. All three are based on an internal structure that contains a quantum mechanical pressure-supported core. How the core transitions to the outer NFW-like dark matter distribution is the subject of these three models. The differences are summarized in Table 3.1.

3.3.1 Cold dark matter distribution – NFW profile

The NFW profile [151] and subsequently its more generalized form [152, 153] are the outcome of N-body dark matter simulations where initial thermal velocities in the dark matter are negligible and do not affect the growth of structure (cold dark matter). The form

[1] For binned analysis and differences between binned and unbinned analyses [107].

of the dark matter distribution is given by a generalized NFW,

$$\rho_{\rm NFW}(r) = \frac{\rho_s}{(r/r_s)^{\gamma}[1+(r/r_s)^{\alpha}]^{(\beta-\gamma)/\alpha}}, \tag{3.24}$$

where ρ_s and r_s are the characteristic density and scale radius respectively, and $\{\alpha, \beta, \gamma\}$ describe the power law behavior of the dark matter distribution. The profile has an inner density profile that goes as $\sim r^{-\gamma}$ and an outer behavior characterised by $\sim r^{-\beta}$. The normalization of such a profile is specified either by the characteristic density ρ_s and the scale radius r_s, or by the mass of the halo $M_\Delta = \int \rho(r) d^3r$ and its concentration $c = R_\Delta/r_s$, where R_Δ is the radius of the halo.

One has the freedom to choose how to define a halo, for example whether a halo is defined as a virial overdensity (in this case $\Delta = \text{vir}$) or a fixed product of Δ times the mean matter density of the universe (e.g., $\Delta = 200$). In what follows, when we refer to the mass of an NFW profile we will be using $\Delta = 200$, i.e., the NFW profile can be characterized by M_{200} and c_{200} (or R_{200}).

This functional form of dark matter distribution has been extensively studied in numerical simulations and has been applied in studies aimed at reconstructing the gravitational potential of dark matter halos on many scales, from galaxy clusters [154] to the Milky Way [155] and dwarf galaxies [106, 156].

When implemented in `MultiNest`, the generalized NFW parameters are sampled over flat priors in linear space for the powers α, β, γ and in logarithmic space for the parameters $(1-\beta_a)$, $M_{200}/M_\odot$, and c_{200}:

$$\begin{aligned} -1 \leq -\log_{10}(1-\beta_a) &\leq +1, \\ \log_{10}(5\times 10^7) \leq \log_{10}(M_{200}/M_\odot) &\leq \log_{10}(5\times 10^9), \\ \log_{10}(2) \leq \log_{10}(c_{200}) &\leq \log_{10}(30), \\ 0.5 \leq \alpha &\leq 3, \\ 3 \leq \beta &\leq 10, \\ 0 \leq \gamma &\leq 1.2. \end{aligned}$$

Note that the original NFW profile has a power law behavior given by $\{\alpha, \beta, \gamma\} = \{1, 3, 1\}$. The priors for M_{200} have an upper limit at $M_{200} = 5\times 10^9 M_\odot$ because increasing that limit

has minimal effect on the posteriors.

3.3.2 Soliton cores

Fuzzy dark matter distribution in collapsed halos is a highly non-linear process that necessitates the use of numerical simulations. The large scale cosmological simulations of [139] found that axion-like dark matter does lead to the formation of cores that reside in the center of dark matter halos. The density of such cores at $z = 0$ (present epoch) is parameterized as

$$\rho_{\rm soliton}(r) = \frac{1.9(10m_{22})^{-2}(r_c/{\rm kpc})^{-4}}{\left[1 + 9.1 \times 10^{-2}\,(r/r_c)^2\right]^8} 10^9 M_\odot {\rm kpc}^{-3}, \tag{3.25}$$

where $m_{22} \equiv m/10^{-22}$eV is the scaled dark matter particle mass and r_c is the characteristic radius, defined to be the radius at which density drops to one half of the halo's peak value defined as $\rho_{\rm soliton}(r \to 0)$. The functional form of Eq. 3.25 is accurate to 2% for $0 < r \lesssim 3r_c$ [139].

The soliton core extends out to the characteristic radius[2],

$$r_c \approx 1.5\, m_{22}^{-1} \left(\frac{M_{200}}{10^9 M_\odot}\right)^{-1/3} {\rm kpc}. \tag{3.26}$$

For the full wave dark matter density profile of Eq. 3.25, the numerical simulations of Schive et al. [139], Mocz et al. [140] show that at $\sim 3r_c$ there is a smooth transition to an NFW-like profile.

There is however ambiguity in how the NFW profile is defined in this case ($\{\rho_s, r_s\}$, or $\{M_{200}, c_{200}\}$) and how it relates to the characteristics of the soliton, namely, $\{M_{200}, m_{22}\}$) in Equations 3.25 & 3.26. In other words, how is the inner part of the halo (formed early on) related to the distribution of matter in the outskirts of the halo?

Previous work proposed different methods on how to make this transition. In this chapter we will examine how choices affect the posteriors using stellar kinematics in dwarf galaxies.

[2]The original fitting function from [139] was in terms of $M_{\rm vir}$. Here, for consistency throughout the paper we use the relationship between M_{200} and $M_{\rm vir}$ for a matter density of $\Omega_{\rm M} = 0.3$ [157] to express Eq. 3.26 in terms of M_{200}.

Soliton core mass

It is vital to the computation time of a velocity dispersion profile to have analytical forms for the mass enclosed at radius r, as this computation happens many times for a given model of dark matter profile. Changing the computation from numerically calculating a triple integral to numerically calculating a double integral significantly reduces computation time.

With this in mind, we can use Equation 3.25 to write the mass enclosed within radius R in the soliton core as

$$M_{\rm core}(\leq R) = \frac{4\pi(1.9)}{a(10m_{22})^2}\left(\frac{r_c}{\rm kpc}\right)^{-4} r_c^2 \int \frac{(r/r_c)^2\,dr}{[1+9.1\times10^2(r/r_c)^2]^8} M_\odot {\rm pc}^{-3}. \tag{3.27}$$

If we define $x \equiv \frac{r}{r_c}$ and $C \equiv 9.1\times10^{-2}$, then:

$$M_{\rm core}(\leq R) = \frac{4\pi(1.9)}{a(10m_{22})^2}\left(\frac{r_c}{\rm kpc}\right)^{-4} r_c^3 \int \frac{x^2\,dx}{[1+Cx^2]^8} M_\odot {\rm pc}^{-3} \tag{3.28}$$

Focusing on just the integral in Equation 3.28, it may be rewritten with partial fractions:

$$M_{\rm core}(\leq R) = \frac{4\pi(1.9)}{a(10m_{22})^2}\left(\frac{r_c}{\rm kpc}\right)^{-4} r_c^3 \int \frac{1}{C}\left[\frac{1}{(1+Cx^2)^7} - \frac{1}{(1+Cx^2)^8}\right] dx\, M_\odot {\rm pc}^{-3} \tag{3.29}$$

Define another change of variables such that $x \equiv \tan(u)/\sqrt{C}$. Then we may rewrite the integrals as follows:

$$\begin{aligned}
\int_0^{R/r_c} \frac{dx}{(1+Cx^2)^7} &= \frac{1}{\sqrt{C}}\int_0^{\tan^{-1}(\sqrt{C}\,R/r_c)} \cos^{12} u\, du \\
\int_0^{R/r_c} \frac{dx}{(1+Cx^2)^8} &= \frac{1}{\sqrt{C}}\int_0^{\tan^{-1}(\sqrt{C}\,R/r_c)} \cos^{14} u\, du
\end{aligned} \tag{3.30}$$

And recombine using the following reduction formula,

$$\int \cos^m u\, du = \frac{\sin u \cos^{m-1} u}{m} + \frac{m-1}{m}\int \cos^{m-2} u\, du \tag{3.31}$$

Such that

$$\begin{aligned}
\mathbb{I}(R) \equiv \int_0^{R/r_c} \frac{x^2}{[1+Cx^2]^8} dx = \\
\frac{(9.1\times10^{-2})^{-3/2}}{573440}\Bigg[&249480u + 215985\sin(2u) + 69685\sin(4u) \\
&+ 21945\sin(6u) + 5495\sin(8u) + 973\sin(10u) \\
&+ 105\sin(12u) + 5\sin(14u)\Bigg]_{u=\tan^{-1}(\sqrt{9.1\times10^{-2}}\,R/r_c)}
\end{aligned} \tag{3.32}$$

Table 3.1: Summary of soliton core models.

Profile	Free Parameters	Assumptions
NFW	$\beta_a, \rho_s, r_s, \alpha, \beta, \gamma$	Cold Dark Matter
Model A	$\beta_a, m_{22}, M_{200}, c_{200}$	Halo mass parameter M_{200} corresponds to both the soliton mass parameter and the NFW halo mass parameter, transition happens at $3r_c$ with a transition to outer NFW. Total halo mass can be different than M_{200}.
Model B	$\beta_a m_{22}, M'_{200}, \epsilon$	Transition happens at $r_\epsilon = f(m_{22}, M'_h, ...)$, density continuity $\rho_{\rm core}(r_\epsilon) = \rho_{\rm NFW}(r_\epsilon)$.
Model C	β_a, m_{22}, M_{200}	Transition happens at $3r_c$, continuous density $\rho_{\rm core}(3r_c) = \rho_{\rm NFW}(3r_c)$, and second NFW parameter defined by mass conservation.

Allowing us to rewrite Equation 3.29 for r_c given in parsecs as the following computationally efficient expression,

$$M_{\rm core}(\leq R) = \frac{(4\pi)1.9\times10^{12}}{a(10m_{22})^2(0.091)^{3/2}r_c}\mathbb{I}(R)\ \ M_\odot {\rm pc}^{-3}. \tag{3.33}$$

Model A

The simplest soliton-like profile is one where the soliton core transitions to an NFW profile at a radius of $\sim 3r_c$ [142]. This is an artificially constructed halo with no physical input other than the characteristics of the soliton core and the outer functional behavior of the NFW profile. There is no imposed physical connection between the two.

It is composed of two profiles that are matched to have equal densities at the transition radius

$$\rho_{\rm soliton}\Big|_{r=3r_c} = \rho_{\rm NFW}\Big|_{r=3r_c}. \tag{3.34}$$

In this model, the free parameters that can define the NFW profile are the mass M_{200}, and concentration c_{200}. The soliton profile is defined by the same mass M_{200} and the mass of the scalar dark matter particle m_{22}.

The normalization, M_{200}, and characteristic functional behavior given by $c_{200}, \alpha, \beta, \gamma$, of the NFW profile do not need to correspond to physical halos as long as Eq.3.34 is satisfied. Here, the NFW mass parameter and the mass that defines the soliton core is the same, but

concentration can vary untethered by the core's form. The model parameters are sampled over the following flat priors:

$$\begin{aligned} -1 \leq -\log_{10}(1-\beta_a) \leq +1, \\ \log_{10}(5\times10^7) \leq \log_{10}\left(M_{200}/M_\odot\right) \leq \log_{10}(5\times10^{10}), \\ \log_{10}(2) \leq \log_{10}(c_{200}) \leq \log_{10}(120), \\ -1 \leq \log_{10}(m_{22}) \leq 3. \end{aligned}$$

This model represents the simplest (alas unphysical) prescription for the dark matter distribution in a dwarf galaxy.

Model B

A different approach for connecting the soliton core to the outer parts of the halo was proposed in González-Morales et al. [158]. Here, the density of the soliton core is fixed to the density of NFW profile at a transition radius that is governed by a free parameter ϵ. In this definition,

$$\frac{\rho_{\rm soliton}}{[1+(r_\epsilon/r_{\rm sol})^2]^8} = \frac{\rho_{\rm NFW}}{(1+r_\epsilon/r_s)^2(r_\epsilon/r_s)} = \epsilon\rho_{\rm sol}, \tag{3.35}$$

where

$$r_\epsilon = r_{\rm sol}(\epsilon^{-1/8}-1)^{1/2} \tag{3.36}$$

and $r_{\rm sol} = r_c/0.091^{0.5}$ with r_c given by Eq.3.26 (note that Schive et al. [139] formulation is equivalent to the formulation by González-Morales et al. [158] and Marsh and Pop [159]).

The density profile in this model is then

$$\rho_{\rm GM}(r) = \rho_{\rm sol}\begin{cases} \dfrac{1}{[1+(r/r_{\rm sol})^2]^8} & r < r_\epsilon \\ \\ \dfrac{\delta_{\rm NFW}}{(1+r/r_s)^2(r/r_s)} & r \geq r_\epsilon \end{cases} \tag{3.37}$$

where

$$\delta_{\rm NFW} = \epsilon\left[\frac{r_\epsilon}{r_s}\left(1+\frac{r_\epsilon}{r_s}\right)^2\right]. \tag{3.38}$$

The free parameters chosen by `MultiNest` in this model are M_{200}, c_{200}, m_{22}, and ϵ. These parameters are sampled over the flat priors:

$$
\begin{aligned}
-1 \leq -\log_{10}(1-\beta_a) \leq +1, \\
\log_{10}(5\times10^7) \leq \log_{10}\left(M_{200}/M_\odot\right) \leq \log_{10}(5\times10^{10}), \\
\log_{10}(2) \leq \log_{10}(c_{200}) \leq \log_{10}(120), \\
\log_{10}(0.5) \leq \log_{10}(m_{22}) \leq 3, \\
-6 \leq \log_{10}(\epsilon) \leq 1
\end{aligned}
$$

Note that for this halo construction it is possible to choose a halo mass parameter that governs core size but results in a different total mass when integrating out to r_{200}.

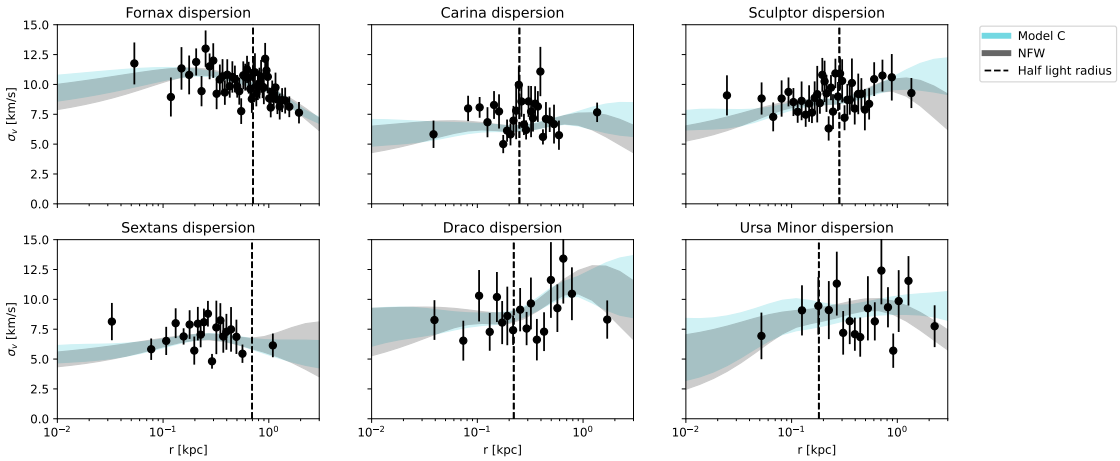

Figure 3.1: Velocity dispersion as a function of radius for the six classical Milky Way Dwarfs. Black points depict binned velocity dispersion measurements (with Poisson error bars). Gray and blue bands represent the 68% unbinned velocity dispersion from the sampled generalized NFW model and the soliton Model C posteriors, respectively. The vertical dashed line shows the half-light radius.

Model C

A more physically motivated formulation of the soliton dark matter profile is proposed by Robles et al. [103]. This formulation connects the inner core of Eq. 3.25 to an outer NFW profile at a transition radius $r_\alpha = \alpha r_c$, where α is found to be $\alpha \approx 3$ (see Schive et al.

[139], Mocz et al. [140]).

$$\rho_{\mathrm{RBBK}}(r) = \begin{cases} \rho_{\mathrm{sol}}(r) & 0 \leq r \leq r_\alpha \\ \rho_{\mathrm{NFW}}(r) & r_\alpha \leq r \leq r_{200}. \end{cases} \tag{3.39}$$

In this model, mass is conserved, and the total mass of a halo is the sum of the mass in the soliton core and the mass of the corresponding NFW profile. In other words,

$$M_{200} = M_{\mathrm{core}} + M_{\mathrm{NFW}}(r_\alpha < r \leq r_\Delta) \tag{3.40}$$

where M_{core} is the total mass contained within the soliton core

$$M_{\mathrm{soliton}} = \int_0^{r_\alpha} \rho_{\mathrm{soliton}} d^3 r. \tag{3.41}$$

Note that we take $r_\alpha = \alpha r_c = 3 r_c$ as before, although this may vary with M_{200} as discussed in Robles et al. [103].

The NFW density profile is given by the generalized NFW Equation 3.24 with $(\alpha, \beta, \gamma) = (1, 3, 1)$, and its shape parameters (ρ_s, r_s) must be solved for using Equations 3.39 and 3.40. Density continuity demands that $\rho_{\mathrm{NFW}}(r_\alpha) = \rho_{\mathrm{core}}(r_\alpha)$, so we can solve for the NFW characteristic density ρ_s,

$$\rho_s = \rho_{\mathrm{core}}(r_\alpha) \frac{r_\alpha}{r_s} \left(1 + \frac{r_\alpha}{r_s}\right)^2. \tag{3.42}$$

To solve for scale radius r_s, we first calculate the mass contained in the outer NFW portion of the halo

$$\begin{aligned} M_{\mathrm{NFW}}(r_\alpha < r \leq r_\Delta) = & \\ &= \rho_s \int_a^b \frac{4\pi r^2}{\left(\frac{r}{r_s}\right)\left(1 + \frac{r}{r_s}\right)^2} dr \\ &= 4\pi \rho_s r_s^3 \left[\frac{r_s(a-b)}{(b + r_s)} + \log\left(\frac{b + r_s}{a + r_s}\right)\right]. \end{aligned} \tag{3.43}$$

Plugging this in to the mass conservation requirement of Equation 3.40, we find an expression that can be used to numerically solve for r_s,

$$\frac{M_\Delta - M_{\mathrm{core}}}{4\pi \rho_{\mathrm{core}}(r_\alpha) r_\alpha^3} = \left(1 + \frac{r_\alpha}{r_s}\right)^2 \left(\frac{r_s}{r_\alpha}\right)^2 \left[\frac{r_s(r_\alpha - r_\Delta)}{(r_\Delta + r_s)(r_\alpha + r_s)} + \log\left(\frac{r_\Delta + r_s}{r_\alpha + r_s}\right)\right]. \tag{3.44}$$

And by varying the values of m_{22} and r_s, we create an interpolation function for the minimum possible halo mass M_{200}^{min} for a given value of m_{22} and wide range of values for r_s.

One important feature of this profile is that not every combination of $\{M_{200}, m_{22}\}$ parameters is valid. This reflects the fact that there is a minimum halo mass set by the core size, which is determined by m_{22} (small halos are not allowed to form because of quantum pressure).

We implement this model in `MultiNest` by sampling over the free parameters with the following flat priors

$$\begin{aligned} -1 \leq -\log_{10}(1-\beta_a) \leq +1, \\ -1 \leq \log_{10}(m_{22}) \leq 3 \\ M_{200}^{\rm min}(m_{22})/M_\odot \leq \log_{10}\left(M_{200}/M_\odot\right) \leq \log_{10}(5\times 10^{10}), \end{aligned}$$

3.4 Observations

For the dwarf galaxies Carina, Fornax, Sculptor and Sextans we adopt the stellar-kinematic data sets of Walker et al. [160]. We refer the reader to Walker et al. [161] for a detailed description of the target selection, observation, and data reduction methods. In order to identify stars that are members of each dwarf galaxy (as opposed to foreground contaminants contributed by the Milky Way), we adopt the membership probabilities estimated by Walker et al. [162], which are derived under the simplifying assumption that the velocity dispersion within each system is constant with projected galactocentric distance. Selecting only those stars having membership probability $> 95\%$, the samples contain 774, 2483, 1365 and 441 probable members of Carina, Fornax, Sculptor and Sextans, respectively.

For Draco and Ursa Minor, we adopt stellar-kinematic data sets of Spencer et al. [163], who include catalogs from multiple literature sources spanning 30 years of observations. Applying the same simple model for distinguishing member stars from foreground contaminants, we obtain a data set containing 692 probable member stars for Draco (341 stars which have multiple observations, that are combined into a single measurement by taking the mean velocity, weighted by the inverse-square of the velocity error) and 680 for Ursa Minor (284 stars that have multiple observations).

For all galaxies, we adopt the half light radii originally published by Irwin and Hatzidimitriou [164]. This research makes use of the VizieR catalogue access tool [165] and was

conducted using computational/visualization resources and services at the Center for Computation and Visualization, Brown University.

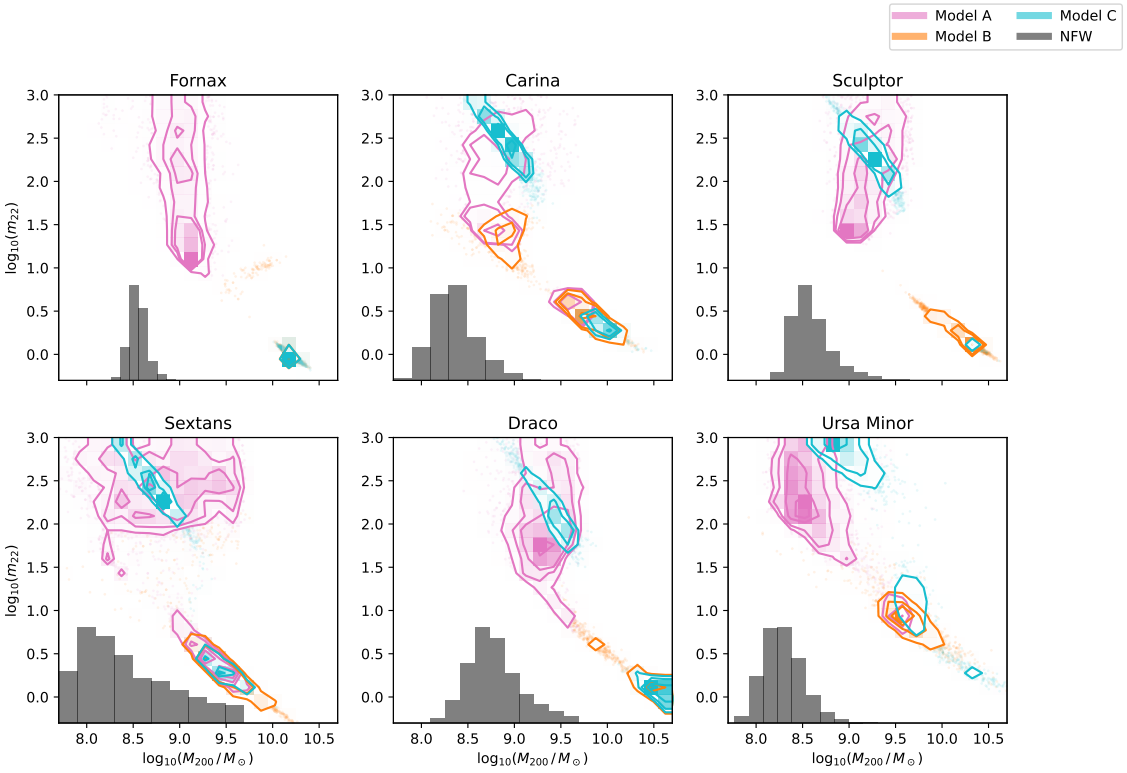

Figure 3.2: Halo mass and m_{22} posteriors for the six Milky Way dwarf galaxies. Pink contours correspond to Model A, orange contours correspond to Model B, and blue contours represent Model C. The gray histogram represents the halo mass posteriors for a generalized NFW profile. Note that Model B's contours in Fornax lie directly under Model C's. This illustrates the anticorrelation between m_{22} and M_{200} – high values of m_{22} require low halo masses, and low values of m_{22} require high halo masses. This result is due to changes in the velocity dispersion anisotropy – see text and Fig. 3.3 for details.

3.5 Results

In Figure 3.1 we show an example of fits to the velocity dispersion data for all six dwarf galaxies. Note that the data shown in Fig. 3.1 is binned (for illustration purposes), but the fits are obtained from the unbinned analysis as described in Section 3.2). We compare the posterior distributions in velocity dispersion of the generalized NFW profile with one of the soliton core profiles, Model C [103]. The reason we choose Model C is because it is the most

physically motivated description, and allows a more direct comparison with the NFW profile as mass is conserved in both cases (the sum of soliton core mass and the mass distributed as NFW in Model C is the same as the total mass of an NFW-only profile). The fits show how the data is most restrictive at the half-light radius, with the outskirts of the halos more unconstrained as expected[3].

Figure 3.2 shows the main result of this chapter. For all dwarf galaxies we find that data allows two distinct regions in the $M_{200} - m_{22}$ parameter space. One requires a low value of m_{22} and high M_{200}, while the other is the opposite, i.e., high values of m_{22} and low M_{200}. The reason is because as halo mass increases, the size of the soliton core gets smaller as $r_c \sim M_{200}^{-1/3}$ and the density is higher as $r_c \sim M_{200}^{4/3}$. In other words, as particle mass increases, quantum effects will become less pronounced and thus the dark matter distribution behaves more classically, and more NFW-like.

This behavior may be related to the same degeneracy that exists between ρ_s and r_s when one fits NFW and/or generalized NFW profiles to dwarf galaxies [166–168]. The origin of such degeneracy is the fact that the Jeans equation is most constraining at the Plummer radius [168]. If all models are then forced to have same mass interior to the Plummer radius, then it is possible to have models with anticorrelated ρ_s and r_s being equally good fits to the data.

There are a few ways to understand why these different regions of the $M_{200} - m_{22}$ parameter space are allowed by the data. One way is to consider the concentration in the distribution of dark matter; a cusped profile will have more mass concentrated in the center as compared to a cored profile of the same total mass, so the total mass for a cored model must increase in order to fit the inner data points.

Another way to understand what drives the fit is to look at the anisotropy (see Section 3.2 as to the physical reasoning of how anisotropy can affect the fit). In Fig. 3.3 we show the m_{22}, M_{200}, and anisotropy posteriors for Model C (shown as a colored scatter plot), as well as M_{200} and anisotropy posteriors for the NFW model (shown as a histogram). It is clear that Model C soliton posteriors tend to have a higher $\log_{10}(1 - \beta_a)$ than NFW[4]. A higher

[3]The other two soliton prescriptions (Model A and Model B [158]) have similar behavior in that regard.
[4]Models A and B have similar behaviour.

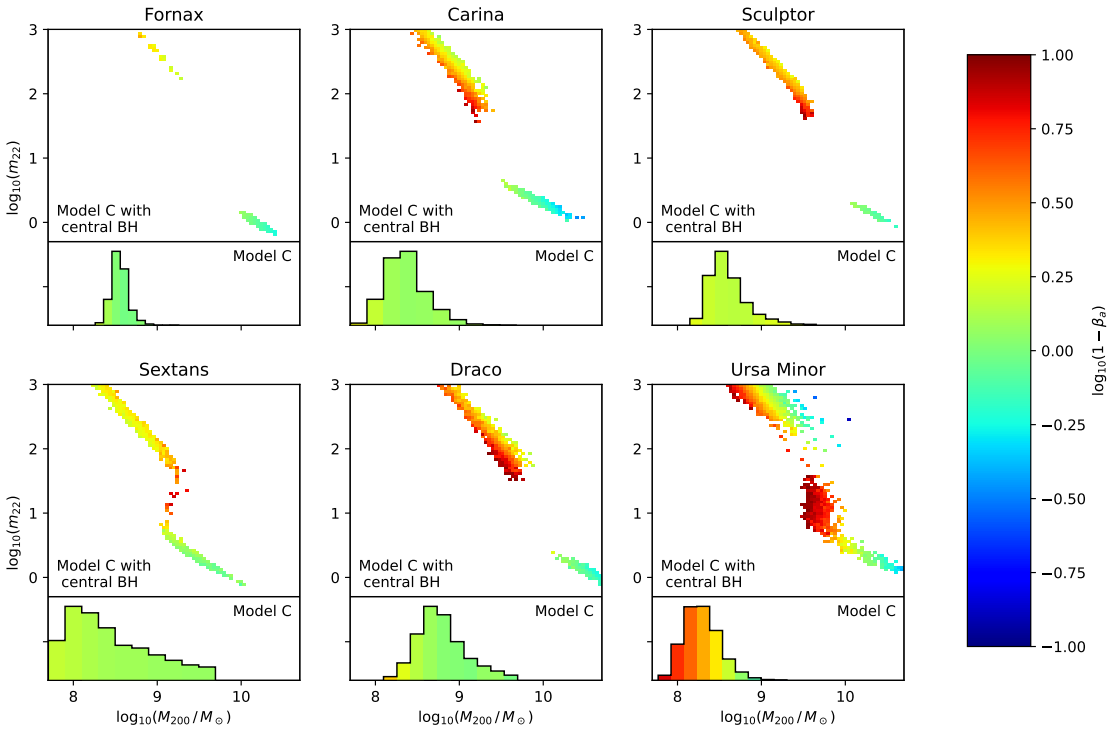

Figure 3.3: Same as Fig. 3.2 but as a posterior scatter plot in the $m_{22} - M_{200}$ parameter space for Model C in all six dwarfs. Color corresponds to the anisotropy parameter. High mass halos that favor $m_{22} \sim 0$ are more radially biased compared to lower mass halos that favor $m_{22} \gtrsim 2$. The histogram corresponds to the mass posterior of an NFW fit to the data, with color corresponding to the average velocity anisotropy in each bin of the histogram.

$\log_{10}(1 - \beta_a)$ means a more tangentially biased halo with lower velocity anisotropy, which causes a suppressed velocity dispersion at low radii. This subtle effect allows models with similar halo mass but different mass distribution and velocity dispersion in the inner radii to both be consistent with data.

A notable feature in Figure 3.3 is a bimodal effect for Model C posteriors, where in addition to high $\log_{10}(1 - \beta_a)$ there is a mode with lower $\log_{10}(1 - \beta_a)$. For models with $\log_{10}(1 - \beta_a) \sim 0$, the velocity dispersion is neither amplified or suppressed. For models with a negative $\log_{10}(1 - \beta_a)$, this corresponds to more radially biased halos (higher β_a), and an amplified velocity dispersion at low radii [61]. As shown in Figure 3.3, these modes also correspond to low m_{22} and high halo mass. As a result, these posteriors fit the velocity

dispersion at low radii well, either because they are cored profiles with high density or the radial anisotropy is radially amplified[5].

Note that if we restrict the maximum limit in the prior of the particle mass to $\log_{10} m_{22} \leq 1.5$, we find similar results as in González-Morales et al. [158], namely a degeneracy between anisotropy and m_{22} (or core size) – lower m_{22} values are preferred when the anisotropy is allowed to be a varying constant instead of fixed at $\beta = 0$. However, when increasing the maximum allowed particle mass to $\log_{10} m_{22} \leq 3$, higher particle masses (and lower core sizes) are also allowed when anisotropy is a varying constant. Therefore, it is not clear that low m_{22} values are a physical outcome of the prior in the anisotropy [158], and instead this effect may be the result of a restrictive prior in m_{22}.

The degeneracy in the $m_{22} - M_{200}$ plane raises a question as to the meaning of halo mass. We can interpret M_{200} as the mass of the halo in the field and before its interaction with the Milky Way. In other words, the mass of the halo today must be less than the mass quoted above. If $m_{22} \sim 0$, then all six dwarfs require that the mass of their host dark matter halo is approximately $M_{200} \sim 10^{9.5-10} M_\odot$. These halo masses are large compared to the masses obtained with NFW fits (see gray histogram in Fig. 3.2). We already know that the most massive dwarfs in the Milky Way are the Large and Small Magellanic Clouds, which means that the six dwarfs as implied here ($m_{22} \sim 0$) are of order $\mathcal{O} \sim 10^{-1}$ the mass of the Large Magellanic Cloud [169].

The question then is whether it is possible for the Milky Way to host at least six dwarf galaxies with masses of order $\mathcal{O} \sim 10^{10} M_\odot$. We can estimate this probability of a dwarf galaxy having a mass of order $\mathcal{O} \sim 10^{10} M_\odot$ by estimating the probability that such halo was formed at some time in the past and it is now part of the Milky Way.

Linear perturbation theory allows such estimate. If a perturbation crosses a critical overdensity threshold, $\delta_{\rm collapse} \approx 1.686$, then the overdensity will virialize and form a halo of mass M at redshift z. The rareness of this fluctuation is encapsulated in the standard

[5]This effect is more pronounced in dwarf galaxies without stars at very low radii. For example in Draco, the inner most star in the unbinned data is ~ 20 pc, as compared to Sculptor with an inner most star at ~ 5 pc.

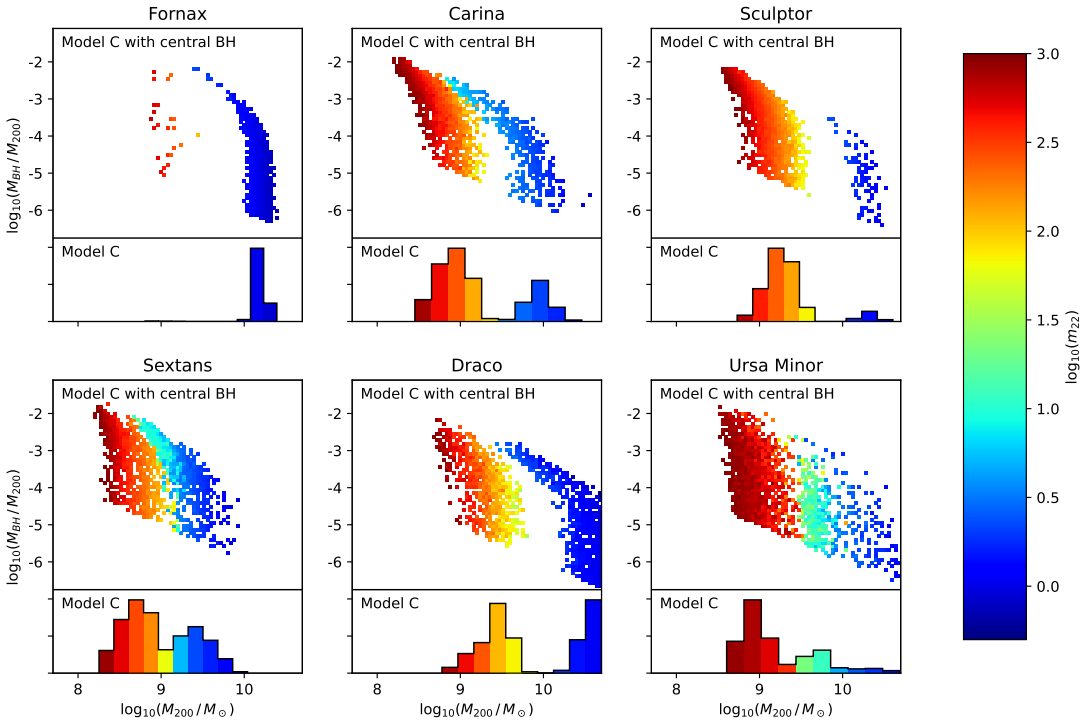

Figure 3.4: Scatter plot of the central black hole posteriors for Model C in the $M_{\rm BH}/M_{200}$ – M_{200} parameter space. Color corresponds to the value of m_{22}. For comparison, the histogram depicts M_{200} posterior for Model C without a black hole. Histogram color represents the average value of m_{22} in a given bin.

deviation of fluctuations that contain a mass M at redshift z.

$$\nu(M_{200}, z) = \frac{\delta_{\rm collapse}}{\sigma(M_{200})\mathcal{D}(z)}, \tag{3.45}$$

where $\sigma(M_{200})$ is the variance on scale M_{200} and $\mathcal{D}(z)$ is the growth factor of linear perturbations, defined such that $\mathcal{D}(z=0) = 1$ [31].

The probability that such object merged with the Milky Way is then obtained by

$$\mathcal{P}(M_{200}, z) = 1 - \Phi[\nu(M_{200}, z)]^{M_{\rm MW}/M_{200}}. \tag{3.46}$$

This formulation accounts for the fact that there are $M_{\rm MW}/M_{200}$ distinct halos that *could* have merged to form the Milky Way (trials factors). The function $\Phi[\nu(M_{200}, z)]$ is the cumulative distribution function of a standard normal distribution (with mean 0 and variance 1), and $\nu(M_{200}, z)$ given by Eq. 3.45.

If we assume $M_{\rm MW} \approx 10^{12} M_\odot$ and $M_{200} \approx 10^{10} M_\odot$ then $M_{\rm MW}/M_{200} \approx 100$, therefore the probability of the Milky Way to have merged with one $10^{10} M_\odot$ object is $P \approx 0.15$ (using $\Omega_M = 0.3$, $\Omega_\Lambda = 0.7$, and $h = 0.7$ in Eq. 3.45). The probability that all six of the dwarfs we study here have originated from a $10^{10} M_\odot$ halo is thus $0.15^6 \approx 10^{-6}$. We therefore conclude that *e*ither m_{22} must be greater than $m_{22} \sim 1$, or that the Milky Way halo is not a typical $10^{12} M_\odot$ halo.

There is however one other possibility for halos to be described with a low m_{22} *a*nd a low M_{200}. And that is the presence of a massive black hole embedded in a soliton core. The physical mechanism that can lead to such objects in dwarf galaxies is highly speculative, but nevertheless it has been considered as a mechanism for generating cored profiles within standard cold dark matter [170]. Such limits have been placed in field dwarf galaxies, as in Reines et al. [171].

Here, we can use the same formalism described in Sections 3.3.1 and 3.3.2 to ask the question whether a Milky Way dwarf galaxy with a soliton core can mimic the velocity dispersion profile of a cusped profile (either described by an NFW profile or by bosonic dark matter with an $m_{22} \sim 10$ or greater.

We can implement this in the `MultiNest` analysis with the addition of a point mass at the center of each dwarf. In both cases, the mass of the black hole is sampled over a flat prior:

$$4 \leq \log_{10}(M_{\rm BH}/M_\odot) \leq 9$$

Figure 3.4 shows a comparison of m_{22}, M_{200}, and $M_{\rm BH}$ posteriors for Model C with a central black hole (shown as a colored scatter plot) to m_{22} and M_{200} posteriors for Model C without a black hole (shown as colored histograms). What is observed at low black hole mass is the two distinct $m_{22} - M_{200}$ regions for low black hole masses. However, as the black hole mass increases, models with low m_{22} and high M_{200} now prefer halos of lower mass. A halo with a black hole of order $\mathcal{O} \gtrsim 10^{-3}$ of the halo mass can have a soliton core with low m_{22}. In other words, by adding a central point mass to a cored profile, it is possible to mimic the effects of a cusped profile (for a similar result but a different analysis in Leo 1 see Bustamante-Rosell et al. [172]).

Given these different models it is illuminating to ask the question whether one model is preferred over another. This can be obtained using the log-likelihood ratio, simply the ratio of the likelihood of one model to the likelihood of another. `MultiNest` is particularly well suited to comparing models; it works by keeping a set of live points sorted by their likelihood, and replacing the lowest point only if the next point drawn has a higher likelihood.

The evidence is the sum of likelihood over the prior volume, which can be calculated efficiently from the live points after convergence. In Figure 3.5 we show the log likelihood ratio $\log(\mathcal{Z}_X/\mathcal{Z}_Y)$ where X and Y are the two models being compared. A log-likelihood ratio of greater than 10 is generally considered to be good evidence preferring one model over the other [173], represented as being outside the shaded purple band. Positive values prefer Model X and negative prefer Model Y.

There is no evidence of one model being preferred over another in most dwarfs, with the exception of Ursa Minor preferring an NFW to the Model C with or without a central black hole. However, Ursa Minor is the dimmest and most irregular of the considered galaxies, with the fewest number of stars, as well as evidence of tidal disruption and so should be not be taken at face value [174, 175]. Note also that even though it is possible to have a central black hole and reasonably low mass halo with low m_{22}, the evidence does not favor the model with a black hole to the model without a black hole.

3.6 Conclusion

In this chapter we explore the viability of ultralight bosons as the dark matter in dwarf galaxies. This is motivated by the large scale properties of the distribution of such dark matter candidates. The formation of a soliton core (on kpc scales) due to quantum pressure has been proposed as a solution to the core/cusp problem in dwarf galaxies [176–179], and other small scale issues in galaxy formation [141].

We use stellar velocity dispersion measurements in six classical Milky Way dwarf galaxies, and employ a Jeans analysis to reconstruct the gravitational potential. The form of the soliton core is a fit to simulations [140, 139] that depends on the boson mass and the halo mass. In the inner parts quantum pressure sets a core which smoothly transitions to an

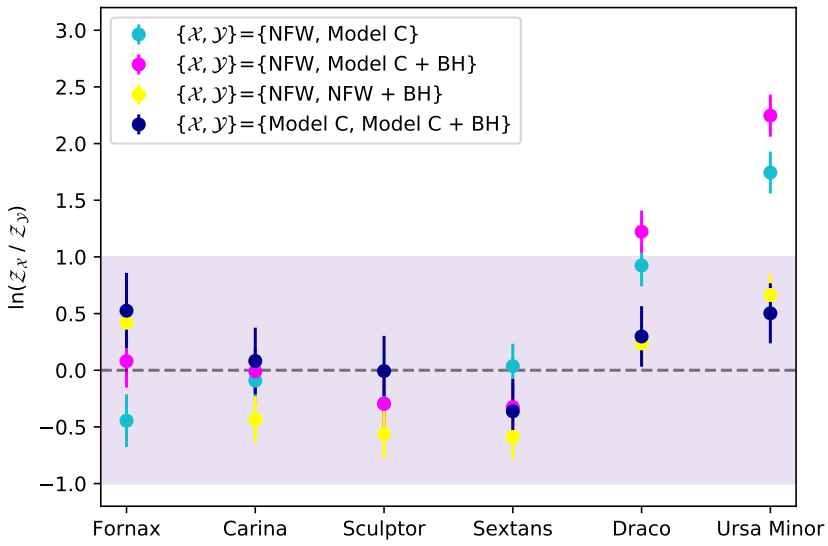

Figure 3.5: Model comparison for the six dwarf galaxies shown as the logarithm of the evidence ratio $\ln(\mathcal{Z}_X/\mathcal{Z}_Y)$. Positive values favor model X, and negative values favor model Y, where X and Y correspond to different models as shown in the legend. Values greater than one, outside of the purple band, are generally considered good evidence. Note that Draco and Ursa Minor have the least number of stars in this sample – see text for details.

NFW-like profile in the outer parts of the halo. We consider four different implementations of the core to NFW-like transition.

We find a multimodal posterior distribution: two distinct anticorrelated regions of particle mass and halo mass. The resulting posteriors show that that there are two allowed regions of the parameter space: low particle masses ($m_{22} \sim 0$) along with high halo masses ($M_{200} \sim 10^{10}$), or high particle masses ($m_{22} \gtrsim 2$, i.e., CDM-like) with lower halo masses ($M_{200} \sim [10^8 - 10^9] M_\odot$), consistent with [102]. This is understood in the context of the velocity anisotropy as shown in Figure 3.3, which can suppress or supplement the velocity dispersion to allow for two regions in parameter space. However taking into consideration the hierarchical merging history of the Milky Way, it is very improbable for a Milky Way size halo to have six $\mathcal{O} \sim 10^{10} M_\odot$ subhalos in addition to the Small and Large Magellanic Clouds. Thus the high mass halos required to have low particle masses are very unlikely.

An alternate viable option for a soliton core to exist in dwarf galaxies is if a black hole is present in the center of the dwarf galaxy. As shown in Figure 3.4, it is possible to have low particle mass with $\mathcal{O} \sim [10^8 - 10^9] M_\odot$ halos with the inclusion of a central black hole with

mass $M_{BH} \sim (10^{-2} - 10^{-3})M_{200}$. This is proportionally a massive black hole in comparison to halo size, especially in context of the black hole and host spheroid mass relationship observed in previous studies (see e.g., [180]). Furthermore, no reliable mechanism through galaxy formation or hierarchical structure formation is known to explain their presence.

Given these models, it is natural then to ask the question whether any of the models is considered favored by the data. Figure 3.5 depicts the evidence, a measure of favorability among any two models. We find that this analysis and with the current state of data there is no appreciable difference between an ultralight bosonic dark matter distribution over cold dark matter, nor does it favor a model with a central black hole over a model without. This holds for all of the classical dwarfs considered, with the exception of Ursa Minor (the most irregular of the considered galaxies, and the one with the least amount of stellar velocity dispersion data).

This work is limited by the assumption that anisotropy is constant for a given system, as opposed to letting it vary with radius. This assumption can be relaxed in two ways: first, one can repeat the aforementioned calculation by allowing anisotropy to vary freely. Alternatively, it may be possible to obtain tangential velocities in the near future. If this observational challenge is accomplished then it will be possible to fully reconstruct the three-dimensional potential without ambiguities arising from assumptions regarding tangential velocities. We plan to address both of these challenging topics in future work.

In summary, we conclude that ultralight bosonic dark matter of mass $m \lesssim 10^{-20}$eV is extremely unlikely in six of the classical Milky Way dwarf galaxies, unless the Milky Way has a very unusual merger history or each dwarf contains a proportionally massive black hole. In lack of evidence for both of these requirements, we constrain the mass of the dark matter particle to be $m \gtrsim 10^{-20}$eV.

CHAPTER 4

Primordial Black Holes in the Gravitational Wave Sky

Though they be mad and dead as nails,
Heads of the characters hammer through daisies;
Break in the sun till the sun breaks down,
And death shall have no dominion.

—Dylan Thomas,
And death shall have no dominion

4.1 Introduction

4.1.1 Primordial Black Holes

Black holes are typically conceived of in the context of stars that can no longer support their own gravity and form a singularity– when the spacetime curvature becomes infinite and not even light can escape, as it is redshifted to infinity. However, stellar collapse is not the only mechanism that could create a black hole. Primordial black holes (PBH) can be created in the very early universe, and can make up a fraction of the dark matter in the universe. There are many mechanisms for the formation of primordial black holes. As discussed in Chapter 2, primordial fluctuations over the Jeans mass will collapse after entering the horizon and source structure formation. Originally it was proposed that if horizon size fluctuations are Gaussian distributed, then PBHs could arise from some of those fluctuations being dense enough to form black holes [181, 182]. Another scenario involves a period of early matter

domination where the universe becomes pressure-less, allowing for collapse. This epoch could be caused by slow reheating after inflation [134, 183] or decays of superheavy particles into non relativistic particles [184]. Other proposals include collapsing fluctuations from a wide variety of inflation models [185, 186], or collapse from cosmic loops [187]. For all of these mechanisms, their mass will be dependent on the horizon size at the time of formation [181] and thus could create a monochromatic mass function (width $\Delta M \approx M_{\rm BH}$), or an extended mass function if formation takes place over a sufficiently long period of time.

Regardless of the formation mechanism, PBHs are of interest to study as possible explanations for astrophysical phenomena [188–191], as objects where Hawking radiation could have significant effects, as binary merger objects in LIGO/VIRGO gravitational wave observations, or as a dark matter candidate. The parameter space for PBHs comprising 100% of dark matter is tightly constrained especially $\sim M_\odot$ PBHs, but it is still possible for them to make up a significant fraction of the dark matter if they are at mass $(\sim 10^{16} - 10^{17})g$ [192, 193]. For them to still exist in the present day with a monochromatic mass spectrum there is a lower limit of $\sim 5 \times 10^{14}$g, as any lighter PBHs would have evaporated away [194]. Additional constraints can be found through gravitational lensing, microlensing, dynamical effects in wide binaries and globular clusters, and large scale structure [192].

4.1.2 Gravitational Waves

To understand the basic derivation of a gravitational wave, let's begin with a linear perturbation around flat space [195]

$$g_{\mu\nu} = \eta_{\mu\nu} + h_{\mu\nu} \tag{4.1}$$

where $\eta_{\mu\nu}$ =diag$(-1, 1, 1, 1)$ is the Minkowski metric for flat space and $|h_{\mu\nu}| \ll 1$. We can then expand Einstein's equations of motions to first order in $h_{\mu\nu}$, in what is called linearized theory using the weak field approximation. The Riemann tensor to linear order becomes

$$R_{\mu\nu\rho\sigma} = \frac{1}{2}(\partial_\nu\partial_\rho h_{\mu\sigma} + \partial_\mu\partial_\sigma h_{\nu\rho} - \partial_\mu\partial_\rho h_{\nu\sigma} - \partial_\nu\partial_\sigma h_{\mu\rho}), \tag{4.2}$$

from which we can write down the Ricci curvature tensor and Ricci scalar,

$$\begin{aligned} R_{\mu\nu} &= \frac{1}{2}\left(\partial_\mu\partial_\lambda h^\lambda_\nu + \partial^\lambda\partial_\nu h_{\mu\lambda} - \partial_\mu\partial_\nu h - \Box h_{\mu\nu}\right) \\ R &= \partial_m u \partial_\nu h^{\mu\nu} - \Box h \end{aligned} \tag{4.3}$$

and the Einstein equations Equation 1.5, taking Λ to equal zero becomes

$$\begin{aligned} G_{\mu\nu} &= R_{\mu\nu} - \frac{1}{2}g_{\mu\nu}R \\ &= \Box\overline{h}_{\mu\nu} + \eta_{\mu\nu}\partial^\rho\partial^\sigma\overline{h}_{\rho\sigma} - \partial^\rho\partial_\nu\overline{h}_{\mu\rho} - \partial^\rho\partial_\mu\overline{h}_{\nu\rho} \\ &= -\frac{16\pi G}{c^4}T_{\mu\nu}, \end{aligned} \tag{4.4}$$

where $\Box$ is the flat space d'Alembertian $\Box = \eta_{\mu\nu}\partial^\mu\partial^\nu = \partial_\mu\partial^\mu$ and we can define

$$\overline{h}_{\mu\nu} \equiv h_{\mu\nu} - \frac{1}{2}\eta_{\mu\nu}h \tag{4.5}$$

with h being the contraction $h \equiv \eta^{\mu\nu}h_{\mu\nu}$. In an analog to the Lorentz gauge in electromagnetism, $\partial_\mu A^\mu = 0$, we can choose the Lorentz gauge $\partial^\nu\overline{h}_{\mu\nu} = 0$ and Equation 4.4 simplifies to

$$\Box\overline{h}_{\mu\nu} = -\frac{16\pi G}{c^4}T_{\mu\nu}. \tag{4.6}$$

This is a wave equation, and implies that a perturbation in flat space can create a gravitational wave. If we are observing from outside the source, $T_{\mu\nu} = 0$, Equation 4.6 becomes $\Box\overline{h}_{\mu\nu} = 0$. Notice that since $\Box = -(1/c^2)\partial_t^2 + \nabla^2$, this also implies gravitational waves travel at the speed of light.

Following the analogy with electromagnetic radiation, it's natural to then ask about the energy radiated in gravitational waves. The radiation can be decomposed into multipoles, but unlike electromagnetism, in a low velocity expansion the leading nonzero term is the quadrupole [195]. Define the quadrupole moment

$$Q^{ij} = \int d^3x \frac{1}{c^2}T^{00}\left(x^i x^j - \frac{1}{3}r^2\delta^{ij}\right) \tag{4.7}$$

where $r = |\mathbf{x}|$ and T^{00}/c^2 can be identified as mass density to the lowest order of v/c. Then the total radiated power is

$$\frac{dE}{dt} = \frac{G}{5c^5}\left\langle \frac{d^3Q_{ij}}{dt^3}\frac{d^3Q_{ij}}{dt^3}\right\rangle \tag{4.8}$$

for $\frac{d^3Q_{ij}}{dt^3}$ evaluated at the retarded time $t - r/c$.

As a gravitational wave propagates, spacetime is distorted a very small but measurable amount. In an observer's frame, this has the effect of changing distances between points on a plane perpendicular to the direction of propagation. This effect can be measured with a Michelson Interferometer [196]. The first detection of a gravitational wave was in 2015, by the Laser Interferometer Gravitational Wave Observatory (LIGO) [197] and since then, many more events have filled the gravitational wave sky. The number of gravitational wave events observed as of the writing of this thesis is 90 [198]. The catalog of black holes and neutrons stars observed as of 2020 is shown in Figure 4.1. An important feature to note is the mass gap– the sparsely populated region between approximately $2.4M_\odot$ and $5M_\odot$ that is heavier than the observed upper limit for neutron star masses [199, 200] and the observed lower limit for stellar collapse black holes [201]. Observations of objects in that mass gap are immediately suspicious, and in particular observations of black holes $< 5M_\odot$ would be an indicator of new physics, either in the formation of stellar black holes or in new ways to form black holes like primordial black holes.

4.2 Could the $2.6M_\odot$ object in GW190814 be a primordial black hole?

In recent years high precision cosmological and astrophysical observations have established ΛCDM as the Standard Cosmological Model [58]. However one of its main components, dark matter, has only been observed through gravitational effects and thus its exact nature remains illusive. Direct and indirect detection experimental searches [202, 203, 64, 204–206, 66, 207–212] as well as the Large Hadron Collider [213–215] have been unsuccessfully searching for a Weakly Interacting Massive Particle (WIMP) as a dark matter candidate. The most recent observed anomaly detected in the XENON1T experiment does not match the required characteristics [216, 217] (however for a possible explanation see [218]), while the parameter space of other popular particle candidates such as axion dark matter is shrinking [219, 220]. Other astrophysical candidates alternative to the particle hypothesis such as dark matter in the form of Massive Compact Halo Objects (MACHOs) have been considered, however they are also heavily constrained from microlensing experiments [221, 222].

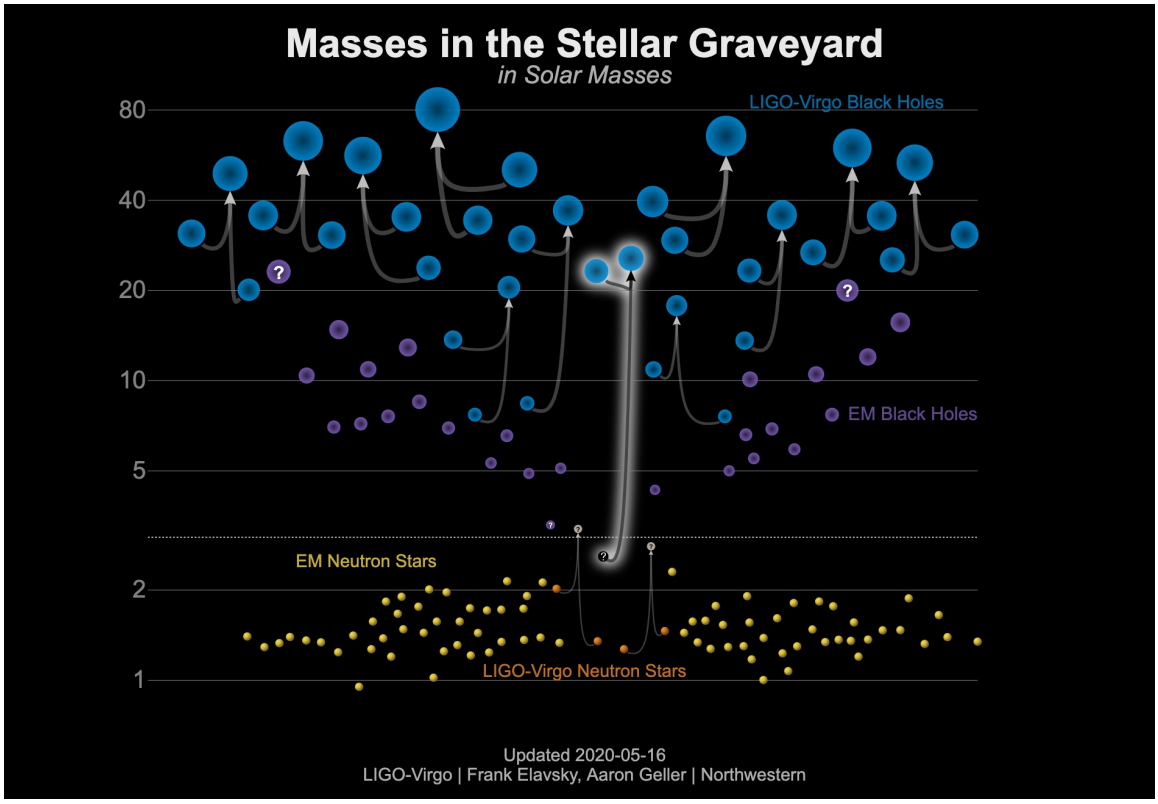

Figure 4.1: A graphic of detected black holes and neutron stars, with gravitational wave observations by LIGO/Virgo. Blue objects are black holes measured with gravitational waves, purple are black holes measured with electromagnetic observations, orange are neutron stars measured with gravitational waves, and yellow are neutron stars measured with electromagnetic observations. The highlighted event is GW190814. Courtesy Caltech/MIT/LIGO Laboratory.

In light of gravitational wave detections by the LIGO Collaboration [223] originating from binary black hole mergers with masses of about $30M_\odot$ another dark matter candidate possibility resurfaced: primordial black holes (PBHs) formed in the early universe prior to Big Bang Nucleosynthesis [181, 224, 182]. The possibility that LIGO has already detected dark matter in the form of $30M_\odot$ PBH mergers is investigated in [225], and a wealth of other work has been done on the merger rate of PBHs [226–230]. These black holes can span numerous orders of magnitude in mass but, similarly to MACHOs, their parameter space has been heavily constrained [192] though a combination of microlensing at lower masses [231–233, 222], Cosmic Microwave Background (CMB) experiments [234, 235], and dynamical effects in Milky Way dwarf galaxies [236–238].

Despite that, there are still three windows for PBH masses in which PBHs can make up $[1-10]\%$ of the dark matter energy budget [193] and thus they remain an interesting option for further investigations, $[10^{16}-10^{17}]$g, $[10^{20}-10^{24}]$g, and $[1-10^{2}]M_{\odot}$. [192] However it's important to note that these constraints typically assume a monochromatic PBH mass function as it is possible that a continuum distribution of masses can be established at formation [239–243].

Recently the LIGO-Virgo collaboration announced the discovery of GW190814 [244], a gravitational wave event originating from a binary system merger with a very small ratio of masses $M_2/M_1 = 0.112^{+0.008}_{-0.009}$. The primary component was identified as a black hole of mass $M_1 = 23.2^{+1.1}_{-1.0}M_{\odot}$ while the secondary object is unidentified with a mass of $M_2 = 2.59^{+0.08}_{-0.09}M_{\odot}$. This event is surprising for two reasons; this is the most asymmetrical binary mass ratio to date and the secondary object's mass lies within the so called "low mass gap". This gap between $\sim 2-5M_{\odot}$ owes to a complete lack of observations, in gravitational and electromagnetic waves, of black holes with mass less than $5M_{\odot}$ or neutron stars with mass above $\sim 2M_{\odot}$ [245–247] which are backed by the fact that current accepted stellar evolutionary models are not able to predict compact objects in that mass range, depending on the progenitor explosion mechanism [248]. Thus if we interpret this event as a new category of binary system mergers the derived merger rate is between $1-23$ Gpc^{-3}yr^{-1}.

Any attempts to explain this relatively high rate struggle to do so within standard astrophysical and cosmological models. As discussed in [244] and in more detail in [249], this observation challenges most results obtained from population synthesis simulations for isolated binaries. The observed rate cannot be explained by dynamical arguments [250] nor a low-mass merger remnant that acquires a BH companion via dynamical interactions in dense environments due to the lack of mass segregation of neutron stars [251]. Other proposals include that this event was subject to gravitational lensing as discussed in [252], accretion of supernova ejecta mass from a neutron star formation that remained bound in a binary system [253], mergers in wide hierarchical quadruple systems [254]. This uncertainty in the predicted rates opens up the possibility that GW190814 is the result of a previously unknown population of mergers. There have also been several analysis considering the possibility that the $2.6M_{\odot}$ object is a neutron star, with resulting constraints on the neutron star equation

of state or exotic degrees of freedom [255–260].

Here, we investigate the possibility that the $2.6M_\odot$ object in GW190814 is a primordial black hole. Such an explanation to GW190814 requires knowledge of the merger rate of stellar mass black holes with primordial black holes, while the dynamics of the formation and merger of such binaries is regulated by the formation rate of heavy stellar mass black holes.

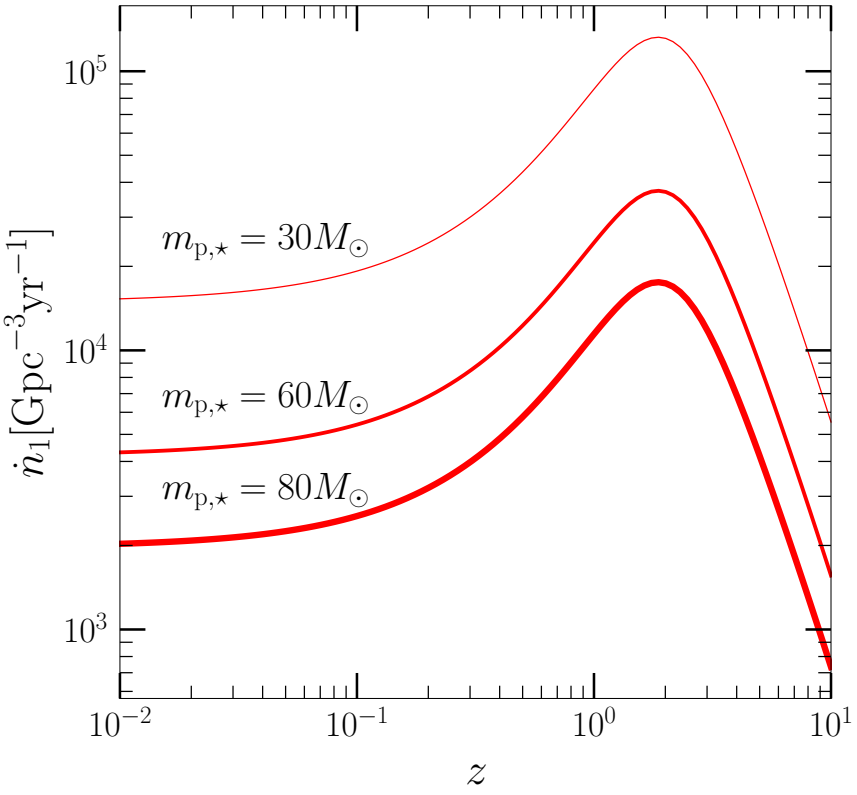

Figure 4.2: The formation rate of $23M_\odot$ black holes, under the maximal assumption that every star with mass greater than $m_{p,*}$ will produce a $23M_\odot$ black hole. The thin, medium and thick curves correspond to $m_{p,*} = [30M_\odot, 60M_\odot, 80M_\odot]$ respectively.

4.2.1 Primordial Black Hole – Stellar Black Hole Merger Rate

We would like to characterize the probability of a $2.6M_\odot$ primordial black hole merger with a $23M_\odot$ stellar remnant. Our plan is to first describe the rate density for such an event and by comparing it with the observed rate density obtained from GW190814 we will be able to assess its probability. In what follows, we will use "2" as a subscript that denotes primordial black holes (e.g., of mass $2.6M_\odot$), and "1" a subscript that denotes a compact

stellar remnant (e.g., a black hole of mass $23M_{\odot}$).

The merger rate between a primordial black hole and a stellar remnant can then be written as

$$\mathcal{R} = \int \mathcal{P}\, \dot{n}_1(z)\, n_2(z)\, \frac{dV}{dz} \frac{dz}{1+z}. \tag{4.9}$$

The rate as given in Equation 4.9 has units of merger events per year per volume, n_2 corresponds to the number density of primordial black holes, $\dot{n}_1$ is the number density of stellar remnant formation at z per unit time, and dV/dz is the cosmological volume element. The factor of $1+z$ in the denominator ensures proper conversion between comoving and physical time intervals.

The quantity $\mathcal{P}$ describes the probability of such a merger to occur. In some ways one may think of $\mathcal{P}$ as a dimensionless “cross section" for such an interaction. It encapsulates all the assumptions and uncertainties that stem from our lack of knowledge of the precise physics that drives such a processes. For example a primordial black hole and a stellar origin black hole will become bound if during weak gravitational scattering the energy loss brings the total energy of the system below the initial kinetic energy of the pair. This process depends on the number density and velocity distribution of black holes. Once the pair is bound, it will take some time, τ, for gravitational wave emission to dissipate the orbital energy of the system and lead to the merger of the two black holes. If during that time, a third black hole interacts with the system then the binary will harden faster with the ejection of the lightest black hole. The quantity $\mathcal{P}$ in Equation 4.9 qualitatively captures the net probability of the merger, and therefore can be used to assess the potential of a merger between a $2.6M_{\odot}$ primordial black hole and a $23M_{\odot}$ black hole of stellar origin.

We will now describe each term that enters in the rate calculation. The number density of primordial black holes of mass M_2 at redshift z can be expressed as

$$n_2(z) = f_2 \frac{\rho_{\rm DM}}{M_2} \tag{4.10}$$

$$= f_2 \Omega_M (1+z)^3 \frac{\rho_{\rm crit}}{M_2}, \tag{4.11}$$

With Ω_M taken to be $\Omega_M = 0.3$. The quantity f_2 is the fraction of the dark matter density in the form of primordial black holes. This fraction is heavily constrained by a swarm of

observational arguments [231, 192, 234, 193], but in general, around $M_2 \approx 2.6M_\odot$, f_2 is less than 1%.

It is important to note that by writing Equation 4.11 in this fashion we make the implicit assumption of a monochromatic distribution of primordial black hole masses (of $M_2 \approx 2.6M_\odot$). If instead we assume a spectrum of masses then the abundance at any given mass will be lower as compared to the monochromatic case. In addition, the number density of primordial black holes in Equation 4.11 is set by the mean dark matter density. This acts as a lower bound because the origin of merger events such as GW190814 is most likely in dark matter dense environments (galactic halos) that imply a higher number density of primordial black holes (e.g., the mean dark matter density of a dark matter halo is ~ 200 times the mean density of dark matter we assume in Equation 4.11.

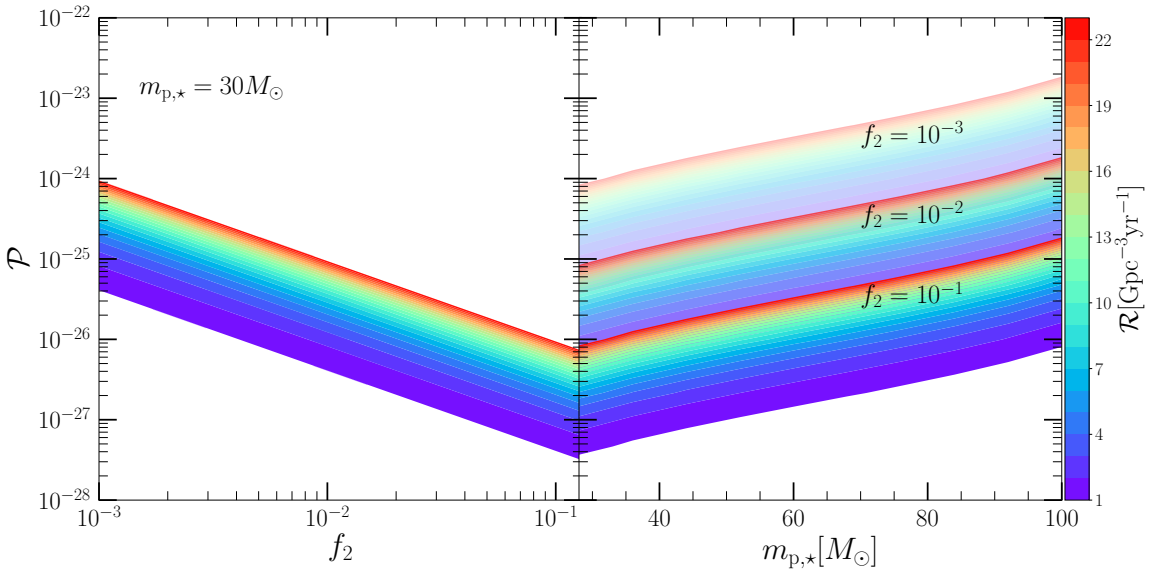

Figure 4.3: Event rate $\mathcal{R}$ of $2.6M_\odot$ primordial black holes with $23M_\odot$ stellar black hole in the $\mathcal{P} - f_2$ (left) and $\mathcal{P} - M_p^{\rm min}$ (right) parameter space. The color coding corresponds to the derived rate from GW190814.

We can obtain the number density of $23M_\odot$ stellar origin black holes in the following way. Assume that the progenitors of such black holes are massive stars whose formation rate is given by the cosmic star formation rate, $\psi(z)$, obtained from observations of star forming galaxies out to high redshift [261],

$$\psi(z) = 0.015 \frac{(1+z)^{2.7}}{1 + [(1+z)/2.9]^{5.6}} {\rm M_\odot yr^{-1} Mpc^{-3}}. \tag{4.12}$$

The mass converted to stars of mass m at redshift z is distributed according to a Salpeter-like [262] mass function rate density,

$$\xi'(m,z) = \frac{dN}{dV\,dt\,d\ln m} \sim m^{-1.35} \tag{4.13}$$

We can normalize the mass function at each redshift by requiring that the integral of the rate density of formation over all stellar masses is given by the star formation rate, i.e, $\psi(z) = \int \xi'(m,z)\,dm$, where the limits of integration are from $0.08M_\odot$ to $120M_\odot$. We assume conservatively that the mass function is independent of redshift (metallicity can change the slope of the Salpeter mass function) – a shallower power law mass function on small scales (e.g., Kroupa [263]) increases the abundance of high mass stars if normalized the same way, and thus make the presented arguments even more stringent. With this formalism, the number density rate of stellar progenitors with mass greater than $m_{\mathrm{p},\star}$ (and up to $m_{\mathrm{p,max}} = 120M_\odot$) is then

$$\dot{n}_\star(z) = \int_{m_{\mathrm{p},\star}}^{m_{\mathrm{p,max}}} \frac{\xi'(m,z)}{m}\,dm. \tag{4.14}$$

We interpret $\dot{n}_\star$ as the rate of formation of stellar progenitors whose stellar remnant is a $23M_\odot$ black hole.This is a maximal assumption as every star whose mass is greater than $23M_\odot$ will produce a $23M_\odot$ black hole. Under this assumption, the number density rate $\dot{n}_2$ of black holes of mass $23M_\odot$ available to merge with a primordial black hole is $\dot{n}_1 = \dot{n}_\star$. Figure 4.3 shows the redshift dependence of the formation rate of $23M_\odot$ black holes from heavier stellar progenitors. The shape of this function is set by the star formation rate, Equation 4.12 (peaking at $z \approx 2$), while the amplitude of the function is set by the initial mass function of stellar masses, Equation 4.13. Finally an important caveat is that only stars with metallicities less than $0.1Z_\odot$ would be able to produce a black hole remnant of the required mass which subsequently reduces $\dot{n}_1$ [264].

4.2.2 Results

The LIGO observation of GW190814 provides an estimate of the merger rate of $23M_\odot$ black holes with $2.6M_\odot$ compact objects. This observed rate is $\mathcal{R}_{\mathrm{obs}} = [1-23]\mathrm{Gpc}^{-3}\mathrm{yr}^{-1}$. In order to assess the probability that the $2.6M_\odot$ object is a primordial black hole, we set

the merger rate of Equation 4.9 equal to the observed rate, i.e., $\mathcal{R} = \mathcal{R}_{\rm obs}$, and then find the values of $\mathcal{P}$ and minimum progenitor mass $m_{\rm p,\star}$ that can satisfy the equality.

Figure 4.3 shows the results of this calculation. We find that if all stars with masses greater than $30M_\odot$ produce $23M_\odot$ black holes then the probability of LIGO GW190814 being due to the merger of a $23M_\odot$ black hole with a $2.6M_\odot$ primordial black hole is between $10^{-27} < \mathcal{P} < 10^{-23}$ for $10^{-3} \leq f_2 \leq 10^{-1}$. The largest the f_2 the smaller $\mathcal{P}$ is to maintain the same rate, while for larger $m_{\rm p,\star}$ it needs to increase to accommodate the smaller number of stellar black holes available.

To interpret this result we need to characterize the physical meaning behind $\mathcal{P}$. The terms in Equation 4.9 (aside from $\mathcal{P}$) give all pairs of primordial and stellar black holes per volume per time. Therefore $\mathcal{P}$ acts as a filter of how many of those black holes are in binaries, and of those how many would have merged per redshift interval. We can parameterize $\mathcal{P}$ as

$$\mathcal{P} = \left(\frac{N_{\rm binary}}{N_{\rm total}}\right)\left(\frac{t_u - \tau}{t_u}\right) \tag{4.15}$$

where $N_{\rm binary}/N_{\rm total}$ is the fraction of objects in binary systems, t_u is the age of the universe, τ is the mean duration between the formation of the stellar black hole, the time to form the binary system and the time it takes for it to merge. In other words, the second term in Equation 4.15 quantifies how many of the binaries would have merged in the lifetime of the universe. A value of $\tau = 0$ means that merging is instantaneous after formation and all the binary systems would have merged. On the other hand a value of $\tau = t_u$ means that no binary system would have enough time to merge by today.

Let's consider the limiting case for which the timescale of the formation and merging of the binary is much less than the age of the universe and thus $\tau \sim 0$. The derived value of $\mathcal{P}$ in this case is just the fraction of primordial black holes in binaries needed to explain the observed rate. Here, the smallness of this number ($\mathcal{P} \approx [10^{-27} - 10^{-23}]$) is extremely important – it implies (unrealistically) that less than one primordial – stellar mass black hole merger is needed in order to satisfy the requirements in the observed cosmological volume of LIGO, $V_{\rm LIGO}$.

The observation of one event requires *at least one* of all the primordial black holes in $V_{\rm LIGO}$ to have formed a binary. Therefore, $\mathcal{P}$ is limited by a minimum value $\mathcal{P}_{\rm min} = 1/(n_2 V_{\rm LIGO})$,

and as a consequence, Equation 4.9 limits the rate to a minimum value $\mathcal{R}_{\rm min}$. This lower bound on the rate depends only on the formation rate of the stellar remnant partner and cannot be modified by adjusting parameters for the primordial black hole population. In other words, the minimum rate $\mathcal{R}_{\rm min}$ is set *only by the rate at which* $23M_\odot$ *black holes become available.*

However there is an important caveat in this case. For example if $m_{\rm p,\star} = 30M_\odot$, $\mathcal{R}_{\rm min}$ is of order $10^5 {\rm Gpc}^{-3}{\rm yr}^{-1}$ (see Figure 4.3) which would immediately exclude the possibility of the $2.6M_\odot$ being a primordial black hole since $\mathcal{R}_{\rm min}$ is 4-5 orders of magnitude larger than the observed rate. In order to get around this obstacle, these 5 orders of magnitude must be attributed to the probability of forming such a system realistically and not instantaneously as previously assumed.

In this particular example we can relax the assumption that $\tau \sim 0$ by setting $(t_u - \tau)/t_u \sim 10^{-5}$, and derive bound limits for the mean duration between forming a binary system and when the system merges, as $t_u \geqslant \tau \geqslant \tau_{\rm min}$, where $\tau_{\rm min} = (1 - 10^{-5})t_u$. This lower limit, $\tau_{\rm min}$, is set by the value $m_{\rm p,\star}$ because of the dependence of $\mathcal{R}_{\rm min}$ on the stellar black holes formation rate $\dot{n}_1$. The larger $m_{\rm p,\star}$ is, the fewer stars and thus stellar black holes are created, reducing $\mathcal{R}_{\rm min}$ and allowing for smaller values of τ while maintaining the observed rate.

Note that $N_{\rm binary}/N_{\rm total}$ doesn't have to be necessarily at its minimum value; there may be more than one such binary system in $V_{\rm LIGO}$. As $N_{\rm binary}/N_{\rm total}$ approaches its maximum value of N_1/N_2, the requirement to maintain the observed rate has to be accounted for by reducing the temporal factor in $\mathcal{P}$. This argument further limits $\tau_{\rm min}$ to values even closer to the age of the universe. One way to relax that constraint would be by lowering the value of N_1 using the fact that only stars with metallicities less than $0.1Z_\odot$ would be able to produce a black hole remnant of the required mass [264]. However, given that n_2 is extremely large (the MW contains of order 10^9 primordial black holes if we assume $f = 0.01$) a reduction in n_1 by even few orders of magnitude will have negligible effect on the results.

4.2.3 Conclusions

We investigated the plausibility of a primordial black hole origin of the secondary object in GW190814. We found that even if primordial black holes account for at most one percent

of the dark matter in the universe, the abundance of primordial black holes leads to an observed rate that highly exceeds the observed rate of such LIGO events. In other words, the large number of primordial black holes imply that *as long as stellar progenitors produce a $23M_\odot$ black hole, it is guaranteed that at least one merger event will take place within a Hubble time.*

More specifically, we showed that if at least one merger event takes place between a primordial black hole and a stellar origin black hole within the LIGO volume implies that the time it takes for the formation of the stellar mass black hole, the capture to a binary and the subsequent inspiral and merger with a primordial black hole must be very close to the age of the universe, $\tau \geq \tau_{\rm min} = (1 - 10^{-5})t_u$. This is a hard bound, as any smaller value of $\tau_{\rm min}$ would give rise to a higher merger rate than what has been observed with LIGO. In other words, if such merger events can occur on faster timescales the merger rate will be higher than observed. However the observation of GW190814 suggests that such a merger did take place on a timescale $t(z = 0.053) \approx 12.97{\rm Gyr} < \tau_{\rm min}$, contradicting our findings.

Therefore to summarize, the large abundance of $\mathcal{O}(20)M_\odot$ stellar origin black holes inferred from the LIGO merger events of such black holes, together with the observed redshift of GW190814 suggest that a primordial black hole origin of the secondary component of GW190814 is rather unlikely.

CHAPTER 5

Concluding Thoughts

And remember, "Patience, Patience," is the watchword of a sage,
Not to-day nor yet to-morrow can complete a perfect age.

—Sarah Williams, *The Old Astronomer*
Twilight Hours: A Legacy of Verse (1868)

In this thesis, I use a Jeans kinematic analysis and gravitational waves to study the viability of dark matter models that are alternatives or complements to Cold Dark Matter: ultralight bosonic dark matter, and primordial black holes.

Ultralight bosonic dark matter is a boson of mass $m \sim 10^{-22}$ eV, a scale light enough for quantum pressure to form a core in the DM density profile on kpc scales. Using stellar velocity dispersion measurements in six classical Milky Way dwarf galaxies, I utilize a Jeans kinematic analysis to reconstruct gravitational potentials and compare how well an ULDM model versus CDM model fits the data. The posterior distribution for ULDM is multimodal with two distinct and anticorrelated regions in particle mass and halo mass. Low particle mass ($m \sim 10^{-22}$eV) and high halo mass ($M_{200} \sim 10^{10}$) or high particle mass ($m \geq 10^{-20}$ eV, CDM-like) with lower halo mass ($M_{200} \sim [10^8 - 10^9]M_\odot$).

Taking into consideration the hierarchical merging history of the Milky Way, it is very unlikely for a Milky Way sized halo to host six subhalos of mass $\sim 10^{10}M_\odot$ along with the Small and Large Magellanic Clouds. Thus it is very unlikely that the dwarf galaxies are of sufficiently high mass to be consistent with particle masses on the order of 10^{-22}eV.

Another possibility allowing low particle mass and low halo mass is the presence of a central black hole of mass $M_{BH} \sim (10^{-2} - 10^{-3})M_{200}$. This is a proportionally massive

black hole. Consider Draco as an example: for a $10^{9.5} M_\odot$ halo and $\sim 10^{-22}$eV particle to be feasible, the central black hole would have to be $\sim 10^{6.5} M_\odot$. Observations of disc galaxies with a central bulge show a relationship between central spheroid and central black hole mass. If we assume the mass of the entire dwarf halo to be equivalent to the mass of the bulge and assume that this relationship holds, you would expect to see a black hole approximately an order of magnitude lighter [180].

Ultimately, none of these models are found to be significantly favored in comparison to each other or CDM. The exception is CDM being favored over ULDM (with or without a central black hole) in Ursa Minor, the most irregular of the considered galaxies, and the one with the least amount of stellar velocity dispersion data.

This work is limited by the assumption of a spherical system, which breaks down in the more irregular Ursa Minor, and in the assumption of a transition from soliton core to outer NFW at three times the characteristic radius. This is a simplification that could be more accurately dealt with by allowing it to vary as a model parameter, or with the halo mass [103]. Velocity anisotropy is also assumed to be constant. This can be relaxed in two ways: first, repeating the calculation while allowing anisotropy to vary with radius. Alternatively, it may be possible to obtain tangential velocities in the near future. If this observational challenge is accomplished then it will be possible to fully reconstruct the three-dimensional potential without ambiguities arising from assumptions regarding tangential velocities. This work can be done in follow up studies.

GW190814 is a gravitational wave event detected on August 14th, 2019 by the LIGO-Virgo collaboration. It was a binary system merger between a black hole of mass $M_1 = 23.2^{+1.1}_{-1.0} M_\odot$ and an unidentified object with a mass of $M_2 = 2.59^{+0.08}_{-0.09} M_\odot$. I investigate the possibility that the $2.6 M_\odot$ object is a primordial black hole. Primordial black holes could make up a fraction of the universe's dark matter; this object is a candidate as it would either be the heaviest neutron star or lightest black hole observed to date. The calculations show that even if primordial black holes account for at most one percent of the dark matter in the universe, the abundance of primordial black holes leads to an observed rate that highly exceeds the observed rate of such LIGO events. In other words, the large number of primordial black holes imply that as long as stellar progenitors produce a $23 M_\odot$ black hole, it is guaranteed

that at least one merger event will take place within a Hubble time. Therefore to summarize, the large abundance of $\mathcal{O}(20)M_{\odot}$ stellar origin black holes inferred from the LIGO merger events of such black holes, together with the observed redshift of GW190814 suggest that a primordial black hole origin of the secondary component of GW190814 is rather unlikely.

Future work can build off of this thesis directly, by relaxing the assumptions and making a more realistic but complex calculation. It could also build from the theory and techniques used here; the physics behind dynamics in combination with merger rates is a powerful tool for studying dark matter through the lens of visible light and gravitational waves. Ultimately, there are many dark matter models still in contention. And while some techniques for investigating them through gravity have existed since the discovery of DM, we are in an era of rapidly expanding observational data and techniques. The completion of missions like Gaia, upgraded LIGO/Virgo, and the Vera Rubin Observatory in the coming years will bring a plethora of data we can use to illuminate the dark universe.

Bibliography

[1] S. Riemer-Sørensen, S. Kotuš, J. K. Webb, K. Ali, V. Dumont, M. T. Murphy, and R. F. Carswell. A precise deuterium abundance: remeasurement of the z = 3.572 absorption system towards the quasar PKS1937-101. *Mon. Not. R. Astron. Soc.*, 468 (3):3239–3250, July 2017. doi: 10.1093/mnras/stx681.

[2] Planck Collaboration, N. Aghanim, Y. Akrami, F. Arroja, M. Ashdown, J. Aumont, C. Baccigalupi, M. Ballardini, A. J. Banday, R. B. Barreiro, N. Bartolo, S. Basak, R. Battye, K. Benabed, J. P. Bernard, M. Bersanelli, P. Bielewicz, J. J. Bock, J. R. Bond, J. Borrill, F. R. Bouchet, F. Boulanger, M. Bucher, C. Burigana, R. C. Butler, E. Calabrese, J. F. Cardoso, J. Carron, B. Casaponsa, A. Challinor, H. C. Chiang, L. P. L. Colombo, C. Combet, D. Contreras, B. P. Crill, F. Cuttaia, P. de Bernardis, G. de Zotti, J. Delabrouille, J. M. Delouis, F. X. Désert, E. Di Valentino, C. Dickinson, J. M. Diego, S. Donzelli, O. Doré, M. Douspis, A. Ducout, X. Dupac, G. Efstathiou, F. Elsner, T. A. Enßlin, H. K. Eriksen, E. Falgarone, Y. Fantaye, J. Fergusson, R. Fernandez-Cobos, F. Finelli, F. Forastieri, M. Frailis, E. Franceschi, A. Frolov, S. Galeotta, S. Galli, K. Ganga, R. T. Génova-Santos, M. Gerbino, T. Ghosh, J. González-Nuevo, K. M. Górski, S. Gratton, A. Gruppuso, J. E. Gudmundsson, J. Hamann, W. Handley, F. K. Hansen, G. Helou, D. Herranz, S. R. Hildebrandt, E. Hivon, Z. Huang, A. H. Jaffe, W. C. Jones, A. Karakci, E. Keihänen, R. Keskitalo, K. Kiiveri, J. Kim, T. S. Kisner, L. Knox, N. Krachmalnicoff, M. Kunz, H. Kurki-Suonio, G. Lagache, J. M. Lamarre, M. Langer, A. Lasenby, M. Lattanzi, C. R. Lawrence, M. Le Jeune, J. P. Leahy, J. Lesgourgues, F. Levrier, A. Lewis, M. Liguori, P. B. Lilje, M. Lilley, V. Lindholm, M. López-Caniego, P. M. Lubin, Y. Z. Ma, J. F. Macías-Pérez, G. Maggio, D. Maino,

N. Mandolesi, A. Mangilli, A. Marcos-Caballero, M. Maris, P. G. Martin, M. Martinelli, E. Martínez-González, S. Matarrese, N. Mauri, J. D. McEwen, P. D. Meerburg, P. R. Meinhold, A. Melchiorri, A. Mennella, M. Migliaccio, M. Millea, S. Mitra, M. A. Miville-Deschênes, D. Molinari, A. Moneti, L. Montier, G. Morgante, A. Moss, S. Mottet, M. Münchmeyer, P. Natoli, H. U. Nørgaard-Nielsen, C. A. Oxborrow, L. Pagano, D. Paoletti, B. Partridge, G. Patanchon, T. J. Pearson, M. Peel, H. V. Peiris, F. Perrotta, V. Pettorino, F. Piacentini, L. Polastri, G. Polenta, J. L. Puget, J. P. Rachen, M. Reinecke, M. Remazeilles, C. Renault, A. Renzi, G. Rocha, C. Rosset, G. Roudier, J. A. Rubiño-Martín, B. Ruiz-Granados, L. Salvati, M. Sandri, M. Savelainen, D. Scott, E. P. S. Shellard, M. Shiraishi, C. Sirignano, G. Sirri, L. D. Spencer, R. Sunyaev, A. S. Suur-Uski, J. A. Tauber, D. Tavagnacco, M. Tenti, L. Terenzi, L. Toffolatti, M. Tomasi, T. Trombetti, J. Valiviita, B. Van Tent, L. Vibert, P. Vielva, F. Villa, N. Vittorio, B. D. Wandelt, I. K. Wehus, M. White, S. D. M. White, A. Zacchei, and A. Zonca. Planck 2018 results. I. Overview and the cosmological legacy of Planck. *Astron. Astrophys.*, 641:A1, September 2020. doi: 10.1051/0004-6361/201833880.

[3] Antony Lewis and Sarah Bridle. Cosmological parameters from CMB and other data: A Monte Carlo approach. *Phys. Rev. D*, 66:103511, 2002. doi: 10.1103/PhysRevD.66.103511.

[4] Michael A. Rappenglück. Palaeolithic timekeepers looking at the golden gate of the ecliptic; the lunar cycle and the pleiades in the cave of la-tete-du-lion (ardéche, france) –21,000 bp. *Earth, Moon, and Planets*, 85(0):391–404, 1999. doi: 10.1023/A:1017069411495. URL https://doi.org/10.1023/A:1017069411495.

[5] John A. Peacock. *Cosmological Physics*. Cambridge University Press, 1999.

[6] Isaac Newton. *Philosophiae Naturalis Principia Mathematica*. 1687. doi: 10.3931/e-rara-440.

[7] A. Einstein. Zur Elektrodynamik bewegter Körper. *Annalen der Physik*, 322(10):891–921, January 1905. doi: 10.1002/andp.19053221004.

[8] A. Einstein. Über die vom Relativitätsprinzip geforderte Trägheit der Energie. *Annalen der Physik*, 328(7):371–384, January 1907. doi: 10.1002/andp.19073280713.

[9] Albert Einstein. Die Feldgleichungen der Gravitation. *Sitzungsberichte der Königlich Preussischen Akademie der Wissenschaften*, pages 844–847, January 1915.

[10] A. Friedmann. Über die Krümmung des Raumes. *Zeitschrift fur Physik*, 10:377–386, January 1922. doi: 10.1007/BF01332580.

[11] Virginia Trimble. The 1920 Shapley-Curtis Discussion: Background, Issues, and Aftermath. *Publ. Astron. Soc. Pac.*, 107:1133, December 1995. doi: 10.1086/133671.

[12] Henrietta S. Leavitt and Edward C. Pickering. Periods of 25 Variable Stars in the Small Magellanic Cloud. *Harvard College Observatory Circular*, 173:1–3, March 1912.

[13] E. P. Hubble. A spiral nebula as a stellar system, Messier 31. *Astrophys. J.*, 69:103–158, March 1929. doi: 10.1086/143167.

[14] Margaret W. Rossiter. "women's work" in science, 1880-1910. *Isis*, 71(3):381–398, 1980. ISSN 00211753, 15456994. URL http://www.jstor.org/stable/230118.

[15] Edwin Hubble. A Relation between Distance and Radial Velocity among Extra-Galactic Nebulae. *Proceedings of the National Academy of Science*, 15(3):168–173, March 1929. doi: 10.1073/pnas.15.3.168.

[16] G. Gamow. The evolution of the universe. *Nature*, 162(4122):680–682, 1948. doi: 10.1038/162680a0. URL https://doi.org/10.1038/162680a0.

[17] R. Alpher and R. Herman. Evolution of the universe. *Nature*, 162(4124):774–775, 1948. doi: 10.1038/162774b0. URL https://doi.org/10.1038/162774b0.

[18] Ralph A. Alpher and Robert C. Herman. On the relative abundance of the elements. *Phys. Rev.*, 74:1737–1742, Dec 1948. doi: 10.1103/PhysRev.74.1737. URL https://link.aps.org/doi/10.1103/PhysRev.74.1737.

[19] G. Gamow. The Origin of Elements and the Separation of Galaxies. *Physical Review*, 74(4):505–506, August 1948. doi: 10.1103/PhysRev.74.505.2.

[20] G. Gamow. Expanding universe and the origin of elements. *Phys. Rev.*, 70:572–573, Oct 1946. doi: 10.1103/PhysRev.70.572.2. URL https://link.aps.org/doi/10.1103/PhysRev.70.572.2.

[21] R. A. Alpher, H. Bethe, and G. Gamow. The origin of chemical elements. *Phys. Rev.*, 73:803–804, Apr 1948. doi: 10.1103/PhysRev.73.803. URL https://link.aps.org/doi/10.1103/PhysRev.73.803.

[22] Adam G. Riess, Alexei V. Filippenko, Peter Challis, Alejandro Clocchiatti, Alan Diercks, Peter M. Garnavich, Ron L. Gilliland, Craig J. Hogan, Saurabh Jha, Robert P. Kirshner, B. Leibundgut, M. M. Phillips, David Reiss, Brian P. Schmidt, Robert A. Schommer, R. Chris Smith, J. Spyromilio, Christopher Stubbs, Nicholas B. Suntzeff, and John Tonry. Observational evidence from supernovae for an accelerating universe and a cosmological constant. *The Astronomical Journal*, 116(3):1009, sep 1998. doi: 10.1086/300499. URL https://dx.doi.org/10.1086/300499.

[23] S. Perlmutter, G. Aldering, G. Goldhaber, R. A. Knop, P. Nugent, P. G. Castro, S. Deustua, S. Fabbro, A. Goobar, D. E. Groom, I. M. Hook, A. G. Kim, M. Y. Kim, J. C. Lee, N. J. Nunes, R. Pain, C. R. Pennypacker, R. Quimby, C. Lidman, R. S. Ellis, M. Irwin, R. G. McMahon, P. Ruiz-Lapuente, N. Walton, B. Schaefer, B. J. Boyle, A. V. Filippenko, T. Matheson, A. S. Fruchter, N. Panagia, H. J. M. Newberg, W. J. Couch, and The Supernova Cosmology Project. Measurements of Ω and Λ from 42 high-redshift supernovae. *The Astrophysical Journal*, 517(2):565, jun 1999. doi: 10.1086/307221. URL https://dx.doi.org/10.1086/307221.

[24] R. H. Dicke, P. J. E. Peebles, P. G. Roll, and D. T. Wilkinson. Cosmic Black-Body Radiation. *Astrophys. J.*, 142:414–419, July 1965. doi: 10.1086/148306.

[25] A. A. Penzias and R. W. Wilson. A Measurement of Excess Antenna Temperature at 4080 Mc/s. *Astrophys. J.*, 142:419–421, July 1965. doi: 10.1086/148307.

[26] A.A. Starobinsky. A new type of isotropic cosmological models without singularity. *Physics Letters B*, 91(1):99–102, 1980. ISSN 0370-2693. doi: https://doi.org/10.1016/0370-2693(80)90670-X. URL https://www.sciencedirect.com/science/article/pii/037026938090670X.

[27] Alan H. Guth. Inflationary universe: A possible solution to the horizon and flatness problems. *Phys. Rev. D*, 23:347–356, Jan 1981. doi: 10.1103/PhysRevD.23.347. URL https://link.aps.org/doi/10.1103/PhysRevD.23.347.

[28] F. Zwicky. Die Rotverschiebung von extragalaktischen Nebeln. *Helvetica Physica Acta*, 6:110–127, January 1933.

[29] V. C. Rubin, Jr. Ford, W. K., and N. Thonnard. Rotational properties of 21 SC galaxies with a large range of luminosities and radii, from NGC 4605 (R=4kpc) to UGC 2885 (R=122kpc). *Astrophys. J.*, 238:471–487, June 1980. doi: 10.1086/158003.

[30] K. C. Freeman. On the Disks of Spiral and S0 Galaxies. *Astrophys. J.*, 160:811, June 1970. doi: 10.1086/150474.

[31] Scott Dodelson and Fabian Schmidt. *Modern Cosmology*. Elsevier Science, 2020. ISBN 9780128159484. doi: 10.1016/C2017-0-01943-2.

[32] Andrew Hozier-Byrne. No Plan, 2019. Track 4 on the album *Wasteland, Baby!*

[33] Steven Weinberg. *Cosmology*. Oxford University Press, 2008. ISBN 978-0-19-852682-7.

[34] David Langlois. Isocurvature cosmological perturbations and the cmb. *Comptes Rendus Physique*, 4(8):953–959, 2003. ISSN 1631-0705. doi: https://doi.org/10.1016/j.crhy.2003.09.004. URL https://www.sciencedirect.com/science/article/pii/S1631070503001282. Dossier: The Cosmic Microwave Background.

[35] Planck Collaboration, Akrami, Y., Arroja, F., Ashdown, M., Aumont, J., Baccigalupi, C., Ballardini, M., Banday, A. J., Barreiro, R. B., Bartolo, N., Basak, S., Benabed, K., Bernard, J.-P., Bersanelli, M., Bielewicz, P., Bock, J. J., Bond, J. R., Borrill, J., Bouchet, F. R., Boulanger, F., Bucher, M., Burigana, C., Butler, R. C., Calabrese, E.,

Cardoso, J.-F., Carron, J., Challinor, A., Chiang, H. C., Colombo, L. P. L., Combet, C., Contreras, D., Crill, B. P., Cuttaia, F., de Bernardis, P., de Zotti, G., Delabrouille, J., Delouis, J.-M., Di Valentino, E., Diego, J. M., Donzelli, S., Doré, O., Douspis, M., Ducout, A., Dupac, X., Dusini, S., Efstathiou, G., Elsner, F., Enßlin, T. A., Eriksen, H. K., Fantaye, Y., Fergusson, J., Fernandez-Cobos, R., Finelli, F., Forastieri, F., Frailis, M., Franceschi, E., Frolov, A., Galeotta, S., Galli, S., Ganga, K., Gauthier, C., Génova-Santos, R. T., Gerbino, M., Ghosh, T., González-Nuevo, J., Górski, K. M., Gratton, S., Gruppuso, A., Gudmundsson, J. E., Hamann, J., Handley, W., Hansen, F. K., Herranz, D., Hivon, E., Hooper, D. C., Huang, Z., Jaffe, A. H., Jones, W. C., Keihänen, E., Keskitalo, R., Kiiveri, K., Kim, J., Kisner, T. S., Krachmalnicoff, N., Kunz, M., Kurki-Suonio, H., Lagache, G., Lamarre, J.-M., Lasenby, A., Lattanzi, M., Lawrence, C. R., Le Jeune, M., Lesgourgues, J., Levrier, F., Lewis, A., Liguori, M., Lilje, P. B., Lindholm, V., López-Caniego, M., Lubin, P. M., Ma, Y.-Z., Macías-Pérez, J. F., Maggio, G., Maino, D., Mandolesi, N., Mangilli, A., Marcos-Caballero, A., Maris, M., Martin, P. G., Martínez-González, E., Matarrese, S., Mauri, N., McEwen, J. D., Meerburg, P. D., Meinhold, P. R., Melchiorri, A., Mennella, A., Migliaccio, M., Mitra, S., Miville-Deschênes, M.-A., Molinari, D., Moneti, A., Montier, L., Morgante, G., Moss, A., Münchmeyer, M., Natoli, P., Nørgaard-Nielsen, H. U., Pagano, L., Paoletti, D., Partridge, B., Patanchon, G., Peiris, H. V., Perrotta, F., Pettorino, V., Piacentini, F., Polastri, L., Polenta, G., Puget, J.-L., Rachen, J. P., Reinecke, M., Remazeilles, M., Renzi, A., Rocha, G., Rosset, C., Roudier, G., Rubiño-Martín, J. A., Ruiz-Granados, B., Salvati, L., Sandri, M., Savelainen, M., Scott, D., Shellard, E. P. S., Shiraishi, M., Sirignano, C., Sirri, G., Spencer, L. D., Sunyaev, R., Suur-Uski, A.-S., Tauber, J. A., Tavagnacco, D., Tenti, M., Toffolatti, L., Tomasi, M., Trombetti, T., Valiviita, J., Van Tent, B., Vielva, P., Villa, F., Vittorio, N., Wandelt, B. D., Wehus, I. K., White, S. D. M., Zacchei, A., Zibin, J. P., and Zonca, A. Planck 2018 results - x. constraints on inflation. *A&A*, 641:A10, 2020. doi: 10.1051/0004-6361/201833887. URL https://doi.org/10.1051/0004-6361/201833887.

[36] David Tytler, John M O'Meara, Nao Suzuki, and Dan Lubin. Review of big bang nu-

cleosynthesis and primordial abundances. *Physica Scripta*, 2000(T85):12, jan 2000. doi: 10.1238/Physica.Topical.085a00012. URL https://dx.doi.org/10.1238/Physica.Topical.085a00012.

[37] Dirk Dubbers and Bastian Märkisch. Precise measurements of the decay of free neutrons. *Annual Review of Nuclear and Particle Science*, 71(1):139–163, 2021. doi: 10.1146/annurev-nucl-102419-043156. URL https://doi.org/10.1146/annurev-nucl-102419-043156.

[38] Keith A Olive, Gary Steigman, and Terry P Walker. Primordial nucleosynthesis: theory and observations. *Physics Reports*, 333-334:389–407, 2000. ISSN 0370-1573. doi: https://doi.org/10.1016/S0370-1573(00)00031-4. URL https://www.sciencedirect.com/science/article/pii/S0370157300000314.

[39] Ryan J. Cooke, Max Pettini, Kenneth M. Nollett, and Regina Jorgenson. The Primordial Deuterium Abundance of the Most Metal-poor Damped Lyman-α System. *Astrophys. J.*, 830(2):148, October 2016. doi: 10.3847/0004-637X/830/2/148.

[40] Irina Dvorkin, Elisabeth Vangioni, Joseph Silk, Patrick Petitjean, and Keith A. Olive. Evolution of dispersion in the cosmic deuterium abundance. *Mon. Not. R. Astron. Soc.*, 458(1):L104–L108, May 2016. doi: 10.1093/mnrasl/slw028.

[41] Arthur B. McDonald and Gary Steigman. Neutrinos and big bang nucleosynthesis. *Advances in High Energy Physics*, 2012:268321, 2012. doi: 10.1155/2012/268321. URL https://doi.org/10.1155/2012/268321.

[42] Megh Nad Saha. Liii. ionization in the solar chromosphere. *The London, Edinburgh, and Dublin Philosophical Magazine and Journal of Science*, 40(238):472–488, 1920. doi: 10.1080/14786441008636148. URL https://doi.org/10.1080/14786441008636148.

[43] M. N. Saha. On a Physical Theory of Stellar Spectra. *Proceedings of the Royal Society of London Series A*, 99(697):135–153, May 1921. doi: 10.1098/rspa.1921.0029.

[44] P. J. E. Peebles. Recombination of the Primeval Plasma. *Astrophys. J.*, 153:1, July 1968. doi: 10.1086/149628.

[45] Planck Collaboration, P. A. R. Ade, N. Aghanim, M. I. R. Alves, C. Armitage-Caplan, M. Arnaud, M. Ashdown, F. Atrio-Barandela, J. Aumont, H. Aussel, C. Baccigalupi, A. J. Banday, R. B. Barreiro, R. Barrena, M. Bartelmann, J. G. Bartlett, N. Bartolo, S. Basak, E. Battaner, R. Battye, K. Benabed, A. Benoît, A. Benoit-Lévy, J. P. Bernard, M. Bersanelli, B. Bertincourt, M. Bethermin, P. Bielewicz, I. Bikmaev, A. Blanchard, J. Bobin, J. J. Bock, H. Böhringer, A. Bonaldi, L. Bonavera, J. R. Bond, J. Borrill, F. R. Bouchet, F. Boulanger, H. Bourdin, J. W. Bowyer, M. Bridges, M. L. Brown, M. Bucher, R. Burenin, C. Burigana, R. C. Butler, E. Calabrese, B. Cappellini, J. F. Cardoso, R. Carr, P. Carvalho, M. Casale, G. Castex, A. Catalano, A. Challinor, A. Chamballu, R. R. Chary, X. Chen, H. C. Chiang, L. Y. Chiang, G. Chon, P. R. Christensen, E. Churazov, S. Church, M. Clemens, D. L. Clements, S. Colombi, L. P. L. Colombo, C. Combet, B. Comis, F. Couchot, A. Coulais, B. P. Crill, M. Cruz, A. Curto, F. Cuttaia, A. Da Silva, H. Dahle, L. Danese, R. D. Davies, R. J. Davis, P. de Bernardis, A. de Rosa, G. de Zotti, T. Déchelette, J. Delabrouille, J. M. Delouis, J. Démoclès, F. X. Désert, J. Dick, C. Dickinson, J. M. Diego, K. Dolag, H. Dole, S. Donzelli, O. Doré, M. Douspis, A. Ducout, J. Dunkley, X. Dupac, G. Efstathiou, F. Elsner, T. A. Enßlin, H. K. Eriksen, O. Fabre, E. Falgarone, M. C. Falvella, Y. Fantaye, J. Fergusson, C. Filliard, F. Finelli, I. Flores-Cacho, S. Foley, O. Forni, P. Fosalba, M. Frailis, A. A. Fraisse, E. Franceschi, M. Freschi, S. Fromenteau, M. Frommert, T. C. Gaier, S. Galeotta, J. Gallegos, S. Galli, B. Gandolfo, K. Ganga, C. Gauthier, R. T. Génova-Santos, T. Ghosh, M. Giard, G. Giardino, M. Gilfanov, D. Girard, Y. Giraud-Héraud, E. Gjerløw, J. González-Nuevo, K. M. Górski, S. Gratton, A. Gregorio, A. Gruppuso, J. E. Gudmundsson, J. Haissinski, J. Hamann, F. K. Hansen, M. Hansen, D. Hanson, D. L. Harrison, A. Heavens, G. Helou, A. Hempel, S. Henrot-Versillé, C. Hernández-Monteagudo, D. Herranz, S. R. Hildebrandt, E. Hivon, S. Ho, M. Hobson, W. A. Holmes, A. Hornstrup, Z. Hou, W. Hovest, G. Huey, K. M. Huffenberger, G. Hurier, S. Ilić, A. H. Jaffe, T. R. Jaffe, J. Jasche, J. Jewell, W. C. Jones, M. Juvela, P. Kalberla, P. Kangaslahti, E. Keihänen, J. Kerp, R. Keskitalo, I. Khamitov, K. Kiiveri, J. Kim, T. S. Kisner, R. Kneissl, J. Knoche, L. Knox, M. Kunz, H. Kurki-Suonio, F. Lacasa, G. Lagache, A. Lähteenmäki, J. M. Lamarre, M. Langer, A. Lasenby, M. Lattanzi,

R. J. Laureijs, A. Lavabre, C. R. Lawrence, M. Le Jeune, S. Leach, J. P. Leahy, R. Leonardi, J. León-Tavares, C. Leroy, J. Lesgourgues, A. Lewis, C. Li, A. Liddle, M. Liguori, P. B. Lilje, M. Linden-Vørnle, V. Lindholm, M. López-Caniego, S. Lowe, P. M. Lubin, J. F. Macías-Pérez, C. J. MacTavish, B. Maffei, G. Maggio, D. Maino, N. Mandolesi, A. Mangilli, A. Marcos-Caballero, D. Marinucci, M. Maris, F. Marleau, D. J. Marshall, P. G. Martin, E. Martínez-González, S. Masi, M. Massardi, S. Matarrese, T. Matsumura, F. Matthai, L. Maurin, P. Mazzotta, A. McDonald, J. D. McEwen, P. McGehee, S. Mei, P. R. Meinhold, A. Melchiorri, J. B. Melin, L. Mendes, E. Menegoni, A. Mennella, M. Migliaccio, K. Mikkelsen, M. Millea, R. Miniscalco, S. Mitra, M. A. Miville-Deschênes, D. Molinari, A. Moneti, L. Montier, G. Morgante, N. Morisset, D. Mortlock, A. Moss, D. Munshi, J. A. Murphy, P. Naselsky, F. Nati, P. Natoli, M. Negrello, N. P. H. Nesvadba, C. B. Netterfield, H. U. Nørgaard-Nielsen, C. North, F. Noviello, D. Novikov, I. Novikov, I. J. O'Dwyer, F. Orieux, S. Osborne, C. O'Sullivan, C. A. Oxborrow, F. Paci, L. Pagano, F. Pajot, R. Paladini, S. Pandolfi, D. Paoletti, B. Partridge, F. Pasian, G. Patanchon, P. Paykari, D. Pearson, T. J. Pearson, M. Peel, H. V. Peiris, O. Perdereau, L. Perotto, F. Perrotta, V. Pettorino, F. Piacentini, M. Piat, E. Pierpaoli, D. Pietrobon, S. Plaszczynski, P. Platania, D. Pogosyan, E. Pointecouteau, G. Polenta, N. Ponthieu, L. Popa, T. Poutanen, G. W. Pratt, G. Prézeau, S. Prunet, J. L. Puget, A. R. Pullen, J. P. Rachen, B. Racine, A. Rahlin, C. Räth, W. T. Reach, R. Rebolo, M. Reinecke, M. Remazeilles, C. Renault, A. Renzi, A. Riazuelo, S. Ricciardi, T. Riller, C. Ringeval, I. Ristorcelli, G. Robbers, G. Rocha, M. Roman, C. Rosset, M. Rossetti, G. Roudier, M. Rowan-Robinson, J. A. Rubiño-Martín, B. Ruiz-Granados, B. Rusholme, E. Salerno, M. Sandri, L. Sanselme, D. Santos, M. Savelainen, G. Savini, B. M. Schaefer, F. Schiavon, D. Scott, M. D. Seiffert, P. Serra, E. P. S. Shellard, K. Smith, G. F. Smoot, T. Souradeep, L. D. Spencer, J. L. Starck, V. Stolyarov, R. Stompor, R. Sudiwala, R. Sunyaev, F. Sureau, P. Sutter, D. Sutton, A. S. Suur-Uski, J. F. Sygnet, J. A. Tauber, D. Tavagnacco, D. Taylor, L. Terenzi, D. Texier, L. Toffolatti, M. Tomasi, J. P. Torre, M. Tristram, M. Tucci, J. Tuovinen, M. Türler, M. Tuttlebee, G. Umana, L. Valenziano, J. Valiviita, B. Van Tent, J. Varis, L. Vibert, M. Viel, P. Vielva, F. Villa, N. Vittorio, L. A. Wade, B. D. Wandelt, C. Watson, R. Watson,

I. K. Wehus, N. Welikala, J. Weller, M. White, S. D. M. White, A. Wilkinson, B. Winkel, J. Q. Xia, D. Yvon, A. Zacchei, J. P. Zibin, and A. Zonca. Planck 2013 results. I. Overview of products and scientific results. *Astron. Astrophys.*, 571:A1, November 2014. doi: 10.1051/0004-6361/201321529.

[46] D. J. Fixsen. The temperature of the cosmic microwave background. *The Astrophysical Journal*, 707(2):916, nov 2009. doi: 10.1088/0004-637X/707/2/916. URL https://dx.doi.org/10.1088/0004-637X/707/2/916.

[47] E. K. Conklin. Velocity of the Earth with Respect to the Cosmic Background Radiation. *Nature*, 222(5197):971–972, June 1969. doi: 10.1038/222971a0.

[48] Ya. B. Zeldovich and R. A. Sunyaev. The Interaction of Matter and Radiation in a Hot-Model Universe. *Astrophys. Space Sci.*, 4(3):301–316, July 1969. doi: 10.1007/BF00661821.

[49] R. A. Sunyaev and Ya. B. Zeldovich. The Spectrum of Primordial Radiation, its Distortions and their Significance. *Comments on Astrophysics and Space Physics*, 2:66, March 1970.

[50] R. A. Sunyaev and Ya. B. Zeldovich. The Observations of Relic Radiation as a Test of the Nature of X-Ray Radiation from the Clusters of Galaxies. *Comments on Astrophysics and Space Physics*, 4:173, November 1972.

[51] R. K. Sachs and A. M. Wolfe. Perturbations of a Cosmological Model and Angular Variations of the Microwave Background. *Astrophys. J.*, 147:73, January 1967. doi: 10.1086/148982.

[52] P. J. E. Peebles and J. T. Yu. Primeval Adiabatic Perturbation in an Expanding Universe. *Astrophys. J.*, 162:815, December 1970. doi: 10.1086/150713.

[53] A. D. Sakharov. The Initial Stage of an Expanding Universe and the Appearance of a Nonuniform Distribution of Matter. *Soviet Journal of Experimental and Theoretical Physics*, 22:241, January 1966.

[54] R. A. Sunyaev and Ya. B. Zeldovich. Small-Scale Fluctuations of Relic Radiation. *Astrophys. Space Sci.*, 7(1):3–19, April 1970. doi: 10.1007/BF00653471.

[55] David H. Weinberg, Michael J. Mortonson, Daniel J. Eisenstein, Christopher Hirata, Adam G. Riess, and Eduardo Rozo. Observational probes of cosmic acceleration. *Physics Reports*, 530(2):87–255, 2013. ISSN 0370-1573. doi: https://doi.org/10.1016/j.physrep.2013.05.001. URL https://www.sciencedirect.com/science/article/pii/S0370157313001592. Observational Probes of Cosmic Acceleration.

[56] N. Bartolo, E. Komatsu, S. Matarrese, and A. Riotto. Non-gaussianity from inflation: theory and observations. *Physics Reports*, 402(3):103–266, 2004. ISSN 0370-1573. doi: https://doi.org/10.1016/j.physrep.2004.08.022. URL https://www.sciencedirect.com/science/article/pii/S0370157304003151.

[57] Planck Collaboration, Y. Akrami, F. Arroja, M. Ashdown, J. Aumont, C. Baccigalupi, M. Ballardini, A. J. Banday, R. B. Barreiro, N. Bartolo, S. Basak, K. Benabed, J. P. Bernard, M. Bersanelli, P. Bielewicz, J. R. Bond, J. Borrill, F. R. Bouchet, M. Bucher, C. Burigana, R. C. Butler, E. Calabrese, J. F. Cardoso, B. Casaponsa, A. Challinor, H. C. Chiang, L. P. L. Colombo, C. Combet, B. P. Crill, F. Cuttaia, P. de Bernardis, A. de Rosa, G. de Zotti, J. Delabrouille, J. M. Delouis, E. Di Valentino, J. M. Diego, O. Doré, M. Douspis, A. Ducout, X. Dupac, S. Dusini, G. Efstathiou, F. Elsner, T. A. Enßlin, H. K. Eriksen, Y. Fantaye, J. Fergusson, R. Fernandez-Cobos, F. Finelli, M. Frailis, A. A. Fraisse, E. Franceschi, A. Frolov, S. Galeotta, S. Galli, K. Ganga, R. T. Génova-Santos, M. Gerbino, J. González-Nuevo, K. M. Górski, S. Gratton, A. Gruppuso, J. E. Gudmundsson, J. Hamann, W. Handley, F. K. Hansen, D. Herranz, E. Hivon, Z. Huang, A. H. Jaffe, W. C. Jones, G. Jung, E. Keihänen, R. Keskitalo, K. Kiiveri, J. Kim, N. Krachmalnicoff, M. Kunz, H. Kurki-Suonio, J. M. Lamarre, A. Lasenby, M. Lattanzi, C. R. Lawrence, M. Le Jeune, F. Levrier, A. Lewis, M. Liguori, P. B. Lilje, V. Lindholm, M. López-Caniego, Y. Z. Ma, J. F. Macías-Pérez, G. Maggio, D. Maino, N. Mandolesi, A. Marcos-Caballero, M. Maris, P. G. Martin, E. Martínez-González, S. Matarrese, N. Mauri, J. D. McEwen, P. D. Meerburg, P. R. Meinhold,

A. Melchiorri, A. Mennella, M. Migliaccio, M. A. Miville-Deschênes, D. Molinari, A. Moneti, L. Montier, G. Morgante, A. Moss, M. Münchmeyer, P. Natoli, F. Oppizzi, L. Pagano, D. Paoletti, B. Partridge, G. Patanchon, F. Perrotta, V. Pettorino, F. Piacentini, G. Polenta, J. L. Puget, J. P. Rachen, B. Racine, M. Reinecke, M. Remazeilles, A. Renzi, G. Rocha, J. A. Rubiño-Martín, B. Ruiz-Granados, L. Salvati, M. Savelainen, D. Scott, E. P. S. Shellard, M. Shiraishi, C. Sirignano, G. Sirri, K. Smith, L. D. Spencer, L. Stanco, R. Sunyaev, A. S. Suur-Uski, J. A. Tauber, D. Tavagnacco, M. Tenti, L. Toffolatti, M. Tomasi, T. Trombetti, J. Valiviita, B. Van Tent, P. Vielva, F. Villa, N. Vittorio, B. D. Wandelt, I. K. Wehus, A. Zacchei, and A. Zonca. Planck 2018 results. IX. Constraints on primordial non-Gaussianity. *Astron. Astrophys.*, 641: A9, September 2020. doi: 10.1051/0004-6361/201935891.

[58] Planck Collaboration, N. Aghanim, Y. Akrami, M. Ashdown, J. Aumont, C. Baccigalupi, M. Ballardini, A. J. Banday, R. B. Barreiro, N. Bartolo, S. Basak, R. Battye, K. Benabed, J. P. Bernard, M. Bersanelli, P. Bielewicz, J. J. Bock, J. R. Bond, J. Borrill, F. R. Bouchet, F. Boulanger, M. Bucher, C. Burigana, R. C. Butler, E. Calabrese, J. F. Cardoso, J. Carron, A. Challinor, H. C. Chiang, J. Chluba, L. P. L. Colombo, C. Combet, D. Contreras, B. P. Crill, F. Cuttaia, P. de Bernardis, G. de Zotti, J. Delabrouille, J. M. Delouis, E. Di Valentino, J. M. Diego, O. Doré, M. Douspis, A. Ducout, X. Dupac, S. Dusini, G. Efstathiou, F. Elsner, T. A. Enßlin, H. K. Eriksen, Y. Fantaye, M. Farhang, J. Fergusson, R. Fernandez-Cobos, F. Finelli, F. Forastieri, M. Frailis, A. A. Fraisse, E. Franceschi, A. Frolov, S. Galeotta, S. Galli, K. Ganga, R. T. Génova-Santos, M. Gerbino, T. Ghosh, J. González-Nuevo, K. M. Górski, S. Gratton, A. Gruppuso, J. E. Gudmundsson, J. Hamann, W. Handley, F. K. Hansen, D. Herranz, S. R. Hildebrandt, E. Hivon, Z. Huang, A. H. Jaffe, W. C. Jones, A. Karakci, E. Keihänen, R. Keskitalo, K. Kiiveri, J. Kim, T. S. Kisner, L. Knox, N. Krachmalnicoff, M. Kunz, H. Kurki-Suonio, G. Lagache, J. M. Lamarre, A. Lasenby, M. Lattanzi, C. R. Lawrence, M. Le Jeune, P. Lemos, J. Lesgourgues, F. Levrier, A. Lewis, M. Liguori, P. B. Lilje, M. Lilley, V. Lindholm, M. López-Caniego, P. M. Lubin, Y. Z. Ma, J. F. Macías-Pérez, G. Maggio, D. Maino, N. Mandolesi, A. Mangilli, A. Marcos-Caballero,

M. Maris, P. G. Martin, M. Martinelli, E. Martínez-González, S. Matarrese, N. Mauri, J. D. McEwen, P. R. Meinhold, A. Melchiorri, A. Mennella, M. Migliaccio, M. Millea, S. Mitra, M. A. Miville-Deschênes, D. Molinari, L. Montier, G. Morgante, A. Moss, P. Natoli, H. U. Nørgaard-Nielsen, L. Pagano, D. Paoletti, B. Partridge, G. Patanchon, H. V. Peiris, F. Perrotta, V. Pettorino, F. Piacentini, L. Polastri, G. Polenta, J. L. Puget, J. P. Rachen, M. Reinecke, M. Remazeilles, A. Renzi, G. Rocha, C. Rosset, G. Roudier, J. A. Rubiño-Martín, B. Ruiz-Granados, L. Salvati, M. Sandri, M. Savelainen, D. Scott, E. P. S. Shellard, C. Sirignano, G. Sirri, L. D. Spencer, R. Sunyaev, A. S. Suur-Uski, J. A. Tauber, D. Tavagnacco, M. Tenti, L. Toffolatti, M. Tomasi, T. Trombetti, L. Valenziano, J. Valiviita, B. Van Tent, L. Vibert, P. Vielva, F. Villa, N. Vittorio, B. D. Wandelt, I. K. Wehus, M. White, S. D. M. White, A. Zacchei, and A. Zonca. Planck 2018 results. VI. Cosmological parameters. *Astron. Astrophys.*, 641: A6, September 2020. doi: 10.1051/0004-6361/201833910.

[59] Antony Lewis and Anthony Challinor. CAMB: Code for Anisotropies in the Microwave Background. Astrophysics Source Code Library, record ascl:1102.026, February 2011.

[60] Joseph Silk. Cosmic Black-Body Radiation and Galaxy Formation. *Astrophys. J.*, 151: 459, February 1968. doi: 10.1086/149449.

[61] James Binney and Scott Tremaine. *Galactic Dynamics: Second Edition*. Princeton University Press, 2008.

[62] A. J. S. Hamilton. Linear Redshift Distortions: a Review. In Donald Hamilton, editor, *The Evolving Universe*, volume 231 of *Astrophysics and Space Science Library*, page 185, January 1998. doi: 10.1007/978-94-011-4960-0_17.

[63] C. Alcock and B. Paczynski. An evolution free test for non-zero cosmological constant. *Nature*, 281:358, October 1979. doi: 10.1038/281358a0.

[64] D. S. Akerib, S. Alsum, H. M. Araújo, X. Bai, A. J. Bailey, J. Balajthy, P. Beltrame, E. P. Bernard, A. Bernstein, T. P. Biesiadzinski, E. M. Boulton, R. Bramante, P. Brás, D. Byram, S. B. Cahn, M. C. Carmona-Benitez, C. Chan, A. A. Chiller, C. Chiller,

A. Currie, J. E. Cutter, T. J. R. Davison, A. Dobi, J. E. Y. Dobson, E. Druszkiewicz, B. N. Edwards, C. H. Faham, S. Fiorucci, R. J. Gaitskell, V. M. Gehman, C. Ghag, K. R. Gibson, M. G. D. Gilchriese, C. R. Hall, M. Hanhardt, S. J. Haselschwardt, S. A. Hertel, D. P. Hogan, M. Horn, D. Q. Huang, C. M. Ignarra, M. Ihm, R. G. Jacobsen, W. Ji, K. Kamdin, K. Kazkaz, D. Khaitan, R. Knoche, N. A. Larsen, C. Lee, B. G. Lenardo, K. T. Lesko, A. Lindote, M. I. Lopes, A. Manalaysay, R. L. Mannino, M. F. Marzioni, D. N. McKinsey, D. M. Mei, J. Mock, M. Moongweluwan, J. A. Morad, A. St. J. Murphy, C. Nehrkorn, H. N. Nelson, F. Neves, K. O'Sullivan, K. C. Oliver-Mallory, K. J. Palladino, E. K. Pease, P. Phelps, L. Reichhart, C. Rhyne, S. Shaw, T. A. Shutt, C. Silva, M. Solmaz, V. N. Solovov, P. Sorensen, S. Stephenson, T. J. Sumner, M. Szydagis, D. J. Taylor, W. C. Taylor, B. P. Tennyson, P. A. Terman, D. R. Tiedt, W. H. To, M. Tripathi, L. Tvrznikova, S. Uvarov, J. R. Verbus, R. C. Webb, J. T. White, T. J. Whitis, M. S. Witherell, F. L. H. Wolfs, J. Xu, K. Yazdani, S. K. Young, C. Zhang, and LUX Collaboration. Results from a Search for Dark Matter in the Complete LUX Exposure. *Phys. Rev. Lett.*, 118(2):021303, January 2017. doi: 10.1103/PhysRevLett.118.021303.

[65] D. S. Akerib, S. Alsum, C. Aquino, H. M. Araújo, X. Bai, A. J. Bailey, J. Balajthy, P. Beltrame, E. P. Bernard, A. Bernstein, T. P. Biesiadzinski, E. M. Boulton, P. Brás, D. Byram, S. B. Cahn, M. C. Carmona-Benitez, C. Chan, A. A. Chiller, C. Chiller, A. Currie, J. E. Cutter, T. J. R. Davison, A. Dobi, J. E. Y. Dobson, E. Druszkiewicz, B. N. Edwards, C. H. Faham, S. R. Fallon, S. Fiorucci, R. J. Gaitskell, V. M. Gehman, C. Ghag, K. R. Gibson, M. G. D. Gilchriese, C. R. Hall, M. Hanhardt, S. J. Haselschwardt, S. A. Hertel, D. P. Hogan, M. Horn, D. Q. Huang, C. M. Ignarra, R. G. Jacobsen, W. Ji, K. Kamdin, K. Kazkaz, D. Khaitan, R. Knoche, N. A. Larsen, C. Lee, B. G. Lenardo, K. T. Lesko, A. Lindote, M. I. Lopes, A. Manalaysay, R. L. Mannino, M. F. Marzioni, D. N. McKinsey, D. M. Mei, J. Mock, M. Moongweluwan, J. A. Morad, A. St. J. Murphy, C. Nehrkorn, H. N. Nelson, F. Neves, K. O'Sullivan, K. C. Oliver-Mallory, K. J. Palladino, E. K. Pease, L. Reichhart, C. Rhyne, S. Shaw, T. A. Shutt, C. Silva, M. Solmaz, V. N. Solovov, P. Sorensen, S. Stephenson, T. J.

Sumner, M. Szydagis, D. J. Taylor, W. C. Taylor, B. P. Tennyson, P. A. Terman, D. R. Tiedt, W. H. To, M. Tripathi, L. Tvrznikova, S. Uvarov, V. Velan, J. R. Verbus, R. C. Webb, J. T. White, T. J. Whitis, M. S. Witherell, F. L. H. Wolfs, J. Xu, K. Yazdani, S. K. Young, C. Zhang, and LUX Collaboration. First Searches for Axions and Axion-like Particles with the LUX Experiment. *Phys. Rev. Lett.*, 118(26):261301, June 2017. doi: 10.1103/PhysRevLett.118.261301.

[66] Alex Geringer-Sameth, Savvas M. Koushiappas, and Matthew G. Walker. Comprehensive search for dark matter annihilation in dwarf galaxies. *Phys. Rev. D*, 91(8):083535, April 2015. doi: 10.1103/PhysRevD.91.083535.

[67] A. Albert, B. Anderson, K. Bechtol, A. Drlica-Wagner, M. Meyer, M. Sánchez-Conde, L. Strigari, M. Wood, T. M. C. Abbott, F. B. Abdalla, A. Benoit-Lévy, G. M. Bernstein, R. A. Bernstein, E. Bertin, D. Brooks, D. L. Burke, A. Carnero Rosell, M. Carrasco Kind, J. Carretero, M. Crocce, C. E. Cunha, C. B. D'Andrea, L. N. da Costa, S. Desai, H. T. Diehl, J. P. Dietrich, P. Doel, T. F. Eifler, A. E. Evrard, A. Fausti Neto, D. A. Finley, B. Flaugher, P. Fosalba, J. Frieman, D. W. Gerdes, D. A. Goldstein, D. Gruen, R. A. Gruendl, K. Honscheid, D. J. James, S. Kent, K. Kuehn, N. Kuropatkin, O. Lahav, T. S. Li, M. A. G. Maia, M. March, J. L. Marshall, P. Martini, C. J. Miller, R. Miquel, E. Neilsen, B. Nord, R. Ogando, A. A. Plazas, K. Reil, A. K. Romer, E. S. Rykoff, E. Sanchez, B. Santiago, M. Schubnell, I. Sevilla-Noarbe, R. C. Smith, M. Soares-Santos, F. Sobreira, E. Suchyta, M. E. C. Swanson, G. Tarle, V. Vikram, A. R. Walker, R. H. Wechsler, Fermi-LAT Collaboration, and DES Collaboration. Searching for Dark Matter Annihilation in Recently Discovered Milky Way Satellites with Fermi-Lat. *Astrophys. J.*, 834(2):110, January 2017. doi: 10.3847/1538-4357/834/2/110.

[68] Antonino Del Popolo and Morgan Le Delliou. Small Scale Problems of the ΛCDM Model: A Short Review. *Galaxies*, 5(1):17, February 2017. doi: 10.3390/galaxies5010017.

[69] Adam G. Riess, Wenlong Yuan, Lucas M. Macri, Dan Scolnic, Dillon Brout, Stefano Casertano, David O. Jones, Yukei Murakami, Gagandeep S. Anand, Louise Breuval, Thomas G. Brink, Alexei V. Filippenko, Samantha Hoffmann, Saurabh W. Jha,

W. D'arcy Kenworthy, John Mackenty, Benjamin E. Stahl, and WeiKang Zheng. A comprehensive measurement of the local value of the hubble constant with 1 km s^{-1} mpc^{-1} uncertainty from the hubble space telescope and the sh0es team. *The Astrophysical Journal Letters*, 934(1):L7, jul 2022. doi: 10.3847/2041-8213/ac5c5b. URL https://dx.doi.org/10.3847/2041-8213/ac5c5b.

[70] Wendy L. Freedman. Measurements of the Hubble Constant: Tensions in Perspective. *Astrophys. J.*, 919(1):16, September 2021. doi: 10.3847/1538-4357/ac0e95.

[71] T. M. C. Abbott, F. B. Abdalla, A. Alarcon, J. Aleksić, S. Allam, S. Allen, A. Amara, J. Annis, J. Asorey, S. Avila, D. Bacon, E. Balbinot, M. Banerji, N. Banik, W. Barkhouse, M. Baumer, E. Baxter, K. Bechtol, M. R. Becker, A. Benoit-Lévy, B. A. Benson, G. M. Bernstein, E. Bertin, J. Blazek, S. L. Bridle, D. Brooks, D. Brout, E. Buckley-Geer, D. L. Burke, M. T. Busha, A. Campos, D. Capozzi, A. Carnero Rosell, M. Carrasco Kind, J. Carretero, F. J. Castander, R. Cawthon, C. Chang, N. Chen, M. Childress, A. Choi, C. Conselice, R. Crittenden, M. Crocce, C. E. Cunha, C. B. D'Andrea, L. N. da Costa, R. Das, T. M. Davis, C. Davis, J. De Vicente, D. L. DePoy, J. DeRose, S. Desai, H. T. Diehl, J. P. Dietrich, S. Dodelson, P. Doel, A. Drlica-Wagner, T. F. Eifler, A. E. Elliott, F. Elsner, J. Elvin-Poole, J. Estrada, A. E. Evrard, Y. Fang, E. Fernandez, A. Ferté, D. A. Finley, B. Flaugher, P. Fosalba, O. Friedrich, J. Frieman, J. García-Bellido, M. Garcia-Fernandez, M. Gatti, E. Gaztanaga, D. W. Gerdes, T. Giannantonio, M. S. S. Gill, K. Glazebrook, D. A. Goldstein, D. Gruen, R. A. Gruendl, J. Gschwend, G. Gutierrez, S. Hamilton, W. G. Hartley, S. R. Hinton, K. Honscheid, B. Hoyle, D. Huterer, B. Jain, D. J. James, M. Jarvis, T. Jeltema, M. D. Johnson, M. W. G. Johnson, T. Kacprzak, S. Kent, A. G. Kim, A. King, D. Kirk, N. Kokron, A. Kovacs, E. Krause, C. Krawiec, A. Kremin, K. Kuehn, S. Kuhlmann, N. Kuropatkin, F. Lacasa, O. Lahav, T. S. Li, A. R. Liddle, C. Lidman, M. Lima, H. Lin, N. MacCrann, M. A. G. Maia, M. Makler, M. Manera, M. March, J. L. Marshall, P. Martini, R. G. McMahon, P. Melchior, F. Menanteau, R. Miquel, V. Miranda, D. Mudd, J. Muir, A. Möller, E. Neilsen, R. C. Nichol, B. Nord, P. Nugent, R. L. C. Ogando, A. Palmese, J. Peacock, H. V. Peiris, J. Peoples, W. J. Percival, D. Petravick,

A. A. Plazas, A. Porredon, J. Prat, A. Pujol, M. M. Rau, A. Refregier, P. M. Ricker, N. Roe, R. P. Rollins, A. K. Romer, A. Roodman, R. Rosenfeld, A. J. Ross, E. Rozo, E. S. Rykoff, M. Sako, A. I. Salvador, S. Samuroff, C. Sánchez, E. Sanchez, B. Santiago, V. Scarpine, R. Schindler, D. Scolnic, L. F. Secco, S. Serrano, I. Sevilla-Noarbe, E. Sheldon, R. C. Smith, M. Smith, J. Smith, M. Soares-Santos, F. Sobreira, E. Suchyta, G. Tarle, D. Thomas, M. A. Troxel, D. L. Tucker, B. E. Tucker, S. A. Uddin, T. N. Varga, P. Vielzeuf, V. Vikram, A. K. Vivas, A. R. Walker, M. Wang, R. H. Wechsler, J. Weller, W. Wester, R. C. Wolf, B. Yanny, F. Yuan, A. Zenteno, B. Zhang, Y. Zhang, J. Zuntz, and Dark Energy Survey Collaboration. Dark Energy Survey year 1 results: Cosmological constraints from galaxy clustering and weak lensing. *Phys. Rev. D*, 98 (4):043526, August 2018. doi: 10.1103/PhysRevD.98.043526.

[72] Julio F. Navarro, Carlos S. Frenk, and Simon D. M. White. A Universal Density Profile from Hierarchical Clustering. *Astrophys. J.*, 490(2):493–508, December 1997. doi: 10.1086/304888.

[73] Ismael Ferrero, Mario G. Abadi, Julio F. Navarro, Laura V. Sales, and Sebastián. Gurovich. The dark matter haloes of dwarf galaxies: a challenge for the Λ cold dark matter paradigm? *Mon. Not. R. Astron. Soc.*, 425(4):2817–2823, October 2012. doi: 10.1111/j.1365-2966.2012.21623.x.

[74] Ben Moore. Evidence against dissipation-less dark matter from observations of galaxy haloes. *Nature*, 370(6491):629–631, 1994. doi: 10.1038/370629a0. URL https://doi.org/10.1038/370629a0.

[75] Marc Davis, George Efstathiou, Carlos S. Frenk, and Simon D. M. White. The Evolution of Large Scale Structure in a Universe Dominated by Cold Dark Matter. *Astrophys. J.*, 292:371–394, 1985. doi: 10.1086/163168.

[76] Matthew G. Walker and Jorge Peñarrubia. A method for measuring (slopes of) the mass profiles of dwarf spheroidal galaxies. *The Astrophysical Journal*, 742(1):20, nov 2011. doi: 10.1088/0004-637X/742/1/20. URL https://dx.doi.org/10.1088/0004-637X/742/1/20.

[77] Anna Genina, Alejandro Benítez-Llambay, Carlos S. Frenk, Shaun Cole, Azadeh Fattahi, Julio F. Navarro, Kyle A. Oman, Till Sawala, and Tom Theuns. The core-cusp problem: a matter of perspective. *Mon. Not. R. Astron. Soc.*, 474(1):1398–1411, February 2018. doi: 10.1093/mnras/stx2855.

[78] G. Kauffmann, S. D. M. White, and B. Guiderdoni. The formation and evolution of galaxies within merging dark matter haloes. *Monthly Notices of the Royal Astronomical Society*, 264(1):201–218, 09 1993. ISSN 0035-8711. doi: 10.1093/mnras/264.1.201. URL https://doi.org/10.1093/mnras/264.1.201.

[79] Anatoly Klypin, Andrey V. Kravtsov, Octavio Valenzuela, and Francisco Prada. Where Are the Missing Galactic Satellites? *Astrophys. J.*, 522(1):82–92, September 1999. doi: 10.1086/307643.

[80] Ben Moore, Sebastiano Ghigna, Fabio Governato, George Lake, Thomas Quinn, Joachim Stadel, and Paolo Tozzi. Dark Matter Substructure within Galactic Halos. *Astrophys. J. Lett.*, 524(1):L19–L22, October 1999. doi: 10.1086/312287.

[81] James S. Bullock. Notes on the Missing Satellites Problem. *arXiv e-prints*, art. arXiv:1009.4505, September 2010. doi: 10.48550/arXiv.1009.4505.

[82] Michael Boylan-Kolchin, James S. Bullock, and Manoj Kaplinghat. Too big to fail? The puzzling darkness of massive Milky Way subhaloes. *Mon. Not. R. Astron. Soc.*, 415(1):L40–L44, July 2011. doi: 10.1111/j.1745-3933.2011.01074.x.

[83] Michael Boylan-Kolchin, James S. Bullock, and Manoj Kaplinghat. The Milky Way's bright satellites as an apparent failure of ΛCDM. *Mon. Not. R. Astron. Soc.*, 422(2): 1203–1218, May 2012. doi: 10.1111/j.1365-2966.2012.20695.x.

[84] Shea Garrison-Kimmel, Michael Boylan-Kolchin, James S. Bullock, and Evan N. Kirby. Too big to fail in the Local Group. *Mon. Not. R. Astron. Soc.*, 444(1):222–236, October 2014. doi: 10.1093/mnras/stu1477.

[85] E. Papastergis, R. Giovanelli, M. P. Haynes, and F. Shankar. Is there a "too big to fail" problem in the field? *Astron. Astrophys.*, 574:A113, February 2015. doi: 10.1051/0004-6361/201424909.

[86] Erik J. Tollerud, Michael Boylan-Kolchin, and James S. Bullock. M31 satellite masses compared to ΛCDM subhaloes. *Mon. Not. R. Astron. Soc.*, 440(4):3511–3519, June 2014. doi: 10.1093/mnras/stu474.

[87] Manoj Kaplinghat, Mauro Valli, and Hai-Bo Yu. Too big to fail in light of Gaia. *Mon. Not. R. Astron. Soc.*, 490(1):231–242, November 2019. doi: 10.1093/mnras/stz2511.

[88] S. Tremaine, M. Henon, and D. Lynden-Bell. H-functions and mixing in violent relaxation. *Mon. Not. R. Astron. Soc.*, 219:285–297, March 1986. doi: 10.1093/mnras/219.2.285.

[89] Walter Dehnen. Phase-space mixing and the merging of cusps. *Mon. Not. R. Astron. Soc.*, 360(3):892–900, July 2005. doi: 10.1111/j.1365-2966.2005.09099.x.

[90] D. Lynden-Bell and J. P. Ostriker. On the stability of differentially rotating bodies. *Mon. Not. R. Astron. Soc.*, 136:293, January 1967. doi: 10.1093/mnras/136.3.293.

[91] John David Jackson. *Classical Electrodynamics, 3rd Edition.* John Wiley & Sons, 1998.

[92] John Dubinski, L. N. da Costa, D. S. Goldwirth, M. Lecar, and T. Piran. Void Evolution and the Large-Scale Structure. *Astrophys. J.*, 410:458, June 1993. doi: 10.1086/172762.

[93] Annalisa Pillepich, Volker Springel, Dylan Nelson, Shy Genel, Jill Naiman, Rüdiger Pakmor, Lars Hernquist, Paul Torrey, Mark Vogelsberger, Rainer Weinberger, and Federico Marinacci. Simulating galaxy formation with the IllustrisTNG model. *Mon. Not. R. Astron. Soc.*, 473(3):4077–4106, January 2018. doi: 10.1093/mnras/stx2656.

[94] S. A. Gregory and L. A. Thompson. The Coma/A1367 supercluster and its environs. *Astrophys. J.*, 222:784–799, June 1978. doi: 10.1086/156198.

[95] V. de Lapparent, M. J. Geller, and J. P. Huchra. A Slice of the Universe. *Astrophys. J. Lett.*, 302:L1, March 1986. doi: 10.1086/184625.

[96] Matthew Colless, Gavin Dalton, Steve Maddox, Will Sutherland, Peder Norberg, Shaun Cole, Joss Bland-Hawthorn, Terry Bridges, Russell Cannon, Chris Collins, Warrick Couch, Nicholas Cross, Kathryn Deeley, Roberto De Propris, Simon P. Driver, George Efstathiou, Richard S. Ellis, Carlos S. Frenk, Karl Glazebrook, Carole Jackson, Ofer Lahav, Ian Lewis, Stuart Lumsden, Darren Madgwick, John A. Peacock, Bruce A. Peterson, Ian Price, Mark Seaborne, and Keith Taylor. The 2dF Galaxy Redshift Survey: spectra and redshifts. *Mon. Not. R. Astron. Soc.*, 328(4):1039–1063, December 2001. doi: 10.1046/j.1365-8711.2001.04902.x.

[97] Cheng Zhao, Andrei Variu, Mengfan He, Daniel Forero-Sánchez, Amélie Tamone, Chia-Hsun Chuang, Francisco-Shu Kitaura, Charling Tao, Jiaxi Yu, Jean-Paul Kneib, Will J. Percival, Huanyuan Shan, Gong-Bo Zhao, Etienne Burtin, Kyle S. Dawson, Graziano Rossi, Donald P. Schneider, and Axel de la Macorra. The completed SDSS-IV extended Baryon Oscillation Spectroscopic Survey: cosmological implications from multitracer BAO analysis with galaxies and voids. *Mon. Not. R. Astron. Soc.*, 511(4): 5492–5524, April 2022. doi: 10.1093/mnras/stac390.

[98] William H. Press and Paul Schechter. Formation of Galaxies and Clusters of Galaxies by Self-Similar Gravitational Condensation. *Astrophys. J.*, 187:425–438, February 1974. doi: 10.1086/152650.

[99] J. R. Bond, S. Cole, G. Efstathiou, and N. Kaiser. Excursion Set Mass Functions for Hierarchical Gaussian Fluctuations. *Astrophys. J.*, 379:440, October 1991. doi: 10.1086/170520.

[100] Cedric Lacey and Shaun Cole. Merger rates in hierarchical models of galaxy formation. *Mon. Not. R. Astron. Soc.*, 262(3):627–649, June 1993. doi: 10.1093/mnras/262.3.627.

[101] J. W. Hsueh, W. Enzi, S. Vegetti, M. W. Auger, C. D. Fassnacht, G. Despali, L. V. E. Koopmans, and J. P. McKean. SHARP - VII. New constraints on the dark matter

free-streaming properties and substructure abundance from gravitationally lensed quasars. *Mon. Not. R. Astron. Soc.*, 492(2):3047–3059, February 2020. doi: 10.1093/mnras/stz3177.

[102] Lam Hui, Jeremiah P. Ostriker, Scott Tremaine, and Edward Witten. Ultralight scalars as cosmological dark matter. *Phys. Rev. D*, 95:043541, Feb 2017. doi: 10.1103/PhysRevD.95.043541. URL https://link.aps.org/doi/10.1103/PhysRevD.95.043541.

[103] Victor H. Robles, James S. Bullock, and Michael Boylan-Kolchin. Scalar Field Dark Matter: Helping or Hurting Small-Scale Problems in Cosmology? *Mon. Not. Roy. Astron. Soc.*, 483(1):289–298, 2019. doi: 10.1093/mnras/sty3190.

[104] M. Ackermann, M. Ajello, A. Albert, W. B. Atwood, L. Baldini, J. Ballet, G. Barbiellini, D. Bastieri, K. Bechtol, R. Bellazzini, B. Berenji, R. D. Blandford, E. D. Bloom, E. Bonamente, A. W. Borgland, J. Bregeon, M. Brigida, P. Bruel, R. Buehler, T. H. Burnett, S. Buson, G. A. Caliandro, R. A. Cameron, B. Cañadas, P. A. Caraveo, J. M. Casandjian, C. Cecchi, E. Charles, A. Chekhtman, J. Chiang, S. Ciprini, R. Claus, J. Cohen-Tanugi, J. Conrad, S. Cutini, A. de Angelis, F. de Palma, C. D. Dermer, S. W. Digel, E. do Couto e Silva, P. S. Drell, A. Drlica-Wagner, L. Falletti, C. Favuzzi, S. J. Fegan, E. C. Ferrara, Y. Fukazawa, S. Funk, P. Fusco, F. Gargano, D. Gasparrini, N. Gehrels, S. Germani, N. Giglietto, F. Giordano, M. Giroletti, T. Glanzman, G. Godfrey, I. A. Grenier, S. Guiriec, M. Gustafsson, D. Hadasch, M. Hayashida, E. Hays, R. E. Hughes, T. E. Jeltema, G. Jóhannesson, R. P. Johnson, A. S. Johnson, T. Kamae, H. Katagiri, J. Kataoka, J. Knödlseder, M. Kuss, J. Lande, L. Latronico, A. M. Lionetto, M. Llena Garde, F. Longo, F. Loparco, B. Lott, M. N. Lovellette, P. Lubrano, G. M. Madejski, M. N. Mazziotta, J. E. McEnery, J. Mehault, P. F. Michelson, W. Mitthumsiri, T. Mizuno, C. Monte, M. E. Monzani, A. Morselli, I. V. Moskalenko, S. Murgia, M. Naumann-Godo, J. P. Norris, E. Nuss, T. Ohsugi, A. Okumura, N. Omodei, E. Orlando, J. F. Ormes, M. Ozaki, D. Paneque, D. Parent, M. Pesce-Rollins, M. Pierbattista, F. Piron, G. Pivato, T. A. Porter, S. Profumo, S. Rainò, M. Razzano, A. Reimer, O. Reimer, S. Ritz, M. Roth, H. F.-W. Sadrozinski, C. Sbarra, J. D. Scargle, T. L. Schalk,

C. Sgrò, E. J. Siskind, G. Spandre, P. Spinelli, L. Strigari, D. J. Suson, H. Tajima, H. Takahashi, T. Tanaka, J. G. Thayer, J. B. Thayer, D. J. Thompson, L. Tibaldo, M. Tinivella, D. F. Torres, E. Troja, Y. Uchiyama, J. Vandenbroucke, V. Vasileiou, G. Vianello, V. Vitale, A. P. Waite, P. Wang, B. L. Winer, K. S. Wood, M. Wood, Z. Yang, S. Zimmer, M. Kaplinghat, and G. D. Martinez. Constraining dark matter models from a combined analysis of milky way satellites with the fermi large area telescope. *Phys. Rev. Lett.*, 107:241302, Dec 2011. doi: 10.1103/PhysRevLett.107.241302. URL https://link.aps.org/doi/10.1103/PhysRevLett.107.241302.

[105] Alex Geringer-Sameth and Savvas M. Koushiappas. Exclusion of Canonical Weakly Interacting Massive Particles by Joint Analysis of Milky Way Dwarf Galaxies with Data from the Fermi Gamma-Ray Space Telescope. *Phys. Rev. Lett.*, 107(24):241303, December 2011. doi: 10.1103/PhysRevLett.107.241303.

[106] Alex Geringer-Sameth, Savvas M. Koushiappas, and Matthew Walker. Dwarf galaxy annihilation and decay emission profiles for dark matter experiments. *Astrophys. J.*, 801(2):74, mar 2015. doi: 10.1088/0004-637x/801/2/74.

[107] V. Bonnivard, C. Combet, M. Daniel, S. Funk, A. Geringer-Sameth, J. A. Hinton, D. Maurin, J. I. Read, S. Sarkar, M. G. Walker, and M. I. Wilkinson. Dark matter annihilation and decay in dwarf spheroidal galaxies: the classical and ultrafaint dSphs. *Mon. Not. R. Astron. Soc.*, 453(1):849–867, October 2015. doi: 10.1093/mnras/stv1601.

[108] Leanna Dugger, Tesla E. Jeltema, and Stefano Profumo. Constraints on decaying dark matter from Fermi observations of nearby galaxies and clusters. *J. Cosmol. Astropart. Phys.*, 2010(12):015, December 2010. doi: 10.1088/1475-7516/2010/12/015.

[109] Manoj Kaplinghat, Sean Tulin, and Hai-Bo Yu. Dark matter halos as particle colliders: Unified solution to small-scale structure puzzles from dwarfs to clusters. *Phys. Rev. Lett.*, 116:041302, Jan 2016. doi: 10.1103/PhysRevLett.116.041302. URL https://link.aps.org/doi/10.1103/PhysRevLett.116.041302.

[110] Scott Tremaine and James E. Gunn. Dynamical role of light neutral leptons in cosmology. *Phys. Rev. Lett.*, 42:407–410, Feb 1979. doi: 10.1103/PhysRevLett.42.407. URL https://link.aps.org/doi/10.1103/PhysRevLett.42.407.

[111] Isabelle S. Goldstein, Savvas M. Koushiappas, and Matthew G. Walker. Viability of ultralight bosonic dark matter in dwarf galaxies. *Phys. Rev. D*, 106(6):063010, September 2022. doi: 10.1103/PhysRevD.106.063010.

[112] Jatan Buch, John Shing Chau Leung, and JiJi Fan. Using Gaia DR2 to constrain local dark matter density and thin dark disk. *J. Cosmol. Astropart. Phys.*, 2019(4): 026, April 2019. doi: 10.1088/1475-7516/2019/04/026.

[113] JiJi Fan, Andrey Katz, Lisa Randall, and Matthew Reece. Double-Disk Dark Matter. *Physics of the Dark Universe*, 2(3):139–156, September 2013. doi: 10.1016/j.dark.2013.07.001.

[114] Kevork Abazajian and Savvas M. Koushiappas. Constraints on sterile neutrino dark matter. *Phys. Rev. D*, 74(2):023527, July 2006. doi: 10.1103/PhysRevD.74.023527.

[115] Mei-Yu Wang, John F. Cherry, Shunsaku Horiuchi, and Louis E. Strigari. Bounds on Resonantly-Produced Sterile Neutrinos from Phase Space Densities of Milky Way Dwarf Galaxies. *arXiv e-prints*, art. arXiv:1712.04597, December 2017.

[116] Kevork N. Abazajian. Sterile neutrinos in cosmology. *Phys. Rep.*, 711:1–28, November 2017. doi: 10.1016/j.physrep.2017.10.003.

[117] Louis E. Strigari, Savvas M. Koushiappas, James S. Bullock, and Manoj Kaplinghat. Precise constraints on the dark matter content of milky way dwarf galaxies for gamma-ray experiments. *Phys. Rev. D*, 75:083526, Apr 2007. doi: 10.1103/PhysRevD.75.083526. URL https://link.aps.org/doi/10.1103/PhysRevD.75.083526.

[118] Louis E. Strigari, Savvas M. Koushiappas, James S. Bullock, Manoj Kaplinghat, Joshua D. Simon, Marla Geha, and Beth Willman. The Most Dark-Matter-dominated Galaxies: Predicted Gamma-Ray Signals from the Faintest Milky Way Dwarfs. *Astrophys. J.*, 678(2):614–620, May 2008. doi: 10.1086/529488.

[119] Matthew Walker. Dark Matter in the Galactic Dwarf Spheroidal Satellites. In Terry D. Oswalt and Gerard Gilmore, editors, *Planets, Stars and Stellar Systems. Volume 5: Galactic Structure and Stellar Populations*, volume 5, page 1039. 2013. doi: 10.1007/978-94-007-5612-0_20.

[120] R. D. Peccei and Helen R. Quinn. CP conservation in the presence of pseudoparticles. *Phys. Rev. Lett.*, 38:1440–1443, Jun 1977. doi: 10.1103/PhysRevLett.38.1440. URL https://link.aps.org/doi/10.1103/PhysRevLett.38.1440.

[121] R. D. Peccei and Helen R. Quinn. Constraints imposed by CP conservation in the presence of pseudoparticles. *Phys. Rev. D*, 16:1791–1797, Sep 1977. doi: 10.1103/PhysRevD.16.1791. URL https://link.aps.org/doi/10.1103/PhysRevD.16.1791.

[122] Steven Weinberg. A new light boson? *Phys. Rev. Lett.*, 40:223–226, Jan 1978. doi: 10.1103/PhysRevLett.40.223. URL https://link.aps.org/doi/10.1103/PhysRevLett.40.223.

[123] David J. E. Marsh. Axion cosmology. *Phys. Rep.*, 643:1–79, July 2016. doi: 10.1016/j.physrep.2016.06.005.

[124] Abril Suárez, Victor H. Robles, and Tonatiuh Matos. A review on the scalar field/bose-einstein condensate dark matter model. In Claudia Moreno González, José Edgar Madriz Aguilar, and Luz Marina Reyes Barrera, editors, *Accelerated Cosmic Expansion*, pages 107–142, Cham, 2014. Springer International Publishing. ISBN 978-3-319-02063-1.

[125] Wayne Hu, Rennan Barkana, and Andrei Gruzinov. Fuzzy cold dark matter: The wave properties of ultralight particles. *Phys. Rev. Lett.*, 85:1158–1161, Aug 2000. doi: 10.1103/PhysRevLett.85.1158. URL https://link.aps.org/doi/10.1103/PhysRevLett.85.1158.

[126] David J. E. Marsh and Joseph Silk. A model for halo formation with axion mixed dark matter. *Mon. Not. R. Astron. Soc.*, 437(3):2652–2663, January 2014. doi: 10.1093/mnras/stt2079.

[127] Hsi-Yu Schive, Tzihong Chiueh, and Tom Broadhurst. Cosmic structure as the quantum interference of a coherent dark wave. *Nature Physics*, 10(7):496–499, July 2014. doi: 10.1038/nphys2996.

[128] Tonatiuh Matos and L. Arturo Ureña López. Further analysis of a cosmological model with quintessence and scalar dark matter. *Phys. Rev. D*, 63:063506, Feb 2001. doi: 10.1103/PhysRevD.63.063506. URL https://link.aps.org/doi/10.1103/PhysRevD.63.063506.

[129] Tonatiuh Matos and L Arturo Ureña-López. Quintessence and scalar dark matter in the universe. *Classical and Quantum Gravity*, 17(13):L75–L81, jun 2000. doi: 10.1088/0264-9381/17/13/101. URL https://doi.org/10.1088/0264-9381/17/13/101.

[130] Varun Sahni and Limin Wang. New cosmological model of quintessence and dark matter. *Phys. Rev. D*, 62:103517, Oct 2000. doi: 10.1103/PhysRevD.62.103517. URL https://link.aps.org/doi/10.1103/PhysRevD.62.103517.

[131] William H. Press, Barbara S. Ryden, and David N. Spergel. Single mechanism for generating large-scale structure and providing dark missing matter. *Phys. Rev. Lett.*, 64:1084–1087, Mar 1990. doi: 10.1103/PhysRevLett.64.1084. URL https://link.aps.org/doi/10.1103/PhysRevLett.64.1084.

[132] Sang-Jin Sin. Late-time phase transition and the galactic halo as a bose liquid. *Phys. Rev. D*, 50:3650–3654, Sep 1994. doi: 10.1103/PhysRevD.50.3650. URL https://link.aps.org/doi/10.1103/PhysRevD.50.3650.

[133] Alexandre Arbey, Julien Lesgourgues, and Pierre Salati. Quintessential halos around galaxies. *Phys. Rev. D*, 64:123528, Nov 2001. doi: 10.1103/PhysRevD.64.123528. URL https://link.aps.org/doi/10.1103/PhysRevD.64.123528.

[134] M. Iu. Khlopov, B. A. Malomed, and Ia. B. Zeldovich. Gravitational instability of scalar fields and formation of primordial black holes. *Mon. Not. R. Astron. Soc.*, 215:575–589, August 1985. doi: 10.1093/mnras/215.4.575.

[135] Tanmay Kumar Poddar, Subhendra Mohanty, and Soumya Jana. Constraints on long range force from perihelion precession of planets in a gauged L_e-$L_{\mu,\tau}$ scenario. *European Physical Journal C*, 81(4):286, April 2021. doi: 10.1140/epjc/s10052-021-09078-9.

[136] L. F. Abbott and P. Sikivie. A cosmological bound on the invisible axion. *Physics Letters B*, 120(1-3):133–136, January 1983. doi: 10.1016/0370-2693(83)90638-X.

[137] Michael Dine and Willy Fischler. The not-so-harmless axion. *Physics Letters B*, 120 (1-3):137–141, January 1983. doi: 10.1016/0370-2693(83)90639-1.

[138] John Preskill, Mark B. Wise, and Frank Wilczek. Cosmology of the invisible axion. *Physics Letters B*, 120(1-3):127–132, January 1983. doi: 10.1016/0370-2693(83)90637-8.

[139] Hsi-Yu Schive, Ming-Hsuan Liao, Tak-Pong Woo, Shing-Kwong Wong, Tzihong Chiueh, Tom Broadhurst, and W-Y. Pauchy Hwang. Understanding the core-halo relation of quantum wave dark matter from 3d simulations. *Phys. Rev. Lett.*, 113:261302, Dec 2014. doi: 10.1103/PhysRevLett.113.261302. URL https://link.aps.org/doi/10.1103/PhysRevLett.113.261302.

[140] Philip Mocz, Lachlan Lancaster, Anastasia Fialkov, Fernando Becerra, and Pierre-Henri Chavanis. Schrödinger-poisson–vlasov-poisson correspondence. *Phys. Rev. D*, 97: 083519, Apr 2018. doi: 10.1103/PhysRevD.97.083519. URL https://link.aps.org/doi/10.1103/PhysRevD.97.083519.

[141] Katelin Schutz. Subhalo mass function and ultralight bosonic dark matter. *Phys. Rev. D*, 101:123026, Jun 2020. doi: 10.1103/PhysRevD.101.123026. URL https://link.aps.org/doi/10.1103/PhysRevD.101.123026.

[142] Mohammadtaher Safarzadeh and David N. Spergel. Ultra-light dark matter is incompatible with the milky way's dwarf satellites. *Astrophys. J.*, 893(1):21, apr 2020. doi: 10.3847/1538-4357/ab7db2. URL https://doi.org/10.3847%2F1538-4357%2Fab7db2.

[143] Abraham Loeb. Quantum Tunneling of Fuzzy Dark Matter out of Satellite Galaxies. *Research Notes of the American Astronomical Society*, 6(6):120, June 2022. doi: 10.3847/2515-5172/ac7646.

[144] J. H. Jeans. Bakerian lecture, 1917: The configurations of rotating compressible masses. *Philosophical Transactions of the Royal Society of London. Series A, Containing Papers of a Mathematical or Physical Character*, 218:157–210, 1919. ISSN 02643952. URL http://www.jstor.org/stable/91076.

[145] K. S. Oh, D. N. C. Lin, and S. J. Aarseth. On the Tidal Disruption of Dwarf Spheroidal Galaxies around the Galaxy. *Astrophys. J.*, 442:142, March 1995. doi: 10.1086/175429.

[146] Slawomir Piatek and Carlton Pryor. The Effect of Galactic Tides on the Apparent Mass-To-Light Ratios in Dwarf Spheroidal Galaxies. *Astron. J.*, 109:1071, March 1995. doi: 10.1086/117342.

[147] J. I. Read, M. I. Wilkinson, N. Wyn Evans, G. Gilmore, and Jan T. Kleyna. The importance of tides for the Local Group dwarf spheroidals. *Mon. Not. R. Astron. Soc.*, 367(1):387–399, March 2006. doi: 10.1111/j.1365-2966.2005.09959.x.

[148] H. C. Plummer. On the problem of distribution in globular star clusters. *Mon. Not. R. Astron. Soc.*, 71:460–470, March 1911. doi: 10.1093/mnras/71.5.460.

[149] F. Feroz, M. P. Hobson, and M. Bridges. MultiNest: an efficient and robust Bayesian inference tool for cosmology and particle physics. *Mon. Not. R. Astron. Soc.*, 398(4): 1601–1614, 09 2009. ISSN 0035-8711. doi: 10.1111/j.1365-2966.2009.14548.x. URL https://doi.org/10.1111/j.1365-2966.2009.14548.x.

[150] J. Buchner, A. Georgakakis, K. Nandra, L. Hsu, C. Rangel, M. Brightman, A. Merloni, M. Salvato, J. Donley, and D. Kocevski. X-ray spectral modelling of the AGN obscuring region in the CDFS: Bayesian model selection and catalogue. *Astronomy and Astrophysics*, 564:A125, April 2014. doi: 10.1051/0004-6361/201322971.

[151] Julio F. Navarro, Carlos S. Frenk, and Simon D. M. White. The Structure of Cold Dark Matter Halos. *Astrophys. J.*, 462:563, May 1996. doi: 10.1086/177173.

[152] Hongsheng Zhao. Analytical models for galactic nuclei. *Mon. Not. R. Astron. Soc.*, 278(2):488–496, January 1996. doi: 10.1093/mnras/278.2.488.

[153] Lars Hernquist. An Analytical Model for Spherical Galaxies and Bulges. *Astrophys. J.*, 356:359, June 1990. doi: 10.1086/168845.

[154] Oleg Y. Gnedin, Daniel Ceverino, Nickolay Y. Gnedin, Anatoly A. Klypin, Andrey V. Kravtsov, Robyn Levine, Daisuke Nagai, and Gustavo Yepes. Halo Contraction Effect in Hydrodynamic Simulations of Galaxy Formation. *arXiv e-prints*, art. arXiv:1108.5736, August 2011.

[155] Anatoly Klypin, HongSheng Zhao, and Rachel S. Somerville. ΛCDM-based Models for the Milky Way and M31. I. Dynamical Models. *Astrophys. J.*, 573(2):597–613, July 2002. doi: 10.1086/340656.

[156] Matthew Walker. *Dark Matter in the Galactic Dwarf Spheroidal Satellites*, pages 1039–1089. Springer Netherlands, Dordrecht, 2013. ISBN 978-94-007-5612-0. doi: 10.1007/978-94-007-5612-0_20. URL https://doi.org/10.1007/978-94-007-5612-0_20.

[157] M. White. The mass of a halo. *Astron. Astrophys.*, 367:27–32, February 2001. doi: 10.1051/0004-6361:20000357.

[158] Alma X. González-Morales, David J. E. Marsh, Jorge Peñarrubia, and Luis A. Ureña-López. Unbiased constraints on ultralight axion mass from dwarf spheroidal galaxies. *Mon. Not. R. Astron. Soc.*, 472(2):1346–1360, 08 2017. ISSN 0035-8711. doi: 10.1093/mnras/stx1941. URL https://doi.org/10.1093/mnras/stx1941.

[159] David J. E. Marsh and Ana-Roxana Pop. Axion dark matter, solitons and the cusp-core problem. *Mon. Not. R. Astron. Soc.*, 451(3):2479–2492, August 2015. doi: 10.1093/mnras/stv1050.

[160] Matthew G. Walker, Mario Mateo, and Edward W. Olszewski. Stellar Velocities in the Carina, Fornax, Sculptor, and Sextans dSph Galaxies: Data From the Magellan/MMFS Survey. *Astrophys. J.*, 137(2):3100–3108, February 2009. doi: 10.1088/0004-6256/137/2/3100.

[161] Matthew G. Walker, Mario Mateo, Edward W. Olszewski, Rebecca Bernstein, Bodhisattva Sen, and Michael Woodroofe. The Michigan/MIKE Fiber System Survey of

Stellar Radial Velocities in Dwarf Spheroidal Galaxies: Acquisition and Reduction of Data. *Astrophys. J. Suppl. Ser.*, 171(2):389–418, August 2007. doi: 10.1086/517886.

[162] Matthew G. Walker, Mario Mateo, Edward W. Olszewski, Bodhisattva Sen, and Michael Woodroofe. Clean Kinematic Samples in Dwarf Spheroidals: An Algorithm for Evaluating Membership and Estimating Distribution Parameters When Contamination is Present. *Astron. J.*, 137(2):3109–3138, February 2009. doi: 10.1088/0004-6256/137/2/3109.

[163] Meghin E. Spencer, Mario Mateo, Edward W. Olszewski, Matthew G. Walker, Alan W. McConnachie, and Evan N. Kirby. The Binary Fraction of Stars in Dwarf Galaxies: The Cases of Draco and Ursa Minor. *Astron. J.*, 156(6):257, December 2018. doi: 10.3847/1538-3881/aae3e4.

[164] M. Irwin and D. Hatzidimitriou. Structural parameters for the Galactic dwarf spheroidals. *Mon. Not. R. Astron. Soc.*, 277(4):1354–1378, December 1995. doi: 10.1093/mnras/277.4.1354.

[165] F. Ochsenbein, P. Bauer, and J. Marcout. The VizieR database of astronomical catalogues. *Astron. Astrophys. Suppl. Ser.*, 143:23–32, April 2000. doi: 10.1051/aas:2000169.

[166] Louis E. Strigari, James S. Bullock, Manoj Kaplinghat, Andrey V. Kravtsov, Oleg Y. Gnedin, Kevork Abazajian, and Anatoly A. Klypin. A Large Dark Matter Core in the Fornax Dwarf Spheroidal Galaxy? *Astrophys. J.*, 652(1):306–312, November 2006. doi: 10.1086/506381.

[167] Matthew G. Walker, Mario Mateo, Edward W. Olszewski, Jorge Peñarrubia, N. Wyn Evans, and Gerard Gilmore. A Universal Mass Profile for Dwarf Spheroidal Galaxies? *Astrophys. J.*, 704(2):1274–1287, October 2009. doi: 10.1088/0004-637X/704/2/1274.

[168] Louis E. Strigari, James S. Bullock, Manoj Kaplinghat, Joshua D. Simon, Marla Geha, Beth Willman, and Matthew G. Walker. A common mass scale for satellite galaxies of the Milky Way. *Nature*, 454(7208):1096–1097, August 2008. doi: 10.1038/nature07222.

[169] D Erkal, V Belokurov, C F P Laporte, S E Koposov, T S Li, C J Grillmair, N Kallivayalil, A M Price-Whelan, N W Evans, K Hawkins, D Hendel, C Mateu, J F Navarro, A del Pino, C T Slater, S T Sohn, and (The OATs: Orphan Aspen Treasury Collaboration). The total mass of the Large Magellanic Cloud from its perturbation on the Orphan stream. *Mon. Not. R. Astron. Soc.*, 487(2):2685–2700, 05 2019. ISSN 0035-8711. doi: 10.1093/mnras/stz1371. URL https://doi.org/10.1093/mnras/stz1371.

[170] Joseph Silk. Feedback by massive black holes in gas-rich dwarf galaxies. *Astrophys. J.*, 839(1):L13, apr 2017. doi: 10.3847/2041-8213/aa67da. URL https://doi.org/10.3847/2041-8213/aa67da.

[171] Amy E. Reines, Gregory R. Sivakoff, Kelsey E. Johnson, and Crystal L. Brogan. An actively accreting massive black hole in the dwarf starburst galaxy Henize2-10. *Nature*, 470(7332):66–68, February 2011. doi: 10.1038/nature09724.

[172] M. J. Bustamante-Rosell, Eva Noyola, Karl Gebhardt, Maximilian H. Fabricius, Ximena Mazzalay, Jens Thomas, and Greg Zeimann. Dynamical Analysis of the Dark Matter and Central Black Hole Mass in the Dwarf Spheroidal Leo I. *Astrophys. J.*, 921(2):107, November 2021. doi: 10.3847/1538-4357/ac0c79.

[173] Harold Jeffreys. *International series of monographs on physics*. Oxford University Press, 1961.

[174] D. Martínez-Delgado, J. Alonso-García, A. Aparicio, and M. A. Gómez-Flechoso. A Tidal Extension in the Ursa Minor Dwarf Spheroidal Galaxy. *Astrophys. J. Lett.*, 549 (1):L63–L66, March 2001. doi: 10.1086/319150.

[175] Andrew B. Pace, Gregory D. Martinez, Manoj Kaplinghat, and Ricardo R. Muñoz. Evidence for substructure in Ursa Minor dwarf spheroidal galaxy using a Bayesian object detection method. *Mon. Not. R. Astron. Soc.*, 442(2):1718–1730, 06 2014. ISSN 0035-8711. doi: 10.1093/mnras/stu938. URL https://doi.org/10.1093/mnras/stu938.

[176] Matthew G. Walker and Jorge Peñarrubia. A Method for Measuring (Slopes of) the Mass Profiles of Dwarf Spheroidal Galaxies. *Astrophys. J.*, 742(1):20, November 2011. doi: 10.1088/0004-637X/742/1/20.

[177] Raffaele Pascale, Lorenzo Posti, Carlo Nipoti, and James Binney. Action-based dynamical models of dwarf spheroidal galaxies: application to Fornax. *Mon. Not. R. Astron. Soc.*, 480(1):927–946, 07 2018. ISSN 0035-8711. doi: 10.1093/mnras/sty1860. URL https://doi.org/10.1093/mnras/sty1860.

[178] Kohei Hayashi, Masashi Chiba, and Tomoaki Ishiyama. Diversity of Dark Matter Density Profiles in the Galactic Dwarf Spheroidal Satellites. *Astrophys. J.*, 904(1):45, November 2020. doi: 10.3847/1538-4357/abbe0a.

[179] J. I. Read, M. G. Walker, and P. Steger. Dark matter heats up in dwarf galaxies. *Mon. Not. R. Astron. Soc.*, 484(1):1401–1420, March 2019. doi: 10.1093/mnras/sty3404.

[180] Savvas M. Koushiappas, James S. Bullock, and Avishai Dekel. Massive black hole seeds from low angular momentum material. *Mon. Not. R. Astron. Soc.*, 354(1):292–304, October 2004. doi: 10.1111/j.1365-2966.2004.08190.x.

[181] Stephen Hawking. Gravitationally Collapsed Objects of Very Low Mass. *Monthly Notices of the Royal Astronomical Society*, 152(1):75–78, 04 1971. ISSN 0035-8711. doi: 10.1093/mnras/152.1.75. URL https://doi.org/10.1093/mnras/152.1.75.

[182] B. J. Carr. The primordial black hole mass spectrum. *The Astrophysical Journal*, 201: 1–19, October 1975. doi: 10.1086/153853.

[183] B. J. Carr, J. H. Gilbert, and James E. Lidsey. Black hole relics and inflation: Limits on blue perturbation spectra. *Phys. Rev. D*, 50:4853–4867, Oct 1994. doi: 10.1103/PhysRevD.50.4853. URL https://link.aps.org/doi/10.1103/PhysRevD.50.4853.

[184] M. Yu. Khlopov and A. G. Polnarev. Primordial black holes as a cosmological test of grand unification. *Physics Letters B*, 97(3-4):383–387, December 1980. doi: 10.1016/0370-2693(80)90624-3.

[185] B. J. Carr and James E. Lidsey. Primordial black holes and generalized constraints on chaotic inflation. *Phys. Rev. D*, 48:543–553, Jul 1993. doi: 10.1103/PhysRevD.48.543. URL https://link.aps.org/doi/10.1103/PhysRevD.48.543.

[186] Bernard Carr and Florian Kühnel. Primordial Black Holes as Dark Matter: Recent Developments. *Annual Review of Nuclear and Particle Science*, 70:355–394, October 2020. doi: 10.1146/annurev-nucl-050520-125911.

[187] S. W. Hawking. Black holes from cosmic strings. *Physics Letters B*, 231(3):237–239, November 1989. doi: 10.1016/0370-2693(89)90206-2.

[188] B. J. Carr. Some cosmological consequences of primordial black-hole evaporations. *Astrophys. J.*, 206:8–25, May 1976. doi: 10.1086/154351.

[189] Sean E. Cutchin, John H. Simonetti, Steven W. Ellingson, Amanda S. Larracuente, and Michael J. Kavic. Constraining the rate of primordial black hole explosions and extra-dimension scale using a low-frequency radio antenna array. *Publications of the Astronomical Society of the Pacific*, 127(958):1269, dec 2015. doi: 10.1086/684195. URL https://dx.doi.org/10.1086/684195.

[190] P. Kiraly, J. Szabelski, J. Wdowczyk, and A. W. Wolfendale. Antiprotons in the cosmic radiation. *Nature*, 293(5828):120–122, September 1981. doi: 10.1038/293120a0.

[191] Jane H. MacGibbon and B. J. Carr. Cosmic Rays from Primordial Black Holes. *Astrophys. J.*, 371:447, April 1991. doi: 10.1086/169909.

[192] Bernard Carr, Kazunori Kohri, Yuuiti Sendouda, and Jun'ichi Yokoyama. Constraints on primordial black holes. *Reports on Progress in Physics*, 84(11):116902, November 2021. doi: 10.1088/1361-6633/ac1e31.

[193] Bernard Carr and Florian Kuhnel. Primordial black holes as dark matter: Recent developments, 2020.

[194] B. J. Carr, Kazunori Kohri, Yuuiti Sendouda, and Jun'ichi Yokoyama. Constraints on primordial black holes from the galactic gamma-ray background. *Phys. Rev. D*, 94:

044029, Aug 2016. doi: 10.1103/PhysRevD.94.044029. URL https://link.aps.org/doi/10.1103/PhysRevD.94.044029.

[195] Michele Maggiore. *Gravitational Waves: Volume 1: Theory and Experiments*. Oxford University Press, 10 2007. ISBN 9780198570745. doi: 10.1093/acprof:oso/9780198570745.001.0001. URL https://doi.org/10.1093/acprof:oso/9780198570745.001.0001.

[196] A. A. Michelson and E. W. Morley. On the relative motion of the earth and the luminiferous ether. *American Journal of Science*, s3-34(203):333–345, 11 1887. doi: 10.2475/ajs.s3-34.203.333.

[197] B. P. Abbott, R. Abbott, T. D. Abbott, M. R. Abernathy, F. Acernese, K. Ackley, C. Adams, T. Adams, P. Addesso, R. X. Adhikari, V. B. Adya, C. Affeldt, M. Agathos, K. Agatsuma, N. Aggarwal, O. D. Aguiar, L. Aiello, A. Ain, P. Ajith, B. Allen, A. Allocca, P. A. Altin, S. B. Anderson, W. G. Anderson, K. Arai, M. A. Arain, M. C. Araya, C. C. Arceneaux, J. S. Areeda, N. Arnaud, K. G. Arun, S. Ascenzi, G. Ashton, M. Ast, S. M. Aston, P. Astone, P. Aufmuth, C. Aulbert, S. Babak, P. Bacon, M. K. M. Bader, P. T. Baker, F. Baldaccini, G. Ballardin, S. W. Ballmer, J. C. Barayoga, S. E. Barclay, B. C. Barish, D. Barker, F. Barone, B. Barr, L. Barsotti, M. Barsuglia, D. Barta, J. Bartlett, M. A. Barton, I. Bartos, R. Bassiri, A. Basti, J. C. Batch, C. Baune, V. Bavigadda, M. Bazzan, B. Behnke, M. Bejger, C. Belczynski, A. S. Bell, C. J. Bell, B. K. Berger, J. Bergman, G. Bergmann, C. P. L. Berry, D. Bersanetti, A. Bertolini, J. Betzwieser, S. Bhagwat, R. Bhandare, I. A. Bilenko, G. Billingsley, J. Birch, R. Birney, O. Birnholtz, S. Biscans, A. Bisht, M. Bitossi, C. Biwer, M. A. Bizouard, J. K. Blackburn, C. D. Blair, D. G. Blair, R. M. Blair, S. Bloemen, O. Bock, T. P. Bodiya, M. Boer, G. Bogaert, C. Bogan, A. Bohe, P. Bojtos, C. Bond, F. Bondu, R. Bonnand, B. A. Boom, R. Bork, V. Boschi, S. Bose, Y. Bouffanais, A. Bozzi, C. Bradaschia, P. R. Brady, V. B. Braginsky, M. Branchesi, J. E. Brau, T. Briant, A. Brillet, M. Brinkmann, V. Brisson, P. Brockill, A. F. Brooks, D. A. Brown, D. D. Brown, N. M. Brown, C. C. Buchanan, A. Buikema, T. Bulik, H. J. Bulten, A. Buonanno, D. Buskulic, C. Buy, R. L. Byer, M. Cabero, L. Cadonati, G. Cagnoli, C. Cahillane, J. Calderón Bustillo,

T. Callister, E. Calloni, J. B. Camp, K. C. Cannon, J. Cao, C. D. Capano, E. Capocasa, F. Carbognani, S. Caride, J. Casanueva Diaz, C. Casentini, S. Caudill, M. Cavaglià, F. Cavalier, R. Cavalieri, G. Cella, C. B. Cepeda, L. Cerboni Baiardi, G. Cerretani, E. Cesarini, R. Chakraborty, T. Chalermsongsak, S. J. Chamberlin, M. Chan, S. Chao, P. Charlton, E. Chassande-Mottin, H. Y. Chen, Y. Chen, C. Cheng, A. Chincarini, A. Chiummo, H. S. Cho, M. Cho, J. H. Chow, N. Christensen, Q. Chu, S. Chua, S. Chung, G. Ciani, F. Clara, J. A. Clark, F. Cleva, E. Coccia, P.-F. Cohadon, A. Colla, C. G. Collette, L. Cominsky, M. Constancio, A. Conte, L. Conti, D. Cook, T. R. Corbitt, N. Cornish, A. Corsi, S. Cortese, C. A. Costa, M. W. Coughlin, S. B. Coughlin, J.-P. Coulon, S. T. Countryman, P. Couvares, E. E. Cowan, D. M. Coward, M. J. Cowart, D. C. Coyne, R. Coyne, K. Craig, J. D. E. Creighton, T. D. Creighton, J. Cripe, S. G. Crowder, A. M. Cruise, A. Cumming, L. Cunningham, E. Cuoco, T. Dal Canton, S. L. Danilishin, S. D'Antonio, K. Danzmann, N. S. Darman, C. F. Da Silva Costa, V. Dattilo, I. Dave, H. P. Daveloza, M. Davier, G. S. Davies, E. J. Daw, R. Day, S. De, D. DeBra, G. Debreczeni, J. Degallaix, M. De Laurentis, S. Deléglise, W. Del Pozzo, T. Denker, T. Dent, H. Dereli, V. Dergachev, R. T. DeRosa, R. De Rosa, R. DeSalvo, S. Dhurandhar, M. C. Díaz, L. Di Fiore, M. Di Giovanni, A. Di Lieto, S. Di Pace, I. Di Palma, A. Di Virgilio, G. Dojcinoski, V. Dolique, F. Donovan, K. L. Dooley, S. Doravari, R. Douglas, T. P. Downes, M. Drago, R. W. P. Drever, J. C. Driggers, Z. Du, M. Ducrot, S. E. Dwyer, T. B. Edo, M. C. Edwards, A. Effler, H.-B. Eggenstein, P. Ehrens, J. Eichholz, S. S. Eikenberry, W. Engels, R. C. Essick, T. Etzel, M. Evans, T. M. Evans, R. Everett, M. Factourovich, V. Fafone, H. Fair, S. Fairhurst, X. Fan, Q. Fang, S. Farinon, B. Farr, W. M. Farr, M. Favata, M. Fays, H. Fehrmann, M. M. Fejer, D. Feldbaum, I. Ferrante, E. C. Ferreira, F. Ferrini, F. Fidecaro, L. S. Finn, I. Fiori, D. Fiorucci, R. P. Fisher, R. Flaminio, M. Fletcher, H. Fong, J.-D. Fournier, S. Franco, S. Frasca, F. Frasconi, M. Frede, Z. Frei, A. Freise, R. Frey, V. Frey, T. T. Fricke, P. Fritschel, V. V. Frolov, P. Fulda, M. Fyffe, H. A. G. Gabbard, J. R. Gair, L. Gammaitoni, S. G. Gaonkar, F. Garufi, A. Gatto, G. Gaur, N. Gehrels, G. Gemme, B. Gendre, E. Genin, A. Gennai, J. George, L. Gergely, V. Germain, Abhirup Ghosh, Archisman Ghosh, S. Ghosh, J. A. Giaime, K. D. Giardina, A. Giazotto, K. Gill,

A. Glaefke, J. R. Gleason, E. Goetz, R. Goetz, L. Gondan, G. González, J. M. Gonzalez Castro, A. Gopakumar, N. A. Gordon, M. L. Gorodetsky, S. E. Gossan, M. Gosselin, R. Gouaty, C. Graef, P. B. Graff, M. Granata, A. Grant, S. Gras, C. Gray, G. Greco, A. C. Green, R. J. S. Greenhalgh, P. Groot, H. Grote, S. Grunewald, G. M. Guidi, X. Guo, A. Gupta, M. K. Gupta, K. E. Gushwa, E. K. Gustafson, R. Gustafson, J. J. Hacker, B. R. Hall, E. D. Hall, G. Hammond, M. Haney, M. M. Hanke, J. Hanks, C. Hanna, M. D. Hannam, J. Hanson, T. Hardwick, J. Harms, G. M. Harry, I. W. Harry, M. J. Hart, M. T. Hartman, C.-J. Haster, K. Haughian, J. Healy, J. Heefner, A. Heidmann, M. C. Heintze, G. Heinzel, H. Heitmann, P. Hello, G. Hemming, M. Hendry, I. S. Heng, J. Hennig, A. W. Heptonstall, M. Heurs, S. Hild, D. Hoak, K. A. Hodge, D. Hofman, S. E. Hollitt, K. Holt, D. E. Holz, P. Hopkins, D. J. Hosken, J. Hough, E. A. Houston, E. J. Howell, Y. M. Hu, S. Huang, E. A. Huerta, D. Huet, B. Hughey, S. Husa, S. H. Huttner, T. Huynh-Dinh, A. Idrisy, N. Indik, D. R. Ingram, R. Inta, H. N. Isa, J.-M. Isac, M. Isi, G. Islas, T. Isogai, B. R. Iyer, K. Izumi, M. B. Jacobson, T. Jacqmin, H. Jang, K. Jani, P. Jaranowski, S. Jawahar, F. Jiménez-Forteza, W. W. Johnson, N. K. Johnson-McDaniel, D. I. Jones, R. Jones, R. J. G. Jonker, L. Ju, K. Haris, C. V. Kalaghatgi, V. Kalogera, S. Kandhasamy, G. Kang, J. B. Kanner, S. Karki, M. Kasprzack, E. Katsavounidis, W. Katzman, S. Kaufer, T. Kaur, K. Kawabe, F. Kawazoe, F. Kéfélian, M. S. Kehl, D. Keitel, D. B. Kelley, W. Kells, R. Kennedy, D. G. Keppel, J. S. Key, A. Khalaidovski, F. Y. Khalili, I. Khan, S. Khan, Z. Khan, E. A. Khazanov, N. Kijbunchoo, C. Kim, J. Kim, K. Kim, Nam-Gyu Kim, Namjun Kim, Y.-M. Kim, E. J. King, P. J. King, D. L. Kinzel, J. S. Kissel, L. Kleybolte, S. Klimenko, S. M. Koehlenbeck, K. Kokeyama, S. Koley, V. Kondrashov, A. Kontos, S. Koranda, M. Korobko, W. Z. Korth, I. Kowalska, D. B. Kozak, V. Kringel, B. Krishnan, A. Królak, C. Krueger, G. Kuehn, P. Kumar, R. Kumar, L. Kuo, A. Kutynia, P. Kwee, B. D. Lackey, M. Landry, J. Lange, B. Lantz, P. D. Lasky, A. Lazzarini, C. Lazzaro, P. Leaci, S. Leavey, E. O. Lebigot, C. H. Lee, H. K. Lee, H. M. Lee, K. Lee, A. Lenon, M. Leonardi, J. R. Leong, N. Leroy, N. Letendre, Y. Levin, B. M. Levine, T. G. F. Li, A. Libson, T. B. Littenberg, N. A. Lockerbie, J. Logue, A. L. Lombardi, L. T. London, J. E. Lord, M. Lorenzini, V. Loriette, M. Lormand, G. Losurdo,

J. D. Lough, C. O. Lousto, G. Lovelace, H. Lück, A. P. Lundgren, J. Luo, R. Lynch, Y. Ma, T. MacDonald, B. Machenschalk, M. MacInnis, D. M. Macleod, F. Magaña Sandoval, R. M. Magee, M. Mageswaran, E. Majorana, I. Maksimovic, V. Malvezzi, N. Man, I. Mandel, V. Mandic, V. Mangano, G. L. Mansell, M. Manske, M. Mantovani, F. Marchesoni, F. Marion, S. Márka, Z. Márka, A. S. Markosyan, E. Maros, F. Martelli, L. Martellini, I. W. Martin, R. M. Martin, D. V. Martynov, J. N. Marx, K. Mason, A. Masserot, T. J. Massinger, M. Masso-Reid, F. Matichard, L. Matone, N. Mavalvala, N. Mazumder, G. Mazzolo, R. McCarthy, D. E. McClelland, S. McCormick, S. C. McGuire, G. McIntyre, J. McIver, D. J. McManus, S. T. McWilliams, D. Meacher, G. D. Meadors, J. Meidam, A. Melatos, G. Mendell, D. Mendoza-Gandara, R. A. Mercer, E. Merilh, M. Merzougui, S. Meshkov, C. Messenger, C. Messick, P. M. Meyers, F. Mezzani, H. Miao, C. Michel, H. Middleton, E. E. Mikhailov, L. Milano, J. Miller, M. Millhouse, Y. Minenkov, J. Ming, S. Mirshekari, C. Mishra, S. Mitra, V. P. Mitrofanov, G. Mitselmakher, R. Mittleman, A. Moggi, M. Mohan, S. R. P. Mohapatra, M. Montani, B. C. Moore, C. J. Moore, D. Moraru, G. Moreno, S. R. Morriss, K. Mossavi, B. Mours, C. M. Mow-Lowry, C. L. Mueller, G. Mueller, A. W. Muir, Arunava Mukherjee, D. Mukherjee, S. Mukherjee, N. Mukund, A. Mullavey, J. Munch, D. J. Murphy, P. G. Murray, A. Mytidis, I. Nardecchia, L. Naticchioni, R. K. Nayak, V. Necula, K. Nedkova, G. Nelemans, M. Neri, A. Neunzert, G. Newton, T. T. Nguyen, A. B. Nielsen, S. Nissanke, A. Nitz, F. Nocera, D. Nolting, M. E. N. Normandin, L. K. Nuttall, J. Oberling, E. Ochsner, J. O'Dell, E. Oelker, G. H. Ogin, J. J. Oh, S. H. Oh, F. Ohme, M. Oliver, P. Oppermann, Richard J. Oram, B. O'Reilly, R. O'Shaughnessy, C. D. Ott, D. J. Ottaway, R. S. Ottens, H. Overmier, B. J. Owen, A. Pai, S. A. Pai, J. R. Palamos, O. Palashov, C. Palomba, A. Pal-Singh, H. Pan, Y. Pan, C. Pankow, F. Pannarale, B. C. Pant, F. Paoletti, A. Paoli, M. A. Papa, H. R. Paris, W. Parker, D. Pascucci, A. Pasqualetti, R. Passaquieti, D. Passuello, B. Patricelli, Z. Patrick, B. L. Pearlstone, M. Pedraza, R. Pedurand, L. Pekowsky, A. Pele, S. Penn, A. Perreca, H. P. Pfeiffer, M. Phelps, O. Piccinni, M. Pichot, M. Pickenpack, F. Piergiovanni, V. Pierro, G. Pillant, L. Pinard, I. M. Pinto, M. Pitkin, J. H. Poeld, R. Poggiani, P. Popolizio, A. Post, J. Powell, J. Prasad, V. Predoi, S. S.

Premachandra, T. Prestegard, L. R. Price, M. Prijatelj, M. Principe, S. Privitera, R. Prix, G. A. Prodi, L. Prokhorov, O. Puncken, M. Punturo, P. Puppo, M. Pürrer, H. Qi, J. Qin, V. Quetschke, E. A. Quintero, R. Quitzow-James, F. J. Raab, D. S. Rabeling, H. Radkins, P. Raffai, S. Raja, M. Rakhmanov, C. R. Ramet, P. Rapagnani, V. Raymond, M. Razzano, V. Re, J. Read, C. M. Reed, T. Regimbau, L. Rei, S. Reid, D. H. Reitze, H. Rew, S. D. Reyes, F. Ricci, K. Riles, N. A. Robertson, R. Robie, F. Robinet, A. Rocchi, L. Rolland, J. G. Rollins, V. J. Roma, J. D. Romano, R. Romano, G. Romanov, J. H. Romie, D. Rosińska, S. Rowan, A. Rüdiger, P. Ruggi, K. Ryan, S. Sachdev, T. Sadecki, L. Sadeghian, L. Salconi, M. Saleem, F. Salemi, A. Samajdar, L. Sammut, L. M. Sampson, E. J. Sanchez, V. Sandberg, B. Sandeen, G. H. Sanders, J. R. Sanders, B. Sassolas, B. S. Sathyaprakash, P. R. Saulson, O. Sauter, R. L. Savage, A. Sawadsky, P. Schale, R. Schilling, J. Schmidt, P. Schmidt, R. Schnabel, R. M. S. Schofield, A. Schönbeck, E. Schreiber, D. Schuette, B. F. Schutz, J. Scott, S. M. Scott, D. Sellers, A. S. Sengupta, D. Sentenac, V. Sequino, A. Sergeev, G. Serna, Y. Setyawati, A. Sevigny, D. A. Shaddock, T. Shaffer, S. Shah, M. S. Shahriar, M. Shaltev, Z. Shao, B. Shapiro, P. Shawhan, A. Sheperd, D. H. Shoemaker, D. M. Shoemaker, K. Siellez, X. Siemens, D. Sigg, A. D. Silva, D. Simakov, A. Singer, L. P. Singer, A. Singh, R. Singh, A. Singhal, A. M. Sintes, B. J. J. Slagmolen, J. R. Smith, M. R. Smith, N. D. Smith, R. J. E. Smith, E. J. Son, B. Sorazu, F. Sorrentino, T. Souradeep, A. K. Srivastava, A. Staley, M. Steinke, J. Steinlechner, S. Steinlechner, D. Steinmeyer, B. C. Stephens, S. P. Stevenson, R. Stone, K. A. Strain, N. Straniero, G. Stratta, N. A. Strauss, S. Strigin, R. Sturani, A. L. Stuver, T. Z. Summerscales, L. Sun, P. J. Sutton, B. L. Swinkels, M. J. Szczepańczyk, M. Tacca, D. Talukder, D. B. Tanner, M. Tápai, S. P. Tarabrin, A. Taracchini, R. Taylor, T. Theeg, M. P. Thirugnanasambandam, E. G. Thomas, M. Thomas, P. Thomas, K. A. Thorne, K. S. Thorne, E. Thrane, S. Tiwari, V. Tiwari, K. V. Tokmakov, C. Tomlinson, M. Tonelli, C. V. Torres, C. I. Torrie, D. Töyrä, F. Travasso, G. Traylor, D. Trifirò, M. C. Tringali, L. Trozzo, M. Tse, M. Turconi, D. Tuyenbayev, D. Ugolini, C. S. Unnikrishnan, A. L. Urban, S. A. Usman, H. Vahlbruch, G. Vajente, G. Valdes, M. Vallisneri, N. van Bakel, M. van Beuzekom, J. F. J. van den Brand, C. Van Den Broeck, D. C. Vander-

Hyde, L. van der Schaaf, J. V. van Heijningen, A. A. van Veggel, M. Vardaro, S. Vass, M. Vasúth, R. Vaulin, A. Vecchio, G. Vedovato, J. Veitch, P. J. Veitch, K. Venkateswara, D. Verkindt, F. Vetrano, A. Viceré, S. Vinciguerra, D. J. Vine, J.-Y. Vinet, S. Vitale, T. Vo, H. Vocca, C. Vorvick, D. Voss, W. D. Vousden, S. P. Vyatchanin, A. R. Wade, L. E. Wade, M. Wade, S. J. Waldman, M. Walker, L. Wallace, S. Walsh, G. Wang, H. Wang, M. Wang, X. Wang, Y. Wang, H. Ward, R. L. Ward, J. Warner, M. Was, B. Weaver, L.-W. Wei, M. Weinert, A. J. Weinstein, R. Weiss, T. Welborn, L. Wen, P. Weßels, T. Westphal, K. Wette, J. T. Whelan, S. E. Whitcomb, D. J. White, B. F. Whiting, K. Wiesner, C. Wilkinson, P. A. Willems, L. Williams, R. D. Williams, A. R. Williamson, J. L. Willis, B. Willke, M. H. Wimmer, L. Winkelmann, W. Winkler, C. C. Wipf, A. G. Wiseman, H. Wittel, G. Woan, J. Worden, J. L. Wright, G. Wu, J. Yablon, I. Yakushin, W. Yam, H. Yamamoto, C. C. Yancey, M. J. Yap, H. Yu, M. Yvert, A. Zadrożny, L. Zangrando, M. Zanolin, J.-P. Zendri, M. Zevin, F. Zhang, L. Zhang, M. Zhang, Y. Zhang, C. Zhao, M. Zhou, Z. Zhou, X. J. Zhu, M. E. Zucker, S. E. Zuraw, and J. Zweizig. Observation of gravitational waves from a binary black hole merger. *Phys. Rev. Lett.*, 116:061102, Feb 2016. doi: 10.1103/PhysRevLett.116.061102. URL https://link.aps.org/doi/10.1103/PhysRevLett.116.061102.

[198] The LIGO Scientific Collaboration, the Virgo Collaboration, the KAGRA Collaboration, R. Abbott, T. D. Abbott, F. Acernese, K. Ackley, C. Adams, N. Adhikari, R. X. Adhikari, V. B. Adya, C. Affeldt, D. Agarwal, M. Agathos, K. Agatsuma, N. Aggarwal, O. D. Aguiar, L. Aiello, A. Ain, P. Ajith, S. Akcay, T. Akutsu, S. Albanesi, A. Allocca, P. A. Altin, A. Amato, C. Anand, S. Anand, A. Ananyeva, S. B. Anderson, W. G. Anderson, M. Ando, T. Andrade, N. Andres, T. Andrić, S. V. Angelova, S. Ansoldi, J. M. Antelis, S. Antier, S. Appert, Koji Arai, Koya Arai, Y. Arai, S. Araki, A. Araya, M. C. Araya, J. S. Areeda, M. Arène, N. Aritomi, N. Arnaud, M. Arogeti, S. M. Aronson, K. G. Arun, H. Asada, Y. Asali, G. Ashton, Y. Aso, M. Assiduo, S. M. Aston, P. Astone, F. Aubin, C. Austin, S. Babak, F. Badaracco, M. K. M. Bader, C. Badger, S. Bae, Y. Bae, A. M. Baer, S. Bagnasco, Y. Bai, L. Baiotti, J. Baird, R. Bajpai, M. Ball, G. Ballardin, S. W. Ballmer, A. Balsamo, G. Baltus, S. Banagiri,

D. Bankar, J. C. Barayoga, C. Barbieri, B. C. Barish, D. Barker, P. Barneo, F. Barone, B. Barr, L. Barsotti, M. Barsuglia, D. Barta, J. Bartlett, M. A. Barton, I. Bartos, R. Bassiri, A. Basti, M. Bawaj, J. C. Bayley, A. C. Baylor, M. Bazzan, B. Bécsy, V. M. Bedakihale, M. Bejger, I. Belahcene, V. Benedetto, D. Beniwal, T. F. Bennett, J. D. Bentley, M. BenYaala, F. Bergamin, B. K. Berger, S. Bernuzzi, C. P. L. Berry, D. Bersanetti, A. Bertolini, J. Betzwieser, D. Beveridge, R. Bhandare, U. Bhardwaj, D. Bhattacharjee, S. Bhaumik, I. A. Bilenko, G. Billingsley, S. Bini, R. Birney, O. Birnholtz, S. Biscans, M. Bischi, S. Biscoveanu, A. Bisht, B. Biswas, M. Bitossi, M. A. Bizouard, J. K. Blackburn, C. D. Blair, D. G. Blair, R. M. Blair, F. Bobba, N. Bode, M. Boer, G. Bogaert, M. Boldrini, L. D. Bonavena, F. Bondu, E. Bonilla, R. Bonnand, P. Booker, B. A. Boom, R. Bork, V. Boschi, N. Bose, S. Bose, V. Bossilkov, V. Boudart, Y. Bouffanais, A. Bozzi, C. Bradaschia, P. R. Brady, A. Bramley, A. Branch, M. Branchesi, J. Brandt, J. E. Brau, M. Breschi, T. Briant, J. H. Briggs, A. Brillet, M. Brinkmann, P. Brockill, A. F. Brooks, J. Brooks, D. D. Brown, S. Brunett, G. Bruno, R. Bruntz, J. Bryant, T. Bulik, H. J. Bulten, A. Buonanno, R. Buscicchio, D. Buskulic, C. Buy, R. L. Byer, G. S. Cabourn Davies, L. Cadonati, G. Cagnoli, C. Cahillane, J. Calderón Bustillo, J. D. Callaghan, T. A. Callister, E. Calloni, J. Cameron, J. B. Camp, M. Canepa, S. Canevarolo, M. Cannavacciuolo, K. C. Cannon, H. Cao, Z. Cao, E. Capocasa, E. Capote, G. Carapella, F. Carbognani, J. B. Carlin, M. F. Carney, M. Carpinelli, G. Carrillo, G. Carullo, T. L. Carver, J. Casanueva Diaz, C. Casentini, G. Castaldi, S. Caudill, M. Cavaglià, F. Cavalier, R. Cavalieri, M. Ceasar, G. Cella, P. Cerdá-Durán, E. Cesarini, W. Chaibi, K. Chakravarti, S. Chalathadka Subrahmanya, E. Champion, C. H. Chan, C. Chan, C. L. Chan, K. Chan, M. Chan, K. Chandra, P. Chanial, S. Chao, C. E. A. Chapman-Bird, P. Charlton, E. A. Chase, E. Chassande-Mottin, C. Chatterjee, Debarati Chatterjee, Deep Chatterjee, M. Chaturvedi, S. Chaty, K. Chatziioannou, C. Chen, H. Y. Chen, J. Chen, K. Chen, X. Chen, Y. B. Chen, Y. R. Chen, Z. Chen, H. Cheng, C. K. Cheong, H. Y. Cheung, H. Y. Chia, F. Chiadini, C-Y. Chiang, G. Chiarini, R. Chierici, A. Chincarini, M. L. Chiofalo, A. Chiummo, G. Cho, H. S. Cho, R. K. Choudhary, S. Choudhary, N. Christensen, H. Chu, Q. Chu, Y-K. Chu, S. Chua, K. W. Chung, G. Ciani, P. Ciecielag, M. Cieślar, M. Cifaldi, A. A.

Ciobanu, R. Ciolfi, F. Cipriano, A. Cirone, F. Clara, E. N. Clark, J. A. Clark, L. Clarke, P. Clearwater, S. Clesse, F. Cleva, E. Coccia, E. Codazzo, P. F. Cohadon, D. E. Cohen, L. Cohen, M. Colleoni, C. G. Collette, A. Colombo, M. Colpi, C. M. Compton, Jr. Constancio, M., L. Conti, S. J. Cooper, P. Corban, T. R. Corbitt, I. Cordero-Carrión, S. Corezzi, K. R. Corley, N. Cornish, D. Corre, A. Corsi, S. Cortese, C. A. Costa, R. Cotesta, M. W. Coughlin, J. P. Coulon, S. T. Countryman, B. Cousins, P. Couvares, D. M. Coward, M. J. Cowart, D. C. Coyne, R. Coyne, J. D. E. Creighton, T. D. Creighton, A. W. Criswell, M. Croquette, S. G. Crowder, J. R. Cudell, T. J. Cullen, A. Cumming, R. Cummings, L. Cunningham, E. Cuoco, M. Curyło, P. Dabadie, T. Dal Canton, S. Dall'Osso, G. Dálya, A. Dana, L. M. DaneshgaranBajastani, B. D'Angelo, B. Danila, S. Danilishin, S. D'Antonio, K. Danzmann, C. Darsow-Fromm, A. Dasgupta, L. E. H. Datrier, S. Datta, V. Dattilo, I. Dave, M. Davier, D. Davis, M. C. Davis, E. J. Daw, P. F. de Alarcón, R. Dean, D. DeBra, M. Deenadayalan, J. Degallaix, M. De Laurentis, S. Deléglise, V. Del Favero, F. De Lillo, N. De Lillo, W. Del Pozzo, L. M. DeMarchi, F. De Matteis, V. D'Emilio, N. Demos, T. Dent, A. Depasse, R. De Pietri, R. De Rosa, C. De Rossi, R. DeSalvo, R. De Simone, S. Dhurandhar, M. C. Díaz, Jr. Diaz-Ortiz, M., N. A. Didio, T. Dietrich, L. Di Fiore, C. Di Fronzo, C. Di Giorgio, F. Di Giovanni, M. Di Giovanni, T. Di Girolamo, A. Di Lieto, B. Ding, S. Di Pace, I. Di Palma, F. Di Renzo, A. K. Divakarla, A. Dmitriev, Z. Doctor, L. D'Onofrio, F. Donovan, K. L. Dooley, S. Doravari, I. Dorrington, M. Drago, J. C. Driggers, Y. Drori, J. G. Ducoin, P. Dupej, O. Durante, D. D'Urso, P. A. Duverne, S. E. Dwyer, C. Eassa, P. J. Easter, M. Ebersold, T. Eckhardt, G. Eddolls, B. Edelman, T. B. Edo, O. Edy, A. Effler, S. Eguchi, J. Eichholz, S. S. Eikenberry, M. Eisenmann, R. A. Eisenstein, A. Ejlli, E. Engelby, Y. Enomoto, L. Errico, R. C. Essick, H. Estellés, D. Estevez, Z. Etienne, T. Etzel, M. Evans, T. M. Evans, B. E. Ewing, V. Fafone, H. Fair, S. Fairhurst, A. M. Farah, S. Farinon, B. Farr, W. M. Farr, N. W. Farrow, E. J. Fauchon-Jones, G. Favaro, M. Favata, M. Fays, M. Fazio, J. Feicht, M. M. Fejer, E. Fenyvesi, D. L. Ferguson, A. Fernandez-Galiana, I. Ferrante, T. A. Ferreira, F. Fidecaro, P. Figura, I. Fiori, M. Fishbach, R. P. Fisher, R. Fittipaldi, V. Fiumara, R. Flaminio, E. Floden, H. Fong, J. A. Font, B. Fornal, P. W. F. Forsyth, A. Franke, S. Frasca, F. Frasconi, C. Frederick,

J. P. Freed, Z. Frei, A. Freise, R. Frey, P. Fritschel, V. V. Frolov, G. G. Fronzé, Y. Fujii, Y. Fujikawa, M. Fukunaga, M. Fukushima, P. Fulda, M. Fyffe, H. A. Gabbard, W. E. Gabella, B. U. Gadre, J. R. Gair, J. Gais, S. Galaudage, R. Gamba, D. Ganapathy, A. Ganguly, D. Gao, S. G. Gaonkar, B. Garaventa, F. García, C. García-Núñez, C. García-Quirós, F. Garufi, B. Gateley, S. Gaudio, V. Gayathri, G. G. Ge, G. Gemme, A. Gennai, J. George, R. N. George, O. Gerberding, L. Gergely, P. Gewecke, S. Ghonge, Abhirup Ghosh, Archisman Ghosh, Shaon Ghosh, Shrobana Ghosh, B. Giacomazzo, L. Giacoppo, J. A. Giaime, K. D. Giardina, D. R. Gibson, C. Gier, M. Giesler, P. Giri, F. Gissi, J. Glanzer, A. E. Gleckl, P. Godwin, E. Goetz, R. Goetz, N. Gohlke, J. Golomb, B. Goncharov, G. González, A. Gopakumar, M. Gosselin, R. Gouaty, D. W. Gould, B. Grace, A. Grado, M. Granata, V. Granata, A. Grant, S. Gras, P. Grassia, C. Gray, R. Gray, G. Greco, A. C. Green, R. Green, A. M. Gretarsson, E. M. Gretarsson, D. Griffith, W. Griffiths, H. L. Griggs, G. Grignani, A. Grimaldi, S. J. Grimm, H. Grote, S. Grunewald, P. Gruning, D. Guerra, G. M. Guidi, A. R. Guimaraes, G. Guixé, H. K. Gulati, H. K. Guo, Y. Guo, Anchal Gupta, Anuradha Gupta, P. Gupta, E. K. Gustafson, R. Gustafson, F. Guzman, S. Ha, L. Haegel, A. Hagiwara, S. Haino, O. Halim, E. D. Hall, E. Z. Hamilton, G. Hammond, W. B. Han, M. Haney, J. Hanks, C. Hanna, M. D. Hannam, O. Hannuksela, H. Hansen, T. J. Hansen, J. Hanson, T. Harder, T. Hardwick, K. Haris, J. Harms, G. M. Harry, I. W. Harry, D. Hartwig, K. Hasegawa, B. Haskell, R. K. Hasskew, C. J. Haster, K. Hattori, K. Haughian, H. Hayakawa, K. Hayama, F. J. Hayes, J. Healy, A. Heidmann, A. Heidt, M. C. Heintze, J. Heinze, J. Heinzel, H. Heitmann, F. Hellman, P. Hello, A. F. Helmling-Cornell, G. Hemming, M. Hendry, I. S. Heng, E. Hennes, J. Hennig, M. H. Hennig, A. G. Hernandez, F. Hernandez Vivanco, M. Heurs, S. Hild, P. Hill, Y. Himemoto, A. S. Hines, Y. Hiranuma, N. Hirata, E. Hirose, S. Hochheim, D. Hofman, J. N. Hohmann, D. G. Holcomb, N. A. Holland, K. Holley-Bockelmann, I. J. Hollows, Z. J. Holmes, K. Holt, D. E. Holz, Z. Hong, P. Hopkins, J. Hough, S. Hourihane, E. J. Howell, C. G. Hoy, D. Hoyland, A. Hreibi, B-H. Hsieh, Y. Hsu, G-Z. Huang, H-Y. Huang, P. Huang, Y-C. Huang, Y. J. Huang, Y. Huang, M. T. Hübner, A. D. Huddart, B. Hughey, D. C. Y. Hui, V. Hui, S. Husa, S. H. Huttner, R. Huxford, T. Huynh-Dinh, S. Ide, B. Idzkowski, A. Iess, B. Ikenoue,

S. Imam, K. Inayoshi, C. Ingram, Y. Inoue, K. Ioka, M. Isi, K. Isleif, K. Ito, Y. Itoh, B. R. Iyer, K. Izumi, V. JaberianHamedan, T. Jacqmin, S. J. Jadhav, S. P. Jadhav, A. L. James, A. Z. Jan, K. Jani, J. Janquart, K. Janssens, N. N. Janthalur, P. Jaranowski, D. Jariwala, R. Jaume, A. C. Jenkins, K. Jenner, C. Jeon, M. Jeunon, W. Jia, H. B. Jin, G. R. Johns, N. K. Johnson-McDaniel, A. W. Jones, D. I. Jones, J. D. Jones, P. Jones, R. Jones, R. J. G. Jonker, L. Ju, P. Jung, K. Jung, J. Junker, V. Juste, K. Kaihotsu, T. Kajita, M. Kakizaki, C. V. Kalaghatgi, V. Kalogera, B. Kamai, M. Kamiizumi, N. Kanda, S. Kandhasamy, G. Kang, J. B. Kanner, Y. Kao, S. J. Kapadia, D. P. Kapasi, S. Karat, C. Karathanasis, S. Karki, R. Kashyap, M. Kasprzack, W. Kastaun, S. Katsanevas, E. Katsavounidis, W. Katzman, T. Kaur, K. Kawabe, K. Kawaguchi, N. Kawai, T. Kawasaki, F. Kéfélian, D. Keitel, J. S. Key, S. Khadka, F. Y. Khalili, S. Khan, E. A. Khazanov, N. Khetan, M. Khursheed, N. Kijbunchoo, C. Kim, J. C. Kim, J. Kim, K. Kim, W. S. Kim, Y. M. Kim, C. Kimball, N. Kimura, M. Kinley-Hanlon, R. Kirchhoff, J. S. Kissel, N. Kita, H. Kitazawa, L. Kleybolte, S. Klimenko, A. M. Knee, T. D. Knowles, E. Knyazev, P. Koch, G. Koekoek, Y. Kojima, K. Kokeyama, S. Koley, P. Kolitsidou, M. Kolstein, K. Komori, V. Kondrashov, A. K. H. Kong, A. Kontos, N. Koper, M. Korobko, K. Kotake, M. Kovalam, D. B. Kozak, C. Kozakai, R. Kozu, V. Kringel, N. V. Krishnendu, A. Królak, G. Kuehn, F. Kuei, P. Kuijer, S. Kulkarni, A. Kumar, P. Kumar, Rahul Kumar, Rakesh Kumar, J. Kume, K. Kuns, C. Kuo, H-S. Kuo, Y. Kuromiya, S. Kuroyanagi, K. Kusayanagi, S. Kuwahara, K. Kwak, P. Lagabbe, D. Laghi, E. Lalande, T. L. Lam, A. Lamberts, M. Landry, B. B. Lane, R. N. Lang, J. Lange, B. Lantz, I. La Rosa, A. Lartaux-Vollard, P. D. Lasky, M. Laxen, A. Lazzarini, C. Lazzaro, P. Leaci, S. Leavey, Y. K. Lecoeuche, H. K. Lee, H. M. Lee, H. W. Lee, J. Lee, K. Lee, R. Lee, J. Lehmann, A. Lemaître, M. Leonardi, N. Leroy, N. Letendre, C. Levesque, Y. Levin, J. N. Leviton, K. Leyde, A. K. Y. Li, B. Li, J. Li, K. L. Li, T. G. F. Li, X. Li, C-Y. Lin, F-K. Lin, F-L. Lin, H. L. Lin, L. C. C. Lin, F. Linde, S. D. Linker, J. N. Linley, T. B. Littenberg, G. C. Liu, J. Liu, K. Liu, X. Liu, F. Llamas, M. Llorens-Monteagudo, R. K. L. Lo, A. Lockwood, M. Loh, L. T. London, A. Longo, D. Lopez, M. Lopez Portilla, M. Lorenzini, V. Loriette, M. Lormand, G. Losurdo, T. P. Lott, J. D. Lough, C. O.

Lousto, G. Lovelace, J. F. Lucaccioni, H. Lück, D. Lumaca, A. P. Lundgren, L. W. Luo, J. E. Lynam, R. Macas, M. MacInnis, D. M. Macleod, I. A. O. MacMillan, A. Macquet, I. Magaña Hernandez, C. Magazzù, R. M. Magee, R. Maggiore, M. Magnozzi, S. Mahesh, E. Majorana, C. Makarem, I. Maksimovic, S. Maliakal, A. Malik, N. Man, V. Mandic, V. Mangano, J. L. Mango, G. L. Mansell, M. Manske, M. Mantovani, M. Mapelli, F. Marchesoni, M. Marchio, F. Marion, Z. Mark, S. Márka, Z. Márka, C. Markakis, A. S. Markosyan, A. Markowitz, E. Maros, A. Marquina, S. Marsat, F. Martelli, I. W. Martin, R. M. Martin, M. Martinez, V. A. Martinez, V. Martinez, K. Martinovic, D. V. Martynov, E. J. Marx, H. Masalehdan, K. Mason, E. Massera, A. Masserot, T. J. Massinger, M. Masso-Reid, S. Mastrogiovanni, A. Matas, M. Mateu-Lucena, F. Matichard, M. Matiushechkina, N. Mavalvala, J. J. McCann, R. McCarthy, D. E. McClelland, P. K. McClincy, S. McCormick, L. McCuller, G. I. McGhee, S. C. McGuire, C. McIsaac, J. McIver, T. McRae, S. T. McWilliams, D. Meacher, M. Mehmet, A. K. Mehta, Q. Meijer, A. Melatos, D. A. Melchor, G. Mendell, A. Menendez-Vazquez, C. S. Menoni, R. A. Mercer, L. Mereni, K. Merfeld, E. L. Merilh, J. D. Merritt, M. Merzougui, S. Meshkov, C. Messenger, C. Messick, P. M. Meyers, F. Meylahn, A. Mhaske, A. Miani, H. Miao, I. Michaloliakos, C. Michel, Y. Michimura, H. Middleton, L. Milano, A. L. Miller, A. Miller, B. Miller, M. Millhouse, J. C. Mills, E. Milotti, O. Minazzoli, Y. Minenkov, N. Mio, Ll. M. Mir, M. Miravet-Tenés, C. Mishra, T. Mishra, T. Mistry, S. Mitra, V. P. Mitrofanov, G. Mitselmakher, R. Mittleman, O. Miyakawa, A. Miyamoto, Y. Miyazaki, K. Miyo, S. Miyoki, Geoffrey Mo, L. M. Modafferi, E. Moguel, K. Mogushi, S. R. P. Mohapatra, S. R. Mohite, I. Molina, M. Molina-Ruiz, M. Mondin, M. Montani, C. J. Moore, D. Moraru, F. Morawski, A. More, C. Moreno, G. Moreno, Y. Mori, S. Morisaki, Y. Moriwaki, G. Morrás, B. Mours, C. M. Mow-Lowry, S. Mozzon, F. Muciaccia, Arunava Mukherjee, D. Mukherjee, Soma Mukherjee, Subroto Mukherjee, Suvodip Mukherjee, N. Mukund, A. Mullavey, J. Munch, E. A. Muñiz, P. G. Murray, R. Musenich, S. Muusse, S. L. Nadji, K. Nagano, S. Nagano, A. Nagar, K. Nakamura, H. Nakano, M. Nakano, R. Nakashima, Y. Nakayama, V. Napolano, I. Nardecchia, T. Narikawa, L. Naticchioni, B. Nayak, R. K. Nayak, R. Negishi, B. F. Neil, J. Neilson, G. Nelemans, T. J. N. Nelson, M. Nery, P. Neubauer, A. Neunzert, K. Y. Ng, S. W. S.

Ng, C. Nguyen, P. Nguyen, T. Nguyen, L. Nguyen Quynh, W. T. Ni, S. A. Nichols, A. Nishizawa, S. Nissanke, E. Nitoglia, F. Nocera, M. Norman, C. North, S. Nozaki, J. F. Nuño Siles, L. K. Nuttall, J. Oberling, B. D. O'Brien, Y. Obuchi, J. O'Dell, E. Oelker, W. Ogaki, G. Oganesyan, J. J. Oh, K. Oh, S. H. Oh, M. Ohashi, N. Ohishi, M. Ohkawa, F. Ohme, H. Ohta, M. A. Okada, Y. Okutani, K. Okutomi, C. Olivetto, K. Oohara, C. Ooi, R. Oram, B. O'Reilly, R. G. Ormiston, N. D. Ormsby, L. F. Ortega, R. O'Shaughnessy, E. O'Shea, S. Oshino, S. Ossokine, C. Osthelder, S. Otabe, D. J. Ottaway, H. Overmier, A. E. Pace, G. Pagano, M. A. Page, G. Pagliaroli, A. Pai, S. A. Pai, J. R. Palamos, O. Palashov, C. Palomba, H. Pan, K. Pan, P. K. Panda, H. Pang, P. T. H. Pang, C. Pankow, F. Pannarale, B. C. Pant, F. H. Panther, F. Paoletti, A. Paoli, A. Paolone, A. Parisi, H. Park, J. Park, W. Parker, D. Pascucci, A. Pasqualetti, R. Passaquieti, D. Passuello, M. Patel, M. Pathak, B. Patricelli, A. S. Patron, S. Paul, E. Payne, M. Pedraza, M. Pegoraro, A. Pele, F. E. Peña Arellano, S. Penn, A. Perego, A. Pereira, T. Pereira, C. J. Perez, C. Périgois, C. C. Perkins, A. Perreca, S. Perriès, J. Petermann, D. Petterson, H. P. Pfeiffer, K. A. Pham, K. S. Phukon, O. J. Piccinni, M. Pichot, M. Piendibene, F. Piergiovanni, L. Pierini, V. Pierro, G. Pillant, M. Pillas, F. Pilo, L. Pinard, I. M. Pinto, M. Pinto, B. Piotrzkowski, K. Piotrzkowski, M. Pirello, M. D. Pitkin, E. Placidi, L. Planas, W. Plastino, C. Pluchar, R. Poggiani, E. Polini, D. Y. T. Pong, S. Ponrathnam, P. Popolizio, E. K. Porter, R. Poulton, J. Powell, M. Pracchia, T. Pradier, A. K. Prajapati, K. Prasai, R. Prasanna, G. Pratten, M. Principe, G. A. Prodi, L. Prokhorov, P. Prosposito, L. Prudenzi, A. Puecher, M. Punturo, F. Puosi, P. Puppo, M. Pürrer, H. Qi, V. Quetschke, R. Quitzow-James, N. Qutob, F. J. Raab, G. Raaijmakers, H. Radkins, N. Radulesco, P. Raffai, S. X. Rail, S. Raja, C. Rajan, K. E. Ramirez, T. D. Ramirez, A. Ramos-Buades, J. Rana, P. Rapagnani, U. D. Rapol, A. Ray, V. Raymond, N. Raza, M. Razzano, J. Read, L. A. Rees, T. Regimbau, L. Rei, S. Reid, S. W. Reid, D. H. Reitze, P. Relton, A. Renzini, P. Rettegno, A. Reza, M. Rezac, F. Ricci, D. Richards, J. W. Richardson, L. Richardson, G. Riemenschneider, K. Riles, S. Rinaldi, K. Rink, M. Rizzo, N. A. Robertson, R. Robie, F. Robinet, A. Rocchi, S. Rodriguez, L. Rolland, J. G. Rollins, M. Romanelli, R. Romano, C. L. Romel, A. Romero-Rodríguez,

I. M. Romero-Shaw, J. H. Romie, S. Ronchini, L. Rosa, C. A. Rose, D. Rosińska, M. P. Ross, S. Rowan, S. J. Rowlinson, S. Roy, Santosh Roy, Soumen Roy, D. Rozza, P. Ruggi, K. Ruiz-Rocha, K. Ryan, S. Sachdev, T. Sadecki, J. Sadiq, N. Sago, S. Saito, Y. Saito, K. Sakai, Y. Sakai, M. Sakellariadou, Y. Sakuno, O. S. Salafia, L. Salconi, M. Saleem, F. Salemi, A. Samajdar, E. J. Sanchez, J. H. Sanchez, L. E. Sanchez, N. Sanchis-Gual, J. R. Sanders, A. Sanuy, T. R. Saravanan, N. Sarin, B. Sassolas, H. Satari, B. S. Sathyaprakash, S. Sato, T. Sato, O. Sauter, R. L. Savage, T. Sawada, D. Sawant, H. L. Sawant, S. Sayah, D. Schaetzl, M. Scheel, J. Scheuer, M. Schiworski, P. Schmidt, S. Schmidt, R. Schnabel, M. Schneewind, R. M. S. Schofield, A. Schönbeck, B. W. Schulte, B. F. Schutz, E. Schwartz, J. Scott, S. M. Scott, M. Seglar-Arroyo, T. Sekiguchi, Y. Sekiguchi, D. Sellers, A. S. Sengupta, D. Sentenac, E. G. Seo, V. Sequino, A. Sergeev, Y. Setyawati, T. Shaffer, M. S. Shahriar, B. Shams, L. Shao, A. Sharma, P. Sharma, P. Shawhan, N. S. Shcheblanov, S. Shibagaki, M. Shikauchi, R. Shimizu, T. Shimoda, K. Shimode, H. Shinkai, T. Shishido, A. Shoda, D. H. Shoemaker, D. M. Shoemaker, S. ShyamSundar, M. Sieniawska, D. Sigg, L. P. Singer, D. Singh, N. Singh, A. Singha, A. M. Sintes, V. Sipala, V. Skliris, B. J. J. Slagmolen, T. J. Slaven-Blair, J. Smetana, J. R. Smith, R. J. E. Smith, J. Soldateschi, S. N. Somala, K. Somiya, E. J. Son, K. Soni, S. Soni, V. Sordini, F. Sorrentino, N. Sorrentino, H. Sotani, R. Soulard, T. Souradeep, E. Sowell, V. Spagnuolo, A. P. Spencer, M. Spera, R. Srinivasan, A. K. Srivastava, V. Srivastava, K. Staats, C. Stachie, D. A. Steer, J. Steinhoff, J. Steinlechner, S. Steinlechner, S. P. Stevenson, D. J. Stops, M. Stover, K. A. Strain, L. C. Strang, G. Stratta, A. Strunk, R. Sturani, A. L. Stuver, S. Sudhagar, V. Sudhir, R. Sugimoto, H. G. Suh, A. G. Sullivan, J. M. Sullivan, T. Z. Summerscales, H. Sun, L. Sun, S. Sunil, A. Sur, J. Suresh, P. J. Sutton, Takamasa Suzuki, Toshikazu Suzuki, B. L. Swinkels, M. J. Szczepańczyk, P. Szewczyk, M. Tacca, H. Tagoshi, S. C. Tait, H. Takahashi, R. Takahashi, A. Takamori, S. Takano, H. Takeda, M. Takeda, C. J. Talbot, C. Talbot, H. Tanaka, Kazuyuki Tanaka, Kenta Tanaka, Taiki Tanaka, Takahiro Tanaka, A. J. Tanasijczuk, S. Tanioka, D. B. Tanner, D. Tao, L. Tao, E. N. Tapia San Martín, C. Taranto, J. D. Tasson, S. Telada, R. Tenorio, J. E. Terhune, L. Terkowski, M. P. Thirugnanasambandam, L. Thomas, M. Thomas, P. Thomas, J. E. Thompson, S. R.

Thondapu, K. A. Thorne, E. Thrane, Shubhanshu Tiwari, Srishti Tiwari, V. Tiwari, A. M. Toivonen, K. Toland, A. E. Tolley, T. Tomaru, Y. Tomigami, T. Tomura, M. Tonelli, A. Torres-Forné, C. I. Torrie, I. Tosta e Melo, D. Töyrä, A. Trapananti, F. Travasso, G. Traylor, M. Trevor, M. C. Tringali, A. Tripathee, L. Troiano, A. Trovato, L. Trozzo, R. J. Trudeau, D. S. Tsai, D. Tsai, K. W. Tsang, T. Tsang, J-S. Tsao, M. Tse, R. Tso, K. Tsubono, S. Tsuchida, L. Tsukada, D. Tsuna, T. Tsutsui, T. Tsuzuki, K. Turbang, M. Turconi, D. Tuyenbayev, A. S. Ubhi, N. Uchikata, T. Uchiyama, R. P. Udall, A. Ueda, T. Uehara, K. Ueno, G. Ueshima, C. S. Unnikrishnan, F. Uraguchi, A. L. Urban, T. Ushiba, A. Utina, H. Vahlbruch, G. Vajente, A. Vajpeyi, G. Valdes, M. Valentini, V. Valsan, N. van Bakel, M. van Beuzekom, J. F. J. van den Brand, C. Van Den Broeck, D. C. Vander-Hyde, L. van der Schaaf, J. V. van Heijningen, J. Vanosky, M. H. P. M. van Putten, N. van Remortel, M. Vardaro, A. F. Vargas, V. Varma, M. Vasúth, A. Vecchio, G. Vedovato, J. Veitch, P. J. Veitch, J. Venneberg, G. Venugopalan, D. Verkindt, P. Verma, Y. Verma, D. Veske, F. Vetrano, A. Viceré, S. Vidyant, A. D. Viets, A. Vijaykumar, V. Villa-Ortega, J. Y. Vinet, A. Virtuoso, S. Vitale, T. Vo, H. Vocca, E. R. G. von Reis, J. S. A. von Wrangel, C. Vorvick, S. P. Vyatchanin, L. E. Wade, M. Wade, K. J. Wagner, R. C. Walet, M. Walker, G. S. Wallace, L. Wallace, S. Walsh, J. Wang, J. Z. Wang, W. H. Wang, R. L. Ward, J. Warner, M. Was, T. Washimi, N. Y. Washington, J. Watchi, B. Weaver, S. A. Webster, M. Weinert, A. J. Weinstein, R. Weiss, C. M. Weller, R. A. Weller, F. Wellmann, L. Wen, P. Weßels, K. Wette, J. T. Whelan, D. D. White, B. F. Whiting, C. Whittle, D. Wilken, D. Williams, M. J. Williams, N. Williams, A. R. Williamson, J. L. Willis, B. Willke, D. J. Wilson, W. Winkler, C. C. Wipf, T. Wlodarczyk, G. Woan, J. Woehler, J. K. Wofford, I. C. F. Wong, C. Wu, D. S. Wu, H. Wu, S. Wu, D. M. Wysocki, L. Xiao, W-R. Xu, T. Yamada, H. Yamamoto, Kazuhiro Yamamoto, Kohei Yamamoto, T. Yamamoto, K. Yamashita, R. Yamazaki, F. W. Yang, L. Yang, Y. Yang, Yang Yang, Z. Yang, M. J. Yap, D. W. Yeeles, A. B. Yelikar, M. Ying, K. Yokogawa, J. Yokoyama, T. Yokozawa, J. Yoo, T. Yoshioka, Hang Yu, Haocun Yu, H. Yuzurihara, A. Zadrożny, M. Zanolin, S. Zeidler, T. Zelenova, J. P. Zendri, M. Zevin, M. Zhan, H. Zhang, J. Zhang, L. Zhang, T. Zhang, Y. Zhang, C. Zhao, G. Zhao, Y. Zhao,

Yue Zhao, Y. Zheng, R. Zhou, Z. Zhou, X. J. Zhu, Z. H. Zhu, A. B. Zimmerman, Y. Zlochower, M. E. Zucker, and J. Zweizig. GWTC-3: Compact Binary Coalescences Observed by LIGO and Virgo During the Second Part of the Third Observing Run. *arXiv e-prints*, art. arXiv:2111.03606, November 2021. doi: 10.48550/arXiv.2111.03606.

[199] Roger W. Romani, D. Kandel, Alexei V. Filippenko, Thomas G. Brink, and WeiKang Zheng. PSR J0952-0607: The fastest and heaviest known galactic neutron star. *The Astrophysical Journal Letters*, 934(2):L17, jul 2022. doi: 10.3847/2041-8213/ac8007. URL https://dx.doi.org/10.3847/2041-8213/ac8007.

[200] Masaru Shibata, Enping Zhou, Kenta Kiuchi, and Sho Fujibayashi. Constraint on the maximum mass of neutron stars using gw170817 event. *Phys. Rev. D*, 100:023015, Jul 2019. doi: 10.1103/PhysRevD.100.023015. URL https://link.aps.org/doi/10.1103/PhysRevD.100.023015.

[201] Will M. Farr, Niharika Sravan, Andrew Cantrell, Laura Kreidberg, Charles D. Bailyn, Ilya Mandel, and Vicky Kalogera. The mass distribution of stellar-mass black holes. *The Astrophysical Journal*, 741(2):103, oct 2011. doi: 10.1088/0004-637X/741/2/103. URL https://dx.doi.org/10.1088/0004-637X/741/2/103.

[202] Francis Froborg and Alan R. Duffy. Annual modulation in direct dark matter searches. *Journal of Physics G: Nuclear and Particle Physics*, 2020. URL http://iopscience.iop.org/10.1088/1361-6471/ab8e93.

[203] Jennifer M. Gaskins. A review of indirect searches for particle dark matter. *Contemporary Physics*, 57(4):496–525, 2016. doi: 10.1080/00107514.2016.1175160. URL https://doi.org/10.1080/00107514.2016.1175160.

[204] SuperCDMS Collaboration, R. Agnese, T. Aramaki, I. J. Arnquist, W. Baker, D. Balakishiyeva, S. Banik, D. Barker, R. Basu Thakur, D. A. Bauer, T. Binder, M. A. Bowles, P. L. Brink, R. Bunker, B. Cabrera, D. O. Caldwell, R. Calkins, C. Cartaro, D. G. Cerdeño, Y. Chang, Y. Chen, J. Cooley, B. Cornell, P. Cushman, M. Daal, P. C. F. Di Stefano, T. Doughty, E. Fascione, E. Figueroa-Feliciano, M. Fritts, G. Gerbier,

R. Germond, M. Ghaith, G. L. Godfrey, S. R. Golwala, J. Hall, H. R. Harris, Z. Hong, E. W. Hoppe, L. Hsu, M. E. Huber, V. Iyer, D. Jardin, A. Jastram, C. Jena, M. H. Kelsey, A. Kennedy, A. Kubik, N. A. Kurinsky, B. Loer, E. Lopez Asamar, P. Lukens, D. MacDonell, R. Mahapatra, V. Mandic, N. Mast, E. H. Miller, N. Mirabolfathi, B. Mohanty, J. D. Morales Mendoza, J. Nelson, J. L. Orrell, S. M. Oser, K. Page, W. A. Page, R. Partridge, M. Penalver Martinez, M. Pepin, A. Phipps, S. Poudel, M. Pyle, H. Qiu, W. Rau, P. Redl, A. Reisetter, T. Reynolds, A. Roberts, A. E. Robinson, H. E. Rogers, T. Saab, B. Sadoulet, J. Sander, K. Schneck, R. W. Schnee, S. Scorza, K. Senapati, B. Serfass, D. Speller, M. Stein, J. Street, H. A. Tanaka, D. Toback, R. Underwood, A. N. Villano, B. von Krosigk, B. Welliver, J. S. Wilson, M. J. Wilson, D. H. Wright, S. Yellin, J. J. Yen, B. A. Young, X. Zhang, and X. Zhao. Results from the Super Cryogenic Dark Matter Search (SuperCDMS) experiment at Soudan. *arXiv e-prints*, art. arXiv:1708.08869, August 2017.

[205] D. Yu. Akimov, H. M. Araújo, E. J. Barnes, V. A. Belov, A. Bewick, A. A. Burenkov, V. Chepel, A. Currie, L. Deviveiros, B. Edwards, C. Ghag, A. Hollingsworth, M. Horn, W. G. Jones, G. E. Kalmus, A. S. Kobyakin, A. G. Kovalenko, V. N. Lebedenko, A. Lindote, M. I. Lopes, R. Lüscher, P. Majewski, A. St. J. Murphy, F. Neves, S. M. Paling, J. Pinto da Cunha, R. Preece, J. J. Quenby, L. Reichhart, P. R. Scovell, C. Silva, V. N. Solovov, N. J. T. Smith, V. N. Stekhanov, T. J. Sumner, C. Thorne, and R. J. Walker. WIMP-nucleon cross-section results from the second science run of ZEPLIN-III. *Physics Letters B*, 709(1):14–20, March 2012. doi: 10.1016/j.physletb.2012.01.064.

[206] Fermi LAT Collaboration. Limits on dark matter annihilation signals from the Fermi LAT 4-year measurement of the isotropic gamma-ray background. *J. Cosmol. Astropart. Phys.*, 2015(9):008, September 2015. doi: 10.1088/1475-7516/2015/09/008.

[207] A. Albert, R. Alfaro, C. Alvarez, J. D. Álvarez, R. Arceo, J. C. Arteaga-Velázquez, D. Avila Rojas, H. A. Ayala Solares, N. Bautista-Elivar, A. Becerril, E. Belmont-Moreno, S. Y. BenZvi, A. Bernal, J. Braun, C. Brisbois, K. S. Caballero-Mora, T. Capistrán, A. Carramiñana, S. Casanova, M. Castillo, U. Cotti, J. Cotzomi, S. Coutiño de León, C. De León, E. De la Fuente, R. Diaz Hernandez, B. L. Dingus, M. A. DuVernois,

J. C. Díaz-Vélez, R. W. Ellsworth, K. Engel, D. W. Fiorino, N. Fraija, J. A. García-González, F. Garfias, M. M. González, J. A. Goodman, Z. Hampel-Arias, J. P. Harding, S. Hernandez, A. Hernandez-Almada, B. Hona, P. Hüntemeyer, A. Iriarte, A. Jardin-Blicq, V. Joshi, S. Kaufmann, D. Kieda, R. J. Lauer, D. Lennarz, H. León Vargas, J. T. Linnemann, A. L. Longinotti, M. Longo Proper, G. Luis Raya, R. Luna-García, R. López-Coto, K. Malone, S. S. Marinelli, I. Martinez-Castellanos, J. Martínez-Castro, H. Martínez-Huerta, J. A. Matthews, P. Miranda-Romagnoli, E. Moreno, M. Mostafá, L. Nellen, M. Newbold, M. U. Nisa, R. Noriega-Papaqui, R. Pelayo, J. Pretz, E. G. Pérez-Pérez, Z. Ren, C. D. Rho, C. Rivière, D. Rosa-González, M. Rosenberg, E. Ruiz-Velasco, F. Salesa Greus, A. Sandoval, M. Schneider, H. Schoorlemmer, G. Sinnis, A. J. Smith, R. W. Springer, P. Surajbali, I. Taboada, O. Tibolla, K. Tollefson, I. Torres, G. Vianello, T. Weisgarber, S. Westerhoff, J. Wood, T. Yapici, P. W. Younk, and H. Zhou. Dark Matter Limits from Dwarf Spheroidal Galaxies with the HAWC Gamma-Ray Observatory. *Astrophys. J.*, 853(2):154, February 2018. doi: 10.3847/1538-4357/aaa6d8.

[208] S. Archambault, A. Archer, W. Benbow, R. Bird, E. Bourbeau, T. Brantseg, M. Buchovecky, J. H. Buckley, V. Bugaev, K. Byrum, M. Cerruti, J. L. Christiansen, M. P. Connolly, W. Cui, M. K. Daniel, Q. Feng, J. P. Finley, H. Fleischhack, L. Fortson, A. Furniss, A. Geringer-Sameth, S. Griffin, J. Grube, M. Hütten, N. Hâkansson, D. Hanna, O. Hervet, J. Holder, G. Hughes, B. Hummensky, C. A. Johnson, P. Kaaret, P. Kar, N. Kelley-Hoskins, M. Kertzman, D. Kieda, S. Koushiappas, M. Krause, F. Krennrich, M. J. Lang, T. T. Y. Lin, S. McArthur, P. Moriarty, R. Mukherjee, D. Nieto, S. O'Brien, R. A. Ong, A. N. Otte, N. Park, M. Pohl, A. Popkow, E. Pueschel, J. Quinn, K. Ragan, P. T. Reynolds, G. T. Richards, E. Roache, C. Rulten, I. Sadeh, M. Santander, G. H. Sembroski, K. Shahinyan, A. W. Smith, D. Staszak, I. Telezhinsky, S. Trepanier, J. V. Tucci, J. Tyler, S. P. Wakely, A. Weinstein, P. Wilcox, D. A. Williams, B. Zitzer, and VERITAS Collaboration. Dark matter constraints from a joint analysis of dwarf Spheroidal galaxy observations with VERITAS. *Phys. Rev. D*, 95(8):082001, April 2017. doi: 10.1103/PhysRevD.95.082001.

[209] Javier Rico. Gamma-Ray Dark Matter Searches in Milky Way Satellites—A Comparative Review of Data Analysis Methods and Current Results. *Galaxies*, 8(1):25, March 2020. doi: 10.3390/galaxies8010025.

[210] MAGIC Collaboration, M. L. Ahnen, S. Ansoldi, L. A. Antonelli, P. Antoranz, A. Babic, B. Banerjee, P. Bangale, U. Barres de Almeida, J. A. Barrio, J. Becerra González, W. Bednarek, E. Bernardini, B. Biasuzzi, A. Biland, O. Blanch, S. Bonnefoy, G. Bonnoli, F. Borracci, T. Bretz, E. Carmona, A. Carosi, A. Chatterjee, R. Clavero, P. Colin, E. Colombo, J. L. Contreras, J. Cortina, S. Covino, P. Da Vela, F. Dazzi, A. De Angelis, B. De Lotto, E. de Oña Wilhelmi, C. Delgado Mendez, F. Di Pierro, D. Dominis Prester, D. Dorner, M. Doro, S. Einecke, D. Eisenacher Glawion, D. Elsaesser, A. Fernández-Barral, D. Fidalgo, M. V. Fonseca, L. Font, K. Frantzen, C. Fruck, D. Galindo, R. J. García López, M. Garczarczyk, D. Garrido Terrats, M. Gaug, P. Giammaria, N. Godinović, A. González Muñoz, D. Guberman, A. Hahn, Y. Hanabata, M. Hayashida, J. Herrera, J. Hose, D. Hrupec, G. Hughes, W. Idec, K. Kodani, Y. Konno, H. Kubo, J. Kushida, A. La Barbera, D. Lelas, E. Lindfors, S. Lombardi, F. Longo, M. López R. López-Coto, A. López-Oramas, E. Lorenz, P. Majumdar, M. Makariev, K. Mallot, G. Maneva, M. Manganaro, K. Mannheim, L. Maraschi, B. Marcote, M. Mariotti, M. Martínez, D. Mazin, U. Menzel, J. M. Mirand a, R. Mirzoyan, A. Moralejo, E. Moretti, D. Nakajima, V. Neustroev, A. Niedzwiecki, M. Nievas Rosillo, K. Nilsson, K. Nishijima, K. Noda, R. Orito, A. Overkemping, S. Paiano, J. Palacio, M. Palatiello, D. Paneque, R. Paoletti, J. M. Paredes, X. Paredes-Fortuny, M. Persic, J. Poutanen, P. G. Prada Moroni, E. Prand ini, I. Puljak, W. Rhode, M. Ribó, J. Rico, J. Rodriguez Garcia, T. Saito, K. Satalecka, C. Schultz, T. Schweizer, S. N. Shore, A. Sillanpää, J. Sitarek, I. Snidaric, D. Sobczynska, A. Stamerra, T. Steinbring, M. Strzys, L. Takalo, H. Takami, F. Tavecchio, P. Temnikov, T. Terzić, D. Tescaro, M. Teshima, J. Thaele, D. F. Torres, T. Toyama, A. Treves, V. Verguilov, I. Vovk, J. E. Ward, M. Will, M. H. Wup, R. Zanins, J. Aleksić, M. Wood, B. Anderson, E. D. Bloom, J. Cohen-Tanugi, A. Drlica-Wagner, M. N. Mazziotta, M. Sánchez-Condeai, and L. Strigarian. Limits to dark matter annihilation cross-section from a combined analysis of MAGIC and

Fermi-LAT observations of dwarf satellite galaxies. *J. Cosmol. Astropart. Phys.*, 2016 (2):039, February 2016. doi: 10.1088/1475-7516/2016/02/039.

[211] IceCube Collaboration, M. G. Aartsen, M. Ackermann, J. Adams, J. A. Aguilar, M. Ahlers, M. Ahrens, I. Al Samarai, D. Altmann, K. Andeen, T. Anderson, I. Ansseau, G. Anton, C. Argüelles, J. Auffenberg, S. Axani, H. Bagherpour, X. Bai, J. P. Barron, S. W. Barwick, V. Baum, R. Bay, J. J. Beatty, J. Becker Tjus, K. H. Becker, S. BenZvi, D. Berley, E. Bernardini, D. Z. Besson, G. Binder, D. Bindig, E. Blaufuss, S. Blot, C. Bohm, M. Börner, F. Bos, D. Bose, S. Böser, O. Botner, J. Bourbeau, F. Bradascio, J. Braun, L. Brayeur, M. Brenzke, H. P. Bretz, S. Bron, A. Burgman, T. Carver, J. Casey, M. Casier, E. Cheung, D. Chirkin, A. Christov, K. Clark, L. Classen, S. Coenders, G. H. Collin, J. M. Conrad, D. F. Cowen, R. Cross, M. Day, J. P. A. M. de André, C. De Clercq, J. J. DeLaunay, H. Dembinski, S. De Ridder, P. Desiati, K. D. de Vries, G. de Wasseige, M. de With, T. DeYoung, J. C. Díaz-Vélez, V. di Lorenzo, H. Dujmovic, J. P. Dumm, M. Dunkman, B. Eberhardt, T. Ehrhardt, B. Eichmann, P. Eller, P. A. Evenson, S. Fahey, A. R. Fazely, J. Felde, K. Filimonov, C. Finley, S. Flis, A. Franckowiak, E. Friedman, T. Fuchs, T. K. Gaisser, J. Gallagher, L. Gerhardt, K. Ghorbani, W. Giang, T. Glauch, T. Glüsenkamp, A. Goldschmidt, J. G. Gonzalez, D. Grant, Z. Griffith, C. Haack, A. Hallgren, F. Halzen, K. Hanson, D. Hebecker, D. Heereman, K. Helbing, R. Hellauer, S. Hickford, J. Hignight, G. C. Hill, K. D. Hoffman, R. Hoffmann, B. Hokanson-Fasig, K. Hoshina, F. Huang, M. Huber, K. Hultqvist, S. In, A. Ishihara, E. Jacobi, G. S. Japaridze, M. Jeong, K. Jero, B. J. P. Jones, P. Kalacynski, W. Kang, A. Kappes, T. Karg, A. Karle, U. Katz, M. Kauer, A. Keivani, J. L. Kelley, A. Kheirandish, J. Kim, M. Kim, T. Kintscher, J. Kiryluk, T. Kittler, S. R. Klein, G. Kohnen, R. Koirala, H. Kolanoski, L. Köpke, C. Kopper, S. Kopper, J. P. Koschinsky, D. J. Koskinen, M. Kowalski, K. Krings, M. Kroll, G. Krückl, J. Kunnen, S. Kunwar, N. Kurahashi, T. Kuwabara, A. Kyriacou, M. Labare, J. L. Lanfranchi, M. J. Larson, F. Lauber, D. Lennarz, M. Lesiak-Bzdak, M. Leuermann, Q. R. Liu, L. Lu, J. Lünemann, W. Luszczak, J. Madsen, G. Maggi, K. B. M. Mahn, S. Mancina, R. Maruyama, K. Mase, R. Maunu, F. McNally, K. Meagher, M. Medici, M. Meier,

T. Menne, G. Merino, T. Meures, S. Miarecki, J. Micallef, G. Momenté, T. Montaruli, R. W. Moore, M. Moulai, R. Nahnhauer, P. Nakarmi, U. Naumann, G. Neer, H. Niederhausen, S. C. Nowicki, D. R. Nygren, A. Obertacke Pollmann, A. Olivas, A. O'Murchadha, T. Palczewski, H. Pand ya, D. V. Pankova, P. Peiffer, J. A. Pepper, C. Pérez de los Heros, D. Pieloth, E. Pinat, M. Plum, P. B. Price, G. T. Przybylski, C. Raab, L. Rädel, M. Rameez, K. Rawlins, R. Reimann, B. Relethford, M. Relich, E. Resconi, W. Rhode, M. Richman, B. Riedel, S. Robertson, M. Rongen, C. Rott, T. Ruhe, D. Ryckbosch, D. Rysewyk, T. Sälzer, S. E. Sanchez Herrera, A. Sandrock, J. Sand roos, S. Sarkar, S. Sarkar, K. Satalecka, P. Schlunder, T. Schmidt, A. Schneider, S. Schoenen, S. Schöneberg, L. Schumacher, D. Seckel, S. Seunarine, D. Soldin, M. Song, G. M. Spiczak, C. Spiering, J. Stachurska, T. Stanev, A. Stasik, J. Stettner, A. Steuer, T. Stezelberger, R. G. Stokstad, A. Stößl, N. L. Strotjohann, G. W. Sullivan, M. Sutherland, I. Taboada, J. Tatar, F. Tenholt, S. Ter-Antonyan, A. Terliuk, G. Tešić, S. Tilav, P. A. Toale, M. N. Tobin, S. Toscano, D. Tosi, M. Tselengidou, C. F. Tung, A. Turcati, C. F. Turley, B. Ty, E. Unger, M. Usner, J. Vand enbroucke, W. Van Driessche, N. van Eijndhoven, S. Vanheule, J. van Santen, M. Vehring, E. Vogel, M. Vraeghe, C. Walck, A. Wallace, M. Wallraff, F. D. Wandler, N. Wandkowsky, A. Waza, C. Weaver, M. J. Weiss, C. Wendt, S. Westerhoff, B. J. Whelan, S. Wickmann, K. Wiebe, C. H. Wiebusch, L. Wille, D. R. Williams, L. Wills, M. Wolf, J. Wood, T. R. Wood, E. Woolsey, K. Woschnagg, D. L. Xu, X. W. Xu, Y. Xu, J. P. Yanez, G. Yodh, S. Yoshida, T. Yuan, and M. Zoll. Search for Neutrinos from Dark Matter Self-Annihilations in the center of the Milky Way with 3 years of IceCube/DeepCore. *arXiv e-prints*, art. arXiv:1705.08103, May 2017.

[212] The Super-Kamiokande Collaboration, :, K. Choi, K. Abe, Y. Haga, Y. Hayato, K. Iyogi, J. Kameda, Y. Kishimoto, M. Miura, S. Moriyama, M. Nakahata, Y. Nakano, S. Nakayama, H. Sekiya, M. Shiozawa, Y. Suzuki, A. Takeda, T. Tomura, R. A. Wendell, T. Irvine, 2 T. Kajita, I. Kametani, 2 K. Kaneyuki, K. P. Lee, Y. Nishimura, 2 K. Okumura, T. McLachlan, 2 L. Labarga, E. Kearns, J. L. Raaf, 4 J. L. Stone, L. R. Sulak, 4 S. Berkman, 5 H. A. Tanaka, 5 S. Tobayama, M. Goldhaber, G. Carminati,

W. R. Kropp, S. Mine, A. Renshaw, M. B. Smy, H. W. Sobel, K. S. Ganezer, J. Hill, N. Hong, J. Y. Kim, I. T. Lim, T. Akiri, A. Himmel, K. Scholberg, C. W. Walter, T. Wongjirad, T. Ishizuka, S. Tasaka, J. S. Jang, J. G. Learned, S. Matsuno, S. N. Smith, T. Hasegawa, T. Ishida, T. Ishii, T. Kobayashi, T. Nakadaira, K. Nakamura, Y. Oyama, K. Sakashita, T. Sekiguchi, T. Tsukamoto, A. T. Suzuki, Y. Takeuchi, C. Bronner, S. Hirota, K. Huang, K. Ieki, M. Ikeda, T. Kikawa, A. Minamino, T. Nakaya, K. Suzuki, S. Takahashi, Y. Fukuda, Y. Itow, G. Mitsuka, P. Mijakowski, J. Hignight, J. Imber, C. K. Jung, C. Yanagisawa, H. Ishino, A. Kibayashi, Y. Koshio, T. Mori, M. Sakuda, T. Yano, Y. Kuno, R. Tacik, S. B. Kim, H. Okazawa, Y. Choi, K. Nishijima, M. Koshiba, Y. Totsuka, M. Yokoyama, K. Martens, Ll. Marti, M. R. Vagins, J. F. Martin, P. de Perio, A. Konaka, M. J. Wilking, S. Chen, Y. Zhang, and R. J. Wilkes. Search for neutrinos from annihilation of captured low-mass dark matter particles in the Sun by Super-Kamiokande. *arXiv e-prints*, art. arXiv:1503.04858, March 2015.

[213] Felix Kahlhoefer. Review of lhc dark matter searches. *International Journal of Modern Physics A*, 32(13):1730006, 2017. doi: 10.1142/S0217751X1730006X. URL https://doi.org/10.1142/S0217751X1730006X.

[214] A. M. Sirunyan, A. Tumasyan, W. Adam, E. Asilar, T. Bergauer, J. Brandstetter, E. Brondolin, M. Dragicevic, J. Erö, M. Flechl, M. Friedl, R. Frühwirth, V. M. Ghete, C. Hartl, N. Hörmann, J. Hrubec, M. Jeitler, A. König, I. Krätschmer, D. Liko, T. Matsushita, I. Mikulec, D. Rabady, N. Rad, B. Rahbaran, H. Rohringer, J. Schieck, J. Strauss, W. Waltenberger, C. E. Wulz, O. Dvornikov, V. Makarenko, V. Mossolov, J. Suarez Gonzalez, V. Zykunov, N. Shumeiko, S. Alderweireldt, E. A. De Wolf, X. Janssen, J. Lauwers, M. Van De Klundert, H. Van Haevermaet, P. Van Mechelen, N. Van Remortel, A. Van Spilbeeck, S. Abu Zeid, F. Blekman, J. D'Hondt, N. Daci, I. De Bruyn, K. Deroover, S. Lowette, S. Moortgat, L. Moreels, A. Olbrechts, Q. Python, K. Skovpen, S. Tavernier, W. Van Doninck, P. Van Mulders, I. Van Parijs, H. Brun, B. Clerbaux, G. De Lentdecker, H. Delannoy, G. Fasanella, L. Favart, R. Goldouzian, A. Grebenyuk, G. Karapostoli, T. Lenzi, A. Léonard, J. Luetic, T. Maerschalk, A. Marinov, A. Randle-conde, T. Seva, C. Vander Velde, P. Vanlaer, D. Vannerom, R. Yon-

amine, F. Zenoni, F. Zhang, T. Cornelis, D. Dobur, A. Fagot, M. Gul, I. Khvastunov, D. Poyraz, S. Salva, R. Schöfbeck, M. Tytgat, W. Van Driessche, W. Verbeke, N. Zaganidis, H. Bakhshiansohi, O. Bondu, S. Brochet, G. Bruno, A. Caudron, S. De Visscher, C. Delaere, M. Delcourt, B. Francois, A. Giammanco, A. Jafari, M. Komm, G. Krintiras, V. Lemaitre, A. Magitteri, A. Mertens, M. Musich, K. Piotrzkowski, L. Quertenmont, M. Vidal Marono, S. Wertz, N. Beliy, W. L. AldáJúnior, F. L. Alves, G. A. Alves, L. Brito, C. Hensel, A. Moraes, M. E. Pol, P. Rebello Teles, E. Belchior Batista Das Chagas, W. Carvalho, J. Chinellato, A. Custódio, E. M. Da Costa, G. G. Da Silveira, D. De Jesus Damiao, C. De Oliveira Martins, S. Fonseca De Souza, L. M. Huertas Guativa, H. Malbouisson, D. Matos Figueiredo, C. Mora Herrera, L. Mundim, H. Nogima, W. L. Prado Da Silva, A. Santoro, A. Sznajder, E. J. Tonelli Manganote, F. Torres Da Silva De Araujo, A. Vilela Pereira, S. Ahuja, C. A. Bernardes, S. Dogra, T. R. Fernandez Perez Tomei, E. M. Gregores, P. G. Mercadante, C. S. Moon, S. F. Novaes, Sandra S. Padula, D. Romero Abad, J. C. Ruiz Vargas, A. Aleksandrov, R. Hadjiiska, P. Iaydjiev, M. Rodozov, S. Stoykova, G. Sultanov, M. Vutova, A. Dimitrov, I. Glushkov, L. Litov, B. Pavlov, P. Petkov, W. Fang, X. Gao, M. Ahmad, J. G. Bian, G. M. Chen, H. S. Chen, M. Chen, Y. Chen, T. Cheng, C. H. Jiang, D. Leggat, Z. Liu, F. Romeo, M. Ruan, S. M. Shaheen, A. Spiezia, J. Tao, C. Wang, Z. Wang, E. Yazgan, H. Zhang, J. Zhao, Y. Ban, G. Chen, Q. Li, S. Liu, Y. Mao, S. J. Qian, D. Wang, Z. Xu, C. Avila, A. Cabrera, L. F. Chaparro Sierra, C. Florez, J. P. Gomez, C. F. González Hernández, J. D. Ruiz Alvarez, J. C. Sanabria, N. Godinovic, D. Lelas, I. Puljak, P. M. Ribeiro Cipriano, T. Sculac, Z. Antunovic, M. Kovac, V. Brigljevic, D. Ferencek, K. Kadija, B. Mesic, T. Susa, M. W. Ather, A. Attikis, G. Mavromanolakis, J. Mousa, C. Nicolaou, F. Ptochos, P. A. Razis, H. Rykaczewski, M. Finger, M. Finger, E. Carrera Jarrin, E. El-khateeb, S. Elgammal, A. Mohamed, M. Kadastik, L. Perrini, M. Raidal, A. Tiko, C. Veelken, P. Eerola, J. Pekkanen, M. Voutilainen, J. Härkönen, T. Järvinen, V. Karimäki, R. Kinnunen, T. Lampén, K. Lassila-Perini, S. Lehti, T. Lindén, P. Luukka, J. Tuominiemi, E. Tuovinen, L. Wendland, J. Talvitie, T. Tuuva, M. Besancon, F. Couderc, M. Dejardin, D. Denegri, B. Fabbro, J. L. Faure, C. Favaro, F. Ferri, S. Ganjour, S. Ghosh, A. Givernaud, P. Gras, G. Hamel de Monchenault,

P. Jarry, I. Kucher, E. Locci, M. Machet, J. Malcles, J. Rander, A. Rosowsky, M. Titov, A. Abdulsalam, I. Antropov, S. Baffioni, F. Beaudette, P. Busson, L. Cadamuro, E. Chapon, C. Charlot, O. Davignon, R. Granier de Cassagnac, M. Jo, S. Lisniak, A. Lobanov, P. Miné, M. Nguyen, C. Ochando, G. Ortona, P. Paganini, P. Pigard, S. Regnard, R. Salerno, Y. Sirois, A. G. Stahl Leiton, and The CMS collaboration. Search for new physics in the monophoton final state in proton-proton collisions at s=13$$ \sqrt{s}=13 $$tev. *Journal of High Energy Physics*, 2017(10):73, 2017. doi: 10.1007/JHEP10(2017)073. URL https://doi.org/10.1007/JHEP10(2017)073.

[215] M. Aaboud, G. Aad, B. Abbott, D. C. Abbott, O. Abdinov, D. K. Abhayasinghe, S. H. Abidi, O. S. AbouZeid, N. L. Abraham, H. Abramowicz, H. Abreu, Y. Abulaiti, B. S. Acharya, S. Adachi, L. Adam, C. Adam Bourdarios, L. Adamczyk, L. Adamek, J. Adelman, M. Adersberger, A. Adiguzel, T. Adye, A. A. Affolder, Y. Afik, C. Agapopoulou, M. N. Agaras, A. Aggarwal, C. Agheorghiesei, J. A. Aguilar-Saavedra, F. Ahmadov, G. Aielli, S. Akatsuka, T. P. A. Åkesson, E. Akilli, A. V. Akimov, K. Al Khoury, G. L. Alberghi, J. Albert, M. J. Alconada Verzini, S. Alderweireldt, M. Aleksa, I. N. Aleksandrov, C. Alexa, D. Alexandre, T. Alexopoulos, M. Alhroob, B. Ali, G. Alimonti, J. Alison, S. P. Alkire, C. Allaire, B. M. M. Allbrooke, B. W. Allen, P. P. Allport, A. Aloisio, A. Alonso, F. Alonso, C. Alpigiani, A. A. Alshehri, M. I. Alstaty, M. Alvarez Estevez, B. Alvarez Gonzalez, D. Álvarez Piqueras, M. G. Alviggi, Y. Amaral Coutinho, A. Ambler, L. Ambroz, C. Amelung, D. Amidei, S. P. Amor Dos Santos, S. Amoroso, C. S. Amrouche, F. An, C. Anastopoulos, N. Andari, T. Andeen, C. F. Anders, J. K. Anders, A. Andreazza, V. Andrei, C. R. Anelli, S. Angelidakis, I. Angelozzi, A. Angerami, A. V. Anisenkov, A. Annovi, C. Antel, M. T. Anthony, M. Antonelli, D. J. A. Antrim, F. Anulli, M. Aoki, J. A. Aparisi Pozo, L. Aperio Bella, G. Arabidze, J. P. Araque, V. Araujo Ferraz, R. Araujo Pereira, A. T. H. Arce, F. A. Arduh, J-F. Arguin, S. Argyropoulos, J. H. Arling, A. J. Armbruster, L. J. Armitage, A. Armstrong, O. Arnaez, H. Arnold, A. Artamonov, G. Artoni, S. Artz, S. Asai, N. Asbah, E. M. Asimakopoulou, L. Asquith, K. Assamagan, R. Astalos, R. J. Atkin, M. Atkinson, N. B. Atlay, K. Augsten, G. Avolio, R. Avramidou, M. K. Ayoub, A. M. Azoulay, G. Azuelos,

A. E. Baas, M. J. Baca, H. Bachacou, K. Bachas, M. Backes, F. Backman, P. Bagnaia, M. Bahmani, H. Bahrasemani, A. J. Bailey, V. R. Bailey, J. T. Baines, M. Bajic, C. Bakalis, O. K. Baker, P. J. Bakker, D. Bakshi Gupta, S. Balaji, E. M. Baldin, P. Balek, F. Balli, W. K. Balunas, J. Balz, E. Banas, A. Bandyopadhyay, Sw. Banerjee, A. A. E. Bannoura, L. Barak, W. M. Barbe, E. L. Barberio, D. Barberis, M. Barbero, T. Barillari, M-S. Barisits, J. Barkeloo, T. Barklow, R. Barnea, S. L. Barnes, B. M. Barnett, R. M. Barnett, Z. Barnovska-Blenessy, A. Baroncelli, G. Barone, A. J. Barr, L. Barranco Navarro, F. Barreiro, J. Barreiro Guimarães da Costa, R. Bartoldus, G. Bartolini, A. E. Barton, P. Bartos, A. Basalaev, A. Bassalat, R. L. Bates, S. J. Batista, S. Batlamous, J. R. Batley, M. Battaglia, M. Bauce, F. Bauer, K. T. Bauer, H. S. Bawa, J. B. Beacham, T. Beau, P. H. Beauchemin, P. Bechtle, H. C. Beck, H. P. Beck, K. Becker, M. Becker, C. Becot, A. Beddall, A. J. Beddall, V. A. Bednyakov, M. Bedognetti, C. P. Bee, T. A. Beermann, M. Begalli, M. Begel, A. Behera, J. K. Behr, F. Beisiegel, A. S. Bell, G. Bella, L. Bellagamba, A. Bellerive, P. Bellos, K. Beloborodov, K. Belotskiy, N. L. Belyaev, O. Benary, D. Benchekroun, N. Benekos, Y. Benhammou, D. P. Benjamin, M. Benoit, J. R. Bensinger, S. Bentvelsen, L. Beresford, M. Beretta, D. Berge, E. Bergeaas Kuutmann, N. Berger, B. Bergmann, L. J. Bergsten, J. Beringer, S. Berlendis, N. R. Bernard, G. Bernardi, C. Bernius, F. U. Bernlochner, T. Berry, P. Berta, C. Bertella, G. Bertoli, I. A. Bertram, G. J. Besjes, O. Bessidskaia Bylund, N. Besson, A. Bethani, S. Bethke, A. Betti, A. J. Bevan, J. Beyer, R. Bi, R. M. Bianchi, O. Biebel, D. Biedermann, R. Bielski, K. Bierwagen, N. V. Biesuz, M. Biglietti, T. R. V. Billoud, M. Bindi, A. Bingul, C. Bini, S. Biondi, M. Birman, T. Bisanz, J. P. Biswal, A. Bitadze, C. Bittrich, D. M. Bjergaard, J. E. Black, K. M. Black, T. Blazek, I. Bloch, C. Blocker, A. Blue, U. Blumenschein, S. Blunier, G. J. Bobbink, V. S. Bobrovnikov, S. S. Bocchetta, A. Bocci, D. Boerner, D. Bogavac, A. G. Bogdanchikov, C. Bohm, V. Boisvert, P. Bokan, T. Bold, A. S. Boldyrev, A. E. Bolz, M. Bomben, M. Bona, J. S. Bonilla, M. Boonekamp, H. M. Borecka-Bielska, A. Borisov, G. Borissov, J. Bortfeldt, D. Bortoletto, and The ATLAS collaboration. Constraints on mediator-based dark matter and scalar dark energy models using s$$ \sqrt{s} $$= 13 tev pp collision data collected by the atlas detector. *Journal of High Energy Physics*, 2019(5):142, 2019. doi:

10.1007/JHEP05(2019)142. URL https://doi.org/10.1007/JHEP05(2019)142.

[216] Kristjan Kannike, Martti Raidal, Hardi Veermäe, Alessandro Strumia, and Daniele Teresi. Dark matter and the xenon1t electron recoil excess, 2020.

[217] Ken Van Tilburg. Stellar Basins of Gravitationally Bound Particles. *arXiv e-prints*, art. arXiv:2006.12431, June 2020.

[218] Jatan Buch, Manuel A. Buen-Abad, JiJi Fan, and John Shing Chau Leung. Galactic Origin of Relativistic Bosons and XENON1T Excess. *arXiv e-prints*, art. arXiv:2006.12488, June 2020.

[219] Peter W. Graham, Igor G. Irastorza, Steven K. Lamoreaux, Axel Lindner, and Karl A. van Bibber. Experimental searches for the axion and axion-like particles. *Annual Review of Nuclear and Particle Science*, 65(1):485–514, 2015. doi: 10.1146/annurev-nucl-102014-022120.

[220] N. Du, N. Force, R. Khatiwada, E. Lentz, R. Ottens, L. J Rosenberg, G. Rybka, G. Carosi, N. Woollett, D. Bowring, A. S. Chou, A. Sonnenschein, W. Wester, C. Boutan, N. S. Oblath, R. Bradley, E. J. Daw, A. V. Dixit, J. Clarke, S. R. O'Kelley, N. Crisosto, J. R. Gleason, S. Jois, P. Sikivie, I. Stern, N. S. Sullivan, D. B Tanner, and G. C. Hilton. Search for invisible axion dark matter with the axion dark matter experiment. *Phys. Rev. Lett.*, 120:151301, Apr 2018. doi: 10.1103/PhysRevLett.120.151301. URL https://link.aps.org/doi/10.1103/PhysRevLett.120.151301.

[221] C. Alcock, R. A. Allsman, D. R. Alves, T. S. Axelrod, A. C. Becker, D. P. Bennett, K. H. Cook, N. Dalal, A. J. Drake, K. C. Freeman, M. Geha, K. Griest, M. J. Lehner, S. L. Marshall, D. Minniti, C. A. Nelson, B. A. Peterson, P. Popowski, M. R. Pratt, P. J. Quinn, C. W. Stubbs, W. Sutherland, A. B. Tomaney, T. Vandehei, and D. Welch. The MACHO project: Microlensing results from 5.7 years of large magellanic cloud observations. *The Astrophysical Journal*, 542(1):281–307, oct 2000. doi: 10.1086/309512.

[222] Tisserand, P., Le Guillou, L., Afonso, C., Albert, J. N., Andersen, J., Ansari, R., Aubourg, É., Bareyre, P., Beaulieu, J. P., Charlot, X., Coutures, C., Ferlet, R., Fouqué, P., Glicenstein, J. F., Goldman, B., Gould, A., Graff, D., Gros, M., Haissinski, J., Hamadache, C., de Kat, J., Lasserre, T., Lesquoy, É., Loup, C., Magneville, C., Marquette, J. B., Maurice, É., Maury, A., Milsztajn, A., Moniez, M., Palanque-Delabrouille, N., Perdereau, O., Rahal, Y. R., Rich, J., Spiro, M., Vidal-Madjar, A., Vigroux, L., and S. Zylberajch (The EROS-2 collaboration). Limits on the macho content of the galactic halo from the eros-2 survey of the magellanic clouds ***. *A&A*, 469(2):387–404, 2007. doi: 10.1051/0004-6361:20066017. URL https://doi.org/10.1051/0004-6361:20066017.

[223] B. P. Abbott, R. Abbott, T. D. Abbott, S. Abraham, F. Acernese, K. Ackley, A. Adams, C. Adams, R. X. Adhikari, V. B. Adya, C. Affeldt, M. Agathos, K. Agatsuma, N. Aggarwal, O. D. Aguiar, L. Aiello, A. Ain, P. Ajith, G. Allen, A. Allocca, M. A. Aloy, P. A. Altin, A. Amato, S. Anand, A. Ananyeva, S. B. Anderson, W. G. Anderson, S. V. Angelova, S. Antier, S. Appert, K. Arai, M. C. Araya, J. S. Areeda, M. Arène, N. Arnaud, S. M. Aronson, K. G. Arun, S. Ascenzi, G. Ashton, S. M. Aston, P. Astone, F. Aubin, P. Aufmuth, K. AultONeal, C. Austin, V. Avendano, A. Avila-Alvarez, S. Babak, P. Bacon, F. Badaracco, M. K. M. Bader, S. Bae, A. M. Baer, J. Baird, P. T. Baker, F. Baldaccini, G. Ballardin, S. W. Ballmer, A. Bals, S. Banagiri, J. C. Barayoga, C. Barbieri, S. E. Barclay, B. C. Barish, D. Barker, K. Barkett, S. Barnum, F. Barone, B. Barr, L. Barsotti, M. Barsuglia, D. Barta, J. Bartlett, I. Bartos, R. Bassiri, A. Basti, M. Bawaj, J. C. Bayley, M. Bazzan, B. Bécsy, M. Bejger, I. Belahcene, A. S. Bell, D. Beniwal, M. G. Benjamin, B. K. Berger, G. Bergmann, S. Bernuzzi, C. P. L. Berry, D. Bersanetti, A. Bertolini, J. Betzwieser, R. Bhandare, J. Bidler, E. Biggs, I. A. Bilenko, S. A. Bilgili, G. Billingsley, R. Birney, O. Birnholtz, S. Biscans, M. Bischi, S. Biscoveanu, A. Bisht, M. Bitossi, M. A. Bizouard, J. K. Blackburn, J. Blackman, C. D. Blair, D. G. Blair, R. M. Blair, S. Bloemen, F. Bobba, N. Bode, M. Boer, Y. Boetzel, G. Bogaert, F. Bondu, R. Bonnand, P. Booker, B. A. Boom, R. Bork, V. Boschi, S. Bose, V. Bossilkov, J. Bosveld, Y. Bouffanais, A. Bozzi, C. Bradaschia, P. R. Brady,

A. Bramley, M. Branchesi, J. E. Brau, M. Breschi, T. Briant, J. H. Briggs, F. Brighenti, A. Brillet, M. Brinkmann, P. Brockill, A. F. Brooks, J. Brooks, D. D. Brown, S. Brunett, A. Buikema, T. Bulik, H. J. Bulten, A. Buonanno, D. Buskulic, C. Buy, R. L. Byer, M. Cabero, L. Cadonati, G. Cagnoli, C. Cahillane, J. Calderón Bustillo, T. A. Callister, E. Calloni, J. B. Camp, W. A. Campbell, M. Canepa, K. C. Cannon, H. Cao, J. Cao, G. Carapella, F. Carbognani, S. Caride, M. F. Carney, G. Carullo, J. Casanueva Diaz, C. Casentini, S. Caudill, M. Cavaglià, F. Cavalier, R. Cavalieri, G. Cella, P. Cerdá-Durán, E. Cesarini, O. Chaibi, K. Chakravarti, S. J. Chamberlin, M. Chan, S. Chao, P. Charlton, E. A. Chase, E. Chassande-Mottin, D. Chatterjee, M. Chaturvedi, B. D. Cheeseboro, H. Y. Chen, X. Chen, Y. Chen, H.-P. Cheng, C. K. Cheong, H. Y. Chia, F. Chiadini, A. Chincarini, A. Chiummo, G. Cho, H. S. Cho, M. Cho, N. Christensen, Q. Chu, S. Chua, K. W. Chung, S. Chung, G. Ciani, M. Cieślar, A. A. Ciobanu, R. Ciolfi, F. Cipriano, A. Cirone, F. Clara, J. A. Clark, P. Clearwater, F. Cleva, E. Coccia, P.-F. Cohadon, D. Cohen, M. Colleoni, C. G. Collette, C. Collins, M. Colpi, L. R. Cominsky, M. Constancio, L. Conti, S. J. Cooper, P. Corban, T. R. Corbitt, I. Cordero-Carrión, S. Corezzi, K. R. Corley, N. Cornish, D. Corre, A. Corsi, S. Cortese, C. A. Costa, R. Cotesta, M. W. Coughlin, S. B. Coughlin, J.-P. Coulon, S. T. Countryman, P. Couvares, P. B. Covas, E. E. Cowan, D. M. Coward, M. J. Cowart, D. C. Coyne, R. Coyne, J. D. E. Creighton, T. D. Creighton, J. Cripe, M. Croquette, S. G. Crowder, T. J. Cullen, A. Cumming, L. Cunningham, E. Cuoco, T. Dal Canton, G. Dálya, B. D'Angelo, S. L. Danilishin, S. D'Antonio, K. Danzmann, A. Dasgupta, C. F. Da Silva Costa, L. E. H. Datrier, V. Dattilo, I. Dave, M. Davier, D. Davis, E. J. Daw, D. DeBra, M. Deenadayalan, J. Degallaix, M. De Laurentis, S. Deléglise, W. Del Pozzo, L. M. DeMarchi, N. Demos, T. Dent, R. De Pietri, R. De Rosa, C. De Rossi, R. DeSalvo, O. de Varona, S. Dhurandhar, M. C. Díaz, T. Dietrich, L. Di Fiore, C. DiFronzo, C. Di Giorgio, F. Di Giovanni, M. Di Giovanni, T. Di Girolamo, A. Di Lieto, B. Ding, S. Di Pace, I. Di Palma, F. Di Renzo, A. K. Divakarla, A. Dmitriev, Z. Doctor, F. Donovan, K. L. Dooley, S. Doravari, I. Dorrington, T. P. Downes, M. Drago, J. C. Driggers, Z. Du, J.-G. Ducoin, P. Dupej, O. Durante, S. E. Dwyer, P. J. Easter, G. Eddolls, T. B. Edo, A. Effler, P. Ehrens, J. Eichholz, S. S. Eikenberry, M. Eisenmann, R. A. Eisenstein, L. Errico,

R. C. Essick, H. Estelles, D. Estevez, Z. B. Etienne, T. Etzel, M. Evans, T. M. Evans, V. Fafone, S. Fairhurst, X. Fan, S. Farinon, B. Farr, W. M. Farr, E. J. Fauchon-Jones, M. Favata, M. Fays, M. Fazio, C. Fee, J. Feicht, M. M. Fejer, F. Feng, D. L. Ferguson, A. Fernandez-Galiana, I. Ferrante, E. C. Ferreira, T. A. Ferreira, F. Fidecaro, I. Fiori, D. Fiorucci, M. Fishbach, R. P. Fisher, J. M. Fishner, R. Fittipaldi, M. Fitz-Axen, V. Fiumara, R. Flaminio, M. Fletcher, E. Floden, E. Flynn, H. Fong, J. A. Font, P. W. F. Forsyth, J.-D. Fournier, Francisco Hernandez Vivanco, S. Frasca, F. Frasconi, Z. Frei, A. Freise, R. Frey, V. Frey, P. Fritschel, V. V. Frolov, G. Fronzè, P. Fulda, M. Fyffe, H. A. Gabbard, B. U. Gadre, S. M. Gaebel, J. R. Gair, L. Gammaitoni, S. G. Gaonkar, C. García-Quirós, F. Garufi, B. Gateley, S. Gaudio, G. Gaur, V. Gayathri, G. Gemme, E. Genin, A. Gennai, D. George, J. George, L. Gergely, S. Ghonge, Abhirup Ghosh, Archisman Ghosh, S. Ghosh, B. Giacomazzo, J. A. Giaime, K. D. Giardina, D. R. Gibson, K. Gill, L. Glover, J. Gniesmer, P. Godwin, E. Goetz, R. Goetz, B. Goncharov, G. González, J. M. Gonzalez Castro, A. Gopakumar, S. E. Gossan, M. Gosselin, R. Gouaty, B. Grace, A. Grado, M. Granata, A. Grant, S. Gras, P. Grassia, C. Gray, R. Gray, G. Greco, A. C. Green, R. Green, E. M. Gretarsson, A. Grimaldi, S. J. Grimm, P. Groot, H. Grote, S. Grunewald, P. Gruning, G. M. Guidi, H. K. Gulati, Y. Guo, A. Gupta, Anchal Gupta, P. Gupta, E. K. Gustafson, R. Gustafson, L. Haegel, O. Halim, B. R. Hall, E. D. Hall, E. Z. Hamilton, G. Hammond, M. Haney, M. M. Hanke, J. Hanks, C. Hanna, M. D. Hannam, O. A. Hannuksela, T. J. Hansen, J. Hanson, T. Harder, T. Hardwick, K. Haris, J. Harms, G. M. Harry, I. W. Harry, R. K. Hasskew, C. J. Haster, K. Haughian, F. J. Hayes, J. Healy, A. Heidmann, M. C. Heintze, H. Heitmann, F. Hellman, P. Hello, G. Hemming, M. Hendry, I. S. Heng, J. Hennig, M. Heurs, S. Hild, T. Hinderer, S. Hochheim, D. Hofman, A. M. Holgado, N. A. Holland, K. Holt, D. E. Holz, P. Hopkins, C. Horst, J. Hough, E. J. Howell, C. G. Hoy, Y. Huang, M. T. Hübner, E. A. Huerta, D. Huet, B. Hughey, V. Hui, S. Husa, S. H. Huttner, T. Huynh-Dinh, B. Idzkowski, A. Iess, H. Inchauspe, C. Ingram, R. Inta, G. Intini, B. Irwin, H. N. Isa, J.-M. Isac, M. Isi, B. R. Iyer, T. Jacqmin, S. J. Jadhav, K. Jani, N. N. Janthalur, P. Jaranowski, D. Jariwala, A. C. Jenkins, J. Jiang, G. R. Johns, D. S. Johnson, A. W. Jones, D. I. Jones, J. D. Jones, R. Jones, R. J. G. Jonker,

L. Ju, J. Junker, C. V. Kalaghatgi, V. Kalogera, B. Kamai, S. Kandhasamy, G. Kang, J. B. Kanner, S. J. Kapadia, S. Karki, R. Kashyap, M. Kasprzack, S. Katsanevas, E. Katsavounidis, W. Katzman, S. Kaufer, K. Kawabe, N. V. Keerthana, F. Kéfélian, D. Keitel, R. Kennedy, J. S. Key, F. Y. Khalili, B. Khamesra, I. Khan, S. Khan, E. A. Khazanov, N. Khetan, M. Khursheed, N. Kijbunchoo, Chunglee Kim, G. J. Kim, J. C. Kim, K. Kim, W. Kim, W. S. Kim, Y.-M. Kim, C. Kimball, P. J. King, M. Kinley-Hanlon, R. Kirchhoff, J. S. Kissel, L. Kleybolte, J. H. Klika, S. Klimenko, T. D. Knowles, P. Koch, S. M. Koehlenbeck, G. Koekoek, S. Koley, V. Kondrashov, A. Kontos, N. Koper, M. Korobko, W. Z. Korth, M. Kovalam, D. B. Kozak, C. Krämer, V. Kringel, N. Krishnendu, A. Królak, N. Krupinski, G. Kuehn, A. Kumar, P. Kumar, Rahul Kumar, Rakesh Kumar, L. Kuo, A. Kutynia, S. Kwang, B. D. Lackey, D. Laghi, P. Laguna, K. H. Lai, T. L. Lam, M. Landry, B. B. Lane, R. N. Lang, J. Lange, B. Lantz, R. K. Lanza, A. Lartaux-Vollard, P. D. Lasky, M. Laxen, A. Lazzarini, C. Lazzaro, P. Leaci, S. Leavey, Y. K. Lecoeuche, C. H. Lee, H. K. Lee, H. M. Lee, H. W. Lee, J. Lee, K. Lee, J. Lehmann, A. K. Lenon, N. Leroy, N. Letendre, Y. Levin, A. Li, J. Li, K. J. L. Li, T. G. F. Li, X. Li, F. Lin, F. Linde, S. D. Linker, T. B. Littenberg, J. Liu, X. Liu, M. Llorens-Monteagudo, R. K. L. Lo, L. T. London, A. Longo, M. Lorenzini, V. Loriette, M. Lormand, G. Losurdo, J. D. Lough, C. O. Lousto, G. Lovelace, M. E. Lower, H. Lück, D. Lumaca, A. P. Lundgren, R. Lynch, Y. Ma, R. Macas, S. Macfoy, M. MacInnis, D. M. Macleod, A. Macquet, I. Magaña Hernandez, F. Magaña Sandoval, R. M. Magee, E. Majorana, I. Maksimovic, A. Malik, N. Man, V. Mandic, V. Mangano, G. L. Mansell, M. Manske, M. Mantovani, M. Mapelli, F. Marchesoni, F. Marion, S. Márka, Z. Márka, C. Markakis, A. S. Markosyan, A. Markowitz, E. Maros, A. Marquina, S. Marsat, F. Martelli, I. W. Martin, R. M. Martin, V. Martinez, D. V. Martynov, H. Masalehdan, K. Mason, E. Massera, A. Masserot, T. J. Massinger, M. Masso-Reid, S. Mastrogiovanni, A. Matas, F. Matichard, L. Matone, N. Mavalvala, J. J. McCann, R. McCarthy, D. E. McClelland, S. McCormick, L. McCuller, S. C. McGuire, C. McIsaac, J. McIver, D. J. McManus, T. McRae, S. T. McWilliams, D. Meacher, G. D. Meadors, M. Mehmet, A. K. Mehta, J. Meidam, E. Mejuto Villa, A. Melatos, G. Mendell, R. A. Mercer, L. Mereni, K. Merfeld, E. L. Merilh, M. Merzougui, S. Meshkov, C. Messenger,

C. Messick, F. Messina, R. Metzdorff, P. M. Meyers, F. Meylahn, A. Miani, H. Miao, C. Michel, H. Middleton, L. Milano, A. L. Miller, M. Millhouse, J. C. Mills, M. C. Milovich-Goff, O. Minazzoli, Y. Minenkov, A. Mishkin, C. Mishra, T. Mistry, S. Mitra, V. P. Mitrofanov, G. Mitselmakher, R. Mittleman, G. Mo, D. Moffa, K. Mogushi, S. R. P. Mohapatra, M. Molina-Ruiz, M. Mondin, M. Montani, C. J. Moore, D. Moraru, F. Morawski, G. Moreno, S. Morisaki, B. Mours, C. M. Mow-Lowry, F. Muciaccia, Arunava Mukherjee, D. Mukherjee, S. Mukherjee, Subroto Mukherjee, N. Mukund, A. Mullavey, J. Munch, E. A. Muñiz, M. Muratore, P. G. Murray, A. Nagar, I. Nardecchia, L. Naticchioni, R. K. Nayak, B. F. Neil, J. Neilson, G. Nelemans, T. J. N. Nelson, M. Nery, A. Neunzert, L. Nevin, K. Y. Ng, S. Ng, C. Nguyen, P. Nguyen, D. Nichols, S. A. Nichols, S. Nissanke, F. Nocera, C. North, L. K. Nuttall, M. Obergaulinger, J. Oberling, B. D. O'Brien, G. Oganesyan, G. H. Ogin, J. J. Oh, S. H. Oh, F. Ohme, H. Ohta, M. A. Okada, M. Oliver, P. Oppermann, Richard J. Oram, B. O'Reilly, R. G. Ormiston, L. F. Ortega, R. O'Shaughnessy, S. Ossokine, D. J. Ottaway, H. Overmier, B. J. Owen, A. E. Pace, G. Pagano, M. A. Page, G. Pagliaroli, A. Pai, S. A. Pai, J. R. Palamos, O. Palashov, C. Palomba, H. Pan, P. K. Panda, P. T. H. Pang, C. Pankow, F. Pannarale, B. C. Pant, F. Paoletti, A. Paoli, A. Parida, W. Parker, D. Pascucci, A. Pasqualetti, R. Passaquieti, D. Passuello, M. Patil, B. Patricelli, E. Payne, B. L. Pearlstone, T. C. Pechsiri, A. J. Pedersen, M. Pedraza, R. Pedurand, A. Pele, S. Penn, A. Perego, C. J. Perez, C. Périgois, A. Perreca, J. Petermann, H. P. Pfeiffer, M. Phelps, K. S. Phukon, O. J. Piccinni, M. Pichot, F. Piergiovanni, V. Pierro, G. Pillant, L. Pinard, I. M. Pinto, M. Pirello, M. Pitkin, W. Plastino, R. Poggiani, D. Y. T. Pong, S. Ponrathnam, P. Popolizio, E. K. Porter, J. Powell, A. K. Prajapati, J. Prasad, K. Prasai, R. Prasanna, G. Pratten, T. Prestegard, M. Principe, G. A. Prodi, L. Prokhorov, M. Punturo, P. Puppo, M. Pürrer, H. Qi, V. Quetschke, P. J. Quinonez, F. J. Raab, G. Raaijmakers, H. Radkins, N. Radulesco, P. Raffai, S. Raja, C. Rajan, B. Rajbhandari, M. Rakhmanov, K. E. Ramirez, A. Ramos-Buades, Javed Rana, K. Rao, P. Rapagnani, V. Raymond, M. Razzano, J. Read, T. Regimbau, L. Rei, S. Reid, D. H. Reitze, P. Rettegno, F. Ricci, C. J. Richardson, J. W. Richardson, P. M. Ricker, G. Riemenschneider, K. Riles, M. Rizzo, N. A. Robertson, F. Robinet,

A. Rocchi, L. Rolland, J. G. Rollins, V. J. Roma, M. Romanelli, R. Romano, C. L. Romel, J. H. Romie, C. A. Rose, D. Rose, K. Rose, D. Rosińska, S. G. Rosofsky, M. P. Ross, S. Rowan, A. Rüdiger, P. Ruggi, G. Rutins, K. Ryan, S. Sachdev, T. Sadecki, M. Sakellariadou, O. S. Salafia, L. Salconi, M. Saleem, A. Samajdar, L. Sammut, E. J. Sanchez, L. E. Sanchez, N. Sanchis-Gual, J. R. Sanders, K. A. Santiago, E. Santos, N. Sarin, B. Sassolas, B. S. Sathyaprakash, O. Sauter, R. L. Savage, P. Schale, M. Scheel, J. Scheuer, P. Schmidt, R. Schnabel, R. M. S. Schofield, A. Schönbeck, E. Schreiber, B. W. Schulte, B. F. Schutz, J. Scott, S. M. Scott, E. Seidel, D. Sellers, A. S. Sengupta, N. Sennett, D. Sentenac, V. Sequino, A. Sergeev, Y. Setyawati, D. A. Shaddock, T. Shaffer, M. S. Shahriar, M. B. Shaner, A. Sharma, P. Sharma, P. Shawhan, H. Shen, R. Shink, D. H. Shoemaker, D. M. Shoemaker, K. Shukla, S. ShyamSundar, K. Siellez, M. Sieniawska, D. Sigg, L. P. Singer, D. Singh, N. Singh, A. Singhal, A. M. Sintes, S. Sitmukhambetov, V. Skliris, B. J. J. Slagmolen, T. J. Slaven-Blair, J. R. Smith, R. J. E. Smith, S. Somala, E. J. Son, S. Soni, B. Sorazu, F. Sorrentino, T. Souradeep, E. Sowell, A. P. Spencer, M. Spera, A. K. Srivastava, V. Srivastava, K. Staats, C. Stachie, M. Standke, D. A. Steer, M. Steinke, J. Steinlechner, S. Steinlechner, D. Steinmeyer, S. P. Stevenson, D. Stocks, G. Stolle-McAllister, R. Stone, D. J. Stops, K. A. Strain, G. Stratta, S. E. Strigin, A. Strunk, R. Sturani, A. L. Stuver, V. Sudhir, T. Z. Summerscales, L. Sun, S. Sunil, A. Sur, J. Suresh, P. J. Sutton, B. L. Swinkels, M. J. Szczepańczyk, M. Tacca, S. C. Tait, C. Talbot, D. B. Tanner, D. Tao, M. Tápai, A. Tapia, J. D. Tasson, R. Taylor, R. Tenorio, L. Terkowski, M. Thomas, P. Thomas, S. R. Thondapu, K. A. Thorne, E. Thrane, Shubhanshu Tiwari, Srishti Tiwari, V. Tiwari, K. Toland, M. Tonelli, Z. Tornasi, A. Torres-Forné, C. I. Torrie, D. Töyrä, F. Travasso, G. Traylor, M. C. Tringali, A. Tripathee, A. Trovato, L. Trozzo, K. W. Tsang, M. Tse, R. Tso, L. Tsukada, D. Tsuna, T. Tsutsui, D. Tuyenbayev, K. Ueno, D. Ugolini, C. S. Unnikrishnan, A. L. Urban, S. A. Usman, H. Vahlbruch, G. Vajente, G. Valdes, M. Valentini, N. van Bakel, M. van Beuzekom, J. F. J. van den Brand, C. Van Den Broeck, D. C. Vander-Hyde, L. van der Schaaf, J. V. VanHeijningen, A. A. van Veggel, M. Vardaro, V. Varma, S. Vass, M. Vasúth, A. Vecchio, G. Vedovato, J. Veitch, P. J. Veitch, K. Venkateswara, G. Venugopalan, D. Verkindt, F. Vetrano,

A. Viceré, A. D. Viets, S. Vinciguerra, D. J. Vine, J.-Y. Vinet, S. Vitale, T. Vo, H. Vocca, C. Vorvick, S. P. Vyatchanin, A. R. Wade, L. E. Wade, M. Wade, R. Walet, M. Walker, L. Wallace, S. Walsh, H. Wang, J. Z. Wang, S. Wang, W. H. Wang, Y. F. Wang, R. L. Ward, Z. A. Warden, J. Warner, M. Was, J. Watchi, B. Weaver, L.-W. Wei, M. Weinert, A. J. Weinstein, R. Weiss, F. Wellmann, L. Wen, E. K. Wessel, P. Weßels, J. W. Westhouse, K. Wette, J. T. Whelan, B. F. Whiting, C. Whittle, D. M. Wilken, D. Williams, A. R. Williamson, J. L. Willis, B. Willke, W. Winkler, C. C. Wipf, H. Wittel, G. Woan, J. Woehler, J. K. Wofford, J. L. Wright, D. S. Wu, D. M. Wysocki, S. Xiao, R. Xu, H. Yamamoto, C. C. Yancey, L. Yang, Y. Yang, Z. Yang, M. J. Yap, M. Yazback, D. W. Yeeles, A. Yoon, Hang Yu, Haocun Yu, S. H. R. Yuen, A. K. Zadrożny, A. Zadrożny, M. Zanolin, T. Zelenova, J.-P. Zendri, M. Zevin, J. Zhang, L. Zhang, T. Zhang, C. Zhao, G. Zhao, M. Zhou, Z. Zhou, X. J. Zhu, M. E. Zucker, J. Zweizig, F. Salemi, and M. A. Papa. Search for intermediate mass black hole binaries in the first and second observing runs of the advanced ligo and virgo network. *Phys. Rev. D*, 100:064064, Sep 2019. doi: 10.1103/PhysRevD.100.064064. URL https://link.aps.org/doi/10.1103/PhysRevD.100.064064.

[224] B. J. Carr and S. W. Hawking. Black Holes in the Early Universe. *Monthly Notices of the Royal Astronomical Society*, 168(2):399–415, 08 1974. ISSN 0035-8711. doi: 10.1093/mnras/168.2.399. URL https://doi.org/10.1093/mnras/168.2.399.

[225] Simeon Bird, Ilias Cholis, Julian B. Muñoz, Yacine Ali-Haïmoud, Marc Kamionkowski, Ely D. Kovetz, Alvise Raccanelli, and Adam G. Riess. Did LIGO detect dark matter? *Phys. Rev. Lett.*, 116(20):201301, 2016. doi: 10.1103/PhysRevLett.116.201301.

[226] Andrew D. Gow, Christian T. Byrnes, Alex Hall, and John A. Peacock. Primordial black hole merger rates: distributions for multiple LIGO observables. *JCAP*, 01:031, 2020. doi: 10.1088/1475-7516/2020/01/031.

[227] Sam Young and Christian T. Byrnes. Initial clustering and the primordial black hole merger rate. *JCAP*, 03:004, 2020. doi: 10.1088/1475-7516/2020/03/004.

[228] Ville Vaskonen and Hardi Veermäe. Lower bound on the primordial black hole merger rate. *Phys. Rev. D*, 101(4):043015, 2020. doi: 10.1103/PhysRevD.101.043015.

[229] Guillermo Ballesteros, Pasquale D. Serpico, and Marco Taoso. On the merger rate of primordial black holes: effects of nearest neighbours distribution and clustering. *JCAP*, 10:043, 2018. doi: 10.1088/1475-7516/2018/10/043.

[230] Zu-Cheng Chen and Qing-Guo Huang. Merger Rate Distribution of Primordial-Black-Hole Binaries. *Astrophys. J.*, 864(1):61, 2018. doi: 10.3847/1538-4357/aad6e2.

[231] Hiroko Niikura, Masahiro Takada, Naoki Yasuda, Robert H. Lupton, Takahiro Sumi, Surhud More, Toshiki Kurita, Sunao Sugiyama, Anupreeta More, Masamune Oguri, and Masashi Chiba. Microlensing constraints on primordial black holes with subaru/hsc andromeda observations. *Nature Astronomy*, 3(6):524–534, 2019. doi: 10.1038/s41550-019-0723-1. URL https://doi.org/10.1038/s41550-019-0723-1.

[232] R.A. Allsman et al. MACHO project limits on black hole dark matter in the 1-30 solar mass range. *Astrophys. J. Lett.*, 550:L169, 2001. doi: 10.1086/319636.

[233] L. Wyrzykowski, J. Skowron, S. Kozłowski, A. Udalski, M. K. Szymański, M. Kubiak, G. Pietrzyński, I. Soszyński, O. Szewczyk, K. Ulaczyk, R. Poleski, and P. Tisserand. The OGLE view of microlensing towards the Magellanic Clouds – IV. OGLE-III SMC data and final conclusions on MACHOs*. *Monthly Notices of the Royal Astronomical Society*, 416(4):2949–2961, 09 2011. ISSN 0035-8711. doi: 10.1111/j.1365-2966.2011.19243.x. URL https://doi.org/10.1111/j.1365-2966.2011.19243.x.

[234] Harry Poulter, Yacine Ali-Haïmoud, Jan Hamann, Martin White, and Anthony G. Williams. Cmb constraints on ultra-light primordial black holes with extended mass distributions, 2019.

[235] Yacine Ali-Haïmoud and Marc Kamionkowski. Cosmic microwave background limits on accreting primordial black holes. *Phys. Rev. D*, 95(4):043534, February 2017. doi: 10.1103/PhysRevD.95.043534.

[236] Savvas M. Koushiappas and Abraham Loeb. Dynamics of Dwarf Galaxies Disfavor Stellar-Mass Black Holes as Dark Matter. *Phys. Rev. Lett.*, 119(4):041102, July 2017. doi: 10.1103/PhysRevLett.119.041102.

[237] Timothy D. Brandt. Constraints on MACHO Dark Matter from Compact Stellar Systems in Ultra-faint Dwarf Galaxies. *Astrophys. J. Lett.*, 824(2):L31, June 2016. doi: 10.3847/2041-8205/824/2/L31.

[238] Jakob Stegmann, Pedro R. Capelo, Elisa Bortolas, and Lucio Mayer. Improved constraints from ultra-faint dwarf galaxies on primordial black holes as dark matter. *Mon. Not. R. Astron. Soc.*, 492(4):5247–5260, March 2020. doi: 10.1093/mnras/staa170.

[239] Alexandre Dolgov and Joseph Silk. Baryon isocurvature fluctuations at small scales and baryonic dark matter. *Phys. Rev. D*, 47:4244–4255, May 1993. doi: 10.1103/PhysRevD.47.4244. URL https://link.aps.org/doi/10.1103/PhysRevD.47.4244.

[240] Jun'ichi Yokoyama. Cosmological constraints on primordial black holes produced in the near-critical gravitational collapse. *Phys. Rev. D*, 58:107502, Oct 1998. doi: 10.1103/PhysRevD.58.107502. URL https://link.aps.org/doi/10.1103/PhysRevD.58.107502.

[241] Anne M. Green. Microlensing and dynamical constraints on primordial black hole dark matter with an extended mass function. *Phys. Rev. D*, 94:063530, Sep 2016. doi: 10.1103/PhysRevD.94.063530. URL https://link.aps.org/doi/10.1103/PhysRevD.94.063530.

[242] Bernard Carr, Martti Raidal, Tommi Tenkanen, Ville Vaskonen, and Hardi Veermäe. Primordial black hole constraints for extended mass functions. *Phys. Rev. D*, 96:023514, Jul 2017. doi: 10.1103/PhysRevD.96.023514. URL https://link.aps.org/doi/10.1103/PhysRevD.96.023514.

[243] Florian Kühnel and Katherine Freese. Constraints on primordial black holes with extended mass functions. *Phys. Rev. D*, 95:083508, Apr 2017. doi: 10.1103/PhysRevD.95.083508. URL https://link.aps.org/doi/10.1103/PhysRevD.95.083508.

[244] R. Abbott, T. D. Abbott, S. Abraham, F. Acernese, K. Ackley, C. Adams, R. X. Adhikari, V. B. Adya, C. Affeldt, M. Agathos, K. Agatsuma, N. Aggarwal, O. D. Aguiar, A. Aich, L. Aiello, A. Ain, P. Ajith, S. Akcay, G. Allen, A. Allocca, P. A. Altin, A. Amato, S. Anand, A. Ananyeva, S. B. Anderson, W. G. Anderson, S. V. Angelova, S. Ansoldi, S. Antier, S. Appert, K. Arai, M. C. Araya, J. S. Areeda, M. Arène, N. Arnaud, S. M. Aronson, K. G. Arun, Y. Asali, S. Ascenzi, G. Ashton, S. M. Aston, P. Astone, F. Aubin, P. Aufmuth, K. AultONeal, C. Austin, V. Avendano, S. Babak, P. Bacon, F. Badaracco, M. K. M. Bader, S. Bae, A. M. Baer, J. Baird, F. Baldaccini, G. Ballardin, S. W. Ballmer, A. Bals, A. Balsamo, G. Baltus, S. Banagiri, D. Bankar, R. S. Bankar, J. C. Barayoga, C. Barbieri, B. C. Barish, D. Barker, K. Barkett, P. Barneo, F. Barone, B. Barr, L. Barsotti, M. Barsuglia, D. Barta, J. Bartlett, I. Bartos, R. Bassiri, A. Basti, M. Bawaj, J. C. Bayley, M. Bazzan, B. Bécsy, M. Bejger, I. Belahcene, A. S. Bell, D. Beniwal, M. G. Benjamin, R. Benkel, J. D. Bentley, F. Bergamin, B. K. Berger, G. Bergmann, S. Bernuzzi, C. P. L. Berry, D. Bersanetti, A. Bertolini, J. Betzwieser, R. Bhandare, A. V. Bhandari, J. Bidler, E. Biggs, I. A. Bilenko, G. Billingsley, R. Birney, O. Birnholtz, S. Biscans, M. Bischi, S. Biscoveanu, A. Bisht, G. Bissenbayeva, M. Bitossi, M. A. Bizouard, J. K. Blackburn, J. Blackman, C. D. Blair, D. G. Blair, R. M. Blair, F. Bobba, N. Bode, M. Boer, Y. Boetzel, G. Bogaert, F. Bondu, E. Bonilla, R. Bonnand, P. Booker, B. A. Boom, R. Bork, V. Boschi, S. Bose, V. Bossilkov, J. Bosveld, Y. Bouffanais, A. Bozzi, C. Bradaschia, P. R. Brady, A. Bramley, M. Branchesi, J. E. Brau, M. Breschi, T. Briant, J. H. Briggs, F. Brighenti, A. Brillet, M. Brinkmann, R. Brito, P. Brockill, A. F. Brooks, J. Brooks, D. D. Brown, S. Brunett, G. Bruno, R. Bruntz, A. Buikema, T. Bulik, H. J. Bulten, A. Buonanno, D. Buskulic, R. L. Byer, M. Cabero, L. Cadonati, G. Cagnoli, C. Cahillane, J. Calderón Bustillo, J. D. Callaghan, T. A. Callister, E. Calloni, J. B. Camp, M. Canepa, K. C. Cannon, H. Cao, J. Cao, G. Carapella, F. Carbognani, S. Caride, M. F. Carney, G. Carullo, J. Casanueva Diaz, C. Casentini, J. Castañeda, S. Caudill, M. Cavaglià, F. Cavalier, R. Cavalieri, G. Cella, P. Cerdá-Durán, E. Cesarini, O. Chaibi, K. Chakravarti, C. Chan, M. Chan, S. Chao, P. Charlton, E. A. Chase, E. Chassande-Mottin, D. Chatterjee, M. Chaturvedi, K. Chatziioannou, H. Y. Chen,

X. Chen, Y. Chen, H.-P. Cheng, C. K. Cheong, H. Y. Chia, F. Chiadini, R. Chierici, A. Chincarini, A. Chiummo, G. Cho, H. S. Cho, M. Cho, N. Christensen, Q. Chu, S. Chua, K. W. Chung, S. Chung, G. Ciani, P. Ciecielag, M. Cieślar, A. A. Ciobanu, R. Ciolfi, F. Cipriano, A. Cirone, F. Clara, J. A. Clark, P. Clearwater, S. Clesse, F. Cleva, E. Coccia, P.-F. Cohadon, D. Cohen, M. Colleoni, C. G. Collette, C. Collins, M. Colpi, M. Constancio, L. Conti, S. J. Cooper, P. Corban, T. R. Corbitt, I. Cordero-Carrión, S. Corezzi, K. R. Corley, N. Cornish, D. Corre, A. Corsi, S. Cortese, C. A. Costa, R. Cotesta, M. W. Coughlin, S. B. Coughlin, J.-P. Coulon, S. T. Countryman, P. Couvares, P. B. Covas, D. M. Coward, M. J. Cowart, D. C. Coyne, R. Coyne, J. D. E. Creighton, T. D. Creighton, J. Cripe, M. Croquette, S. G. Crowder, J.-R. Cudell, T. J. Cullen, A. Cumming, R. Cummings, L. Cunningham, E. Cuoco, M. Curylo, T. Dal Canton, G. Dálya, A. Dana, L. M. Daneshgaran-Bajastani, B. D'Angelo, S. L. Danilishin, S. D'Antonio, K. Danzmann, C. Darsow-Fromm, A. Dasgupta, L. E. H. Datrier, V. Dattilo, I. Dave, M. Davier, G. S. Davies, D. Davis, E. J. Daw, D. DeBra, M. Deenadayalan, J. Degallaix, M. De Laurentis, S. Deléglise, M. Delfavero, N. De Lillo, W. Del Pozzo, L. M. DeMarchi, V. D'Emilio, N. Demos, T. Dent, R. De Pietri, R. De Rosa, C. De Rossi, R. DeSalvo, O. de Varona, S. Dhurandhar, M. C. Díaz, M. Diaz-Ortiz, T. Dietrich, L. Di Fiore, C. Di Fronzo, C. Di Giorgio, F. Di Giovanni, M. Di Giovanni, T. Di Girolamo, A. Di Lieto, B. Ding, S. Di Pace, I. Di Palma, F. Di Renzo, A. K. Divakarla, A. Dmitriev, Z. Doctor, F. Donovan, K. L. Dooley, S. Doravari, I. Dorrington, T. P. Downes, M. Drago, J. C. Driggers, Z. Du, J.-G. Ducoin, P. Dupej, O. Durante, D. D'Urso, S. E. Dwyer, P. J. Easter, G. Eddolls, B. Edelman, T. B. Edo, O. Edy, A. Effler, P. Ehrens, J. Eichholz, S. S. Eikenberry, M. Eisenmann, R. A. Eisenstein, A. Ejlli, L. Errico, R. C. Essick, H. Estelles, D. Estevez, Z. B. Etienne, T. Etzel, M. Evans, T. M. Evans, B. E. Ewing, V. Fafone, S. Fairhurst, X. Fan, S. Farinon, B. Farr, W. M. Farr, E. J. Fauchon-Jones, M. Favata, M. Fays, M. Fazio, J. Feicht, M. M. Fejer, F. Feng, E. Fenyvesi, D. L. Ferguson, A. Fernandez-Galiana, I. Ferrante, E. C. Ferreira, T. A. Ferreira, F. Fidecaro, I. Fiori, D. Fiorucci, M. Fishbach, R. P. Fisher, R. Fittipaldi, M. Fitz-Axen, V. Fiumara, R. Flaminio, E. Floden, E. Flynn, H. Fong, J. A. Font, P. W. F. Forsyth, J.-D. Fournier, S. Frasca, F. Frasconi, Z. Frei,

A. Freise, R. Frey, V. Frey, P. Fritschel, V. V. Frolov, G. Fronzè, P. Fulda, M. Fyffe, H. A. Gabbard, B. U. Gadre, S. M. Gaebel, J. R. Gair, S. Galaudage, D. Ganapathy, A. Ganguly, S. G. Gaonkar, C. García-Quirós, F. Garufi, B. Gateley, S. Gaudio, V. Gayathri, G. Gemme, E. Genin, A. Gennai, D. George, J. George, L. Gergely, S. Ghonge, Abhirup Ghosh, Archisman Ghosh, S. Ghosh, B. Giacomazzo, J. A. Giaime, K. D. Giardina, D. R. Gibson, C. Gier, K. Gill, J. Glanzer, J. Gniesmer, P. Godwin, E. Goetz, R. Goetz, N. Gohlke, B. Goncharov, G. González, A. Gopakumar, S. E. Gossan, M. Gosselin, R. Gouaty, B. Grace, A. Grado, M. Granata, A. Grant, S. Gras, P. Grassia, C. Gray, R. Gray, G. Greco, A. C. Green, R. Green, E. M. Gretarsson, H. L. Griggs, G. Grignani, A. Grimaldi, S. J. Grimm, H. Grote, S. Grunewald, P. Gruning, G. M. Guidi, A. R. Guimaraes, G. Guixé, H. K. Gulati, Y. Guo, A. Gupta, Anchal Gupta, P. Gupta, E. K. Gustafson, R. Gustafson, L. Haegel, O. Halim, E. D. Hall, E. Z. Hamilton, G. Hammond, M. Haney, M. M. Hanke, J. Hanks, C. Hanna, M. D. Hannam, O. A. Hannuksela, T. J. Hansen, J. Hanson, T. Harder, T. Hardwick, K. Haris, J. Harms, G. M. Harry, I. W. Harry, R. K. Hasskew, C.-J. Haster, K. Haughian, F. J. Hayes, J. Healy, A. Heidmann, M. C. Heintze, J. Heinze, H. Heitmann, F. Hellman, P. Hello, G. Hemming, M. Hendry, I. S. Heng, E. Hennes, J. Hennig, M. Heurs, S. Hild, T. Hinderer, S. Y. Hoback, S. Hochheim, E. Hofgard, D. Hofman, A. M. Holgado, N. A. Holland, K. Holt, D. E. Holz, P. Hopkins, C. Horst, J. Hough, E. J. Howell, C. G. Hoy, Y. Huang, M. T. Hübner, E. A. Huerta, D. Huet, B. Hughey, V. Hui, S. Husa, S. H. Huttner, R. Huxford, T. Huynh-Dinh, B. Idzkowski, A. Iess, H. Inchauspe, C. Ingram, G. Intini, J.-M. Isac, M. Isi, B. R. Iyer, T. Jacqmin, S. J. Jadhav, S. P. Jadhav, A. L. James, K. Jani, N. N. Janthalur, P. Jaranowski, D. Jariwala, R. Jaume, A. C. Jenkins, J. Jiang, G. R. Johns, N. K. Johnson-McDaniel, A. W. Jones, D. I. Jones, J. D. Jones, P. Jones, R. Jones, R. J. G. Jonker, L. Ju, J. Junker, C. V. Kalaghatgi, V. Kalogera, B. Kamai, S. Kandhasamy, G. Kang, J. B. Kanner, S. J. Kapadia, S. Karki, R. Kashyap, M. Kasprzack, W. Kastaun, S. Katsanevas, E. Katsavounidis, W. Katzman, S. Kaufer, K. Kawabe, F. Kéfélian, D. Keitel, A. Keivani, R. Kennedy, J. S. Key, S. Khadka, F. Y. Khalili, I. Khan, S. Khan, Z. A. Khan, E. A. Khazanov, N. Khetan, M. Khursheed, N. Kijbunchoo, Chunglee Kim, G. J. Kim, J. C. Kim, K. Kim, W. Kim,

W. S. Kim, Y.-M. Kim, C. Kimball, P. J. King, M. Kinley-Hanlon, R. Kirchhoff, J. S. Kissel, L. Kleybolte, S. Klimenko, T. D. Knowles, E. Knyazev, P. Koch, S. M. Koehlenbeck, G. Koekoek, S. Koley, V. Kondrashov, A. Kontos, N. Koper, M. Korobko, W. Z. Korth, M. Kovalam, D. B. Kozak, V. Kringel, N. V. Krishnendu, A. Królak, N. Krupinski, G. Kuehn, A. Kumar, P. Kumar, Rahul Kumar, Rakesh Kumar, S. Kumar, L. Kuo, A. Kutynia, B. D. Lackey, D. Laghi, E. Lalande, T. L. Lam, A. Lamberts, M. Landry, P. Landry, B. B. Lane, R. N. Lang, J. Lange, B. Lantz, R. K. Lanza, I. La Rosa, A. Lartaux-Vollard, P. D. Lasky, M. Laxen, A. Lazzarini, C. Lazzaro, P. Leaci, S. Leavey, Y. K. Lecoeuche, C. H. Lee, H. M. Lee, H. W. Lee, J. Lee, K. Lee, J. Lehmann, N. Leroy, N. Letendre, Y. Levin, A. K. Y. Li, J. Li, K. li, T. G. F. Li, X. Li, F. Linde, S. D. Linker, J. N. Linley, T. B. Littenberg, J. Liu, X. Liu, M. Llorens-Monteagudo, R. K. L. Lo, A. Lockwood, L. T. London, A. Longo, M. Lorenzini, V. Loriette, M. Lormand, G. Losurdo, J. D. Lough, C. O. Lousto, G. Lovelace, H. Lück, D. Lumaca, A. P. Lundgren, Y. Ma, R. Macas, S. Macfoy, M. MacInnis, D. M. Macleod, I. A. O. MacMillan, A. Macquet, I. Magaña Hernandez, F. Magaña-Sandoval, R. M. Magee, E. Majorana, I. Maksimovic, A. Malik, N. Man, V. Mandic, V. Mangano, G. L. Mansell, M. Manske, M. Mantovani, M. Mapelli, F. Marchesoni, F. Marion, S. Márka, Z. Márka, C. Markakis, A. S. Markosyan, A. Markowitz, E. Maros, A. Marquina, S. Marsat, F. Martelli, I. W. Martin, R. M. Martin, V. Martinez, D. V. Martynov, H. Masalehdan, K. Mason, E. Massera, A. Masserot, T. J. Massinger, M. Masso-Reid, S. Mastrogiovanni, A. Matas, F. Matichard, N. Mavalvala, E. Maynard, J. J. McCann, R. McCarthy, D. E. McClelland, S. McCormick, L. McCuller, S. C. McGuire, C. McIsaac, J. McIver, D. J. McManus, T. McRae, S. T. McWilliams, D. Meacher, G. D. Meadors, M. Mehmet, A. K. Mehta, E. Mejuto Villa, A. Melatos, G. Mendell, R. A. Mercer, L. Mereni, K. Merfeld, E. L. Merilh, J. D. Merritt, M. Merzougui, S. Meshkov, C. Messenger, C. Messick, R. Metzdorff, P. M. Meyers, F. Meylahn, A. Mhaske, A. Miani, H. Miao, I. Michaloliakos, C. Michel, H. Middleton, L. Milano, A. L. Miller, M. Millhouse, J. C. Mills, E. Milotti, M. C. Milovich-Goff, O. Minazzoli, Y. Minenkov, A. Mishkin, C. Mishra, T. Mistry, S. Mitra, V. P. Mitrofanov, G. Mitselmakher, R. Mittleman, G. Mo, K. Mogushi, S. R. P. Mohapatra, S. R. Mohite,

M. Molina-Ruiz, M. Mondin, M. Montani, C. J. Moore, D. Moraru, F. Morawski, G. Moreno, S. Morisaki, B. Mours, C. M. Mow-Lowry, S. Mozzon, F. Muciaccia, Arunava Mukherjee, D. Mukherjee, S. Mukherjee, Subroto Mukherjee, N. Mukund, A. Mullavey, J. Munch, E. A. Muñiz, P. G. Murray, A. Nagar, I. Nardecchia, L. Naticchioni, R. K. Nayak, B. F. Neil, J. Neilson, G. Nelemans, T. J. N. Nelson, M. Nery, A. Neunzert, K. Y. Ng, S. Ng, C. Nguyen, P. Nguyen, D. Nichols, S. A. Nichols, S. Nissanke, F. Nocera, M. Noh, C. North, D. Nothard, L. K. Nuttall, J. Oberling, B. D. O'Brien, G. Oganesyan, G. H. Ogin, J. J. Oh, S. H. Oh, F. Ohme, H. Ohta, M. A. Okada, M. Oliver, C. Olivetto, P. Oppermann, Richard J. Oram, B. O'Reilly, R. G. Ormiston, L. F. Ortega, R. O'Shaughnessy, S. Ossokine, C. Osthelder, D. J. Ottaway, H. Overmier, B. J. Owen, A. E. Pace, G. Pagano, M. A. Page, G. Pagliaroli, A. Pai, S. A. Pai, J. R. Palamos, O. Palashov, C. Palomba, H. Pan, P. K. Panda, P. T. H. Pang, C. Pankow, F. Pannarale, B. C. Pant, F. Paoletti, A. Paoli, A. Parida, W. Parker, D. Pascucci, A. Pasqualetti, R. Passaquieti, D. Passuello, B. Patricelli, E. Payne, B. L. Pearlstone, T. C. Pechsiri, A. J. Pedersen, M. Pedraza, A. Pele, S. Penn, A. Perego, C. J. Perez, C. Périgois, A. Perreca, S. Perriès, J. Petermann, H. P. Pfeiffer, M. Phelps, K. S. Phukon, O. J. Piccinni, M. Pichot, M. Piendibene, F. Piergiovanni, V. Pierro, G. Pillant, L. Pinard, I. M. Pinto, K. Piotrzkowski, M. Pirello, M. Pitkin, W. Plastino, R. Poggiani, D. Y. T. Pong, S. Ponrathnam, P. Popolizio, E. K. Porter, J. Powell, A. K. Prajapati, K. Prasai, R. Prasanna, G. Pratten, T. Prestegard, M. Principe, G. A. Prodi, L. Prokhorov, M. Punturo, P. Puppo, M. Pürrer, H. Qi, V. Quetschke, P. J. Quinonez, F. J. Raab, G. Raaijmakers, H. Radkins, N. Radulesco, P. Raffai, H. Rafferty, S. Raja, C. Rajan, B. Rajbhandari, M. Rakhmanov, K. E. Ramirez, A. Ramos-Buades, Javed Rana, K. Rao, P. Rapagnani, V. Raymond, M. Razzano, J. Read, T. Regimbau, L. Rei, S. Reid, D. H. Reitze, P. Rettegno, F. Ricci, C. J. Richardson, J. W. Richardson, P. M. Ricker, G. Riemenschneider, K. Riles, M. Rizzo, N. A. Robertson, F. Robinet, A. Rocchi, R. D. Rodriguez-Soto, L. Rolland, J. G. Rollins, V. J. Roma, M. Romanelli, R. Romano, C. L. Romel, I. M. Romero-Shaw, J. H. Romie, C. A. Rose, D. Rose, K. Rose, D. Rosińska, S. G. Rosofsky, M. P. Ross, S. Rowan, S. J. Rowlinson, P. K. Roy, Santosh Roy, Soumen Roy, P. Ruggi, G. Rutins,

K. Ryan, S. Sachdev, T. Sadecki, M. Sakellariadou, O. S. Salafia, L. Salconi, M. Saleem, F. Salemi, A. Samajdar, E. J. Sanchez, L. E. Sanchez, N. Sanchis-Gual, J. R. Sanders, K. A. Santiago, E. Santos, N. Sarin, B. Sassolas, B. S. Sathyaprakash, O. Sauter, R. L. Savage, V. Savant, D. Sawant, S. Sayah, D. Schaetzl, P. Schale, M. Scheel, J. Scheuer, P. Schmidt, R. Schnabel, R. M. S. Schofield, A. Schönbeck, E. Schreiber, B. W. Schulte, B. F. Schutz, O. Schwarm, E. Schwartz, J. Scott, S. M. Scott, E. Seidel, D. Sellers, A. S. Sengupta, N. Sennett, D. Sentenac, V. Sequino, A. Sergeev, Y. Setyawati, D. A. Shaddock, T. Shaffer, M. S. Shahriar, A. Sharma, P. Sharma, P. Shawhan, H. Shen, M. Shikauchi, R. Shink, D. H. Shoemaker, D. M. Shoemaker, K. Shukla, S. ShyamSundar, K. Siellez, M. Sieniawska, D. Sigg, L. P. Singer, D. Singh, N. Singh, A. Singha, A. Singhal, A. M. Sintes, V. Sipala, V. Skliris, B. J. J. Slagmolen, T. J. Slaven-Blair, J. Smetana, J. R. Smith, R. J. E. Smith, S. Somala, E. J. Son, S. Soni, B. Sorazu, V. Sordini, F. Sorrentino, T. Souradeep, E. Sowell, A. P. Spencer, M. Spera, A. K. Srivastava, V. Srivastava, K. Staats, C. Stachie, M. Standke, D. A. Steer, J. Steinhoff, M. Steinke, J. Steinlechner, S. Steinlechner, D. Steinmeyer, S. Stevenson, D. Stocks, D. J. Stops, M. Stover, K. A. Strain, G. Stratta, A. Strunk, R. Sturani, A. L. Stuver, S. Sudhagar, V. Sudhir, T. Z. Summerscales, L. Sun, S. Sunil, A. Sur, J. Suresh, P. J. Sutton, B. L. Swinkels, M. J. Szczepańczyk, M. Tacca, S. C. Tait, C. Talbot, A. J. Tanasijczuk, D. B. Tanner, D. Tao, M. Tápai, A. Tapia, E. N. Tapia San Martin, J. D. Tasson, R. Taylor, R. Tenorio, L. Terkowski, M. P. Thirugnanasambandam, M. Thomas, P. Thomas, J. E. Thompson, S. R. Thondapu, K. A. Thorne, E. Thrane, C. L. Tinsman, T. R. Saravanan, Shubhanshu Tiwari, S. Tiwari, V. Tiwari, K. Toland, M. Tonelli, Z. Tornasi, A. Torres-Forné, C. I. Torrie, I. Tosta e Melo, D. Töyrä, E. A. Trail, F. Travasso, G. Traylor, M. C. Tringali, A. Tripathee, A. Trovato, R. J. Trudeau, K. W. Tsang, M. Tse, R. Tso, L. Tsukada, D. Tsuna, T. Tsutsui, M. Turconi, A. S. Ubhi, K. Ueno, D. Ugolini, C. S. Unnikrishnan, A. L. Urban, S. A. Usman, A. C. Utina, H. Vahlbruch, G. Vajente, G. Valdes, M. Valentini, N. van Bakel, M. van Beuzekom, J. F. J. van den Brand, C. Van Den Broeck, D. C. Vander-Hyde, L. van der Schaaf, J. V. Van Heijningen, A. A. van Veggel, M. Vardaro, V. Varma, S. Vass, M. Vasúth, A. Vecchio, G. Vedovato, J. Veitch, P. J. Veitch, K. Venkateswara, G. Venugopalan,

D. Verkindt, D. Veske, F. Vetrano, A. Viceré, A. D. Viets, S. Vinciguerra, D. J. Vine, J.-Y. Vinet, S. Vitale, Francisco Hernandez Vivanco, T. Vo, H. Vocca, C. Vorvick, S. P. Vyatchanin, A. R. Wade, L. E. Wade, M. Wade, R. Walet, M. Walker, G. S. Wallace, L. Wallace, S. Walsh, J. Z. Wang, S. Wang, W. H. Wang, R. L. Ward, Z. A. Warden, J. Warner, M. Was, J. Watchi, B. Weaver, L.-W. Wei, M. Weinert, A. J. Weinstein, R. Weiss, F. Wellmann, L. Wen, P. Weßels, J. W. Westhouse, K. Wette, J. T. Whelan, B. F. Whiting, C. Whittle, D. M. Wilken, D. Williams, J. L. Willis, B. Willke, W. Winkler, C. C. Wipf, H. Wittel, G. Woan, J. Woehler, J. K. Wofford, C. Wong, J. L. Wright, D. S. Wu, D. M. Wysocki, L. Xiao, H. Yamamoto, L. Yang, Y. Yang, Z. Yang, M. J. Yap, M. Yazback, D. W. Yeeles, Hang Yu, Haocun Yu, S. H. R. Yuen, A. K. Zadrożny, A. Zadrożny, M. Zanolin, T. Zelenova, J.-P. Zendri, M. Zevin, J. Zhang, L. Zhang, T. Zhang, C. Zhao, G. Zhao, M. Zhou, Z. Zhou, X. J. Zhu, A. B. Zimmerman, M. E. Zucker, and J. Zweizig and. GW190814: Gravitational waves from the coalescence of a 23 solar mass black hole with a 2.6 solar mass compact object. *The Astrophysical Journal*, 896(2):L44, jun 2020. doi: 10.3847/2041-8213/ab960f. URL https://doi.org/10.3847%2F2041-8213%2Fab960f.

[245] Feryal Özel, Dimitrios Psaltis, Ramesh Narayan, and Jeffrey E. McClintock. The Black Hole Mass Distribution in the Galaxy. *Astrophys. J.*, 725(2):1918–1927, December 2010. doi: 10.1088/0004-637X/725/2/1918.

[246] Will M. Farr, Niharika Sravan, Andrew Cantrell, Laura Kreidberg, Charles D. Bailyn, Ilya Mandel, and Vicky Kalogera. The Mass Distribution of Stellar-mass Black Holes. *Astrophys. J.*, 741(2):103, November 2011. doi: 10.1088/0004-637X/741/2/103.

[247] Feryal Özel, Dimitrios Psaltis, Ramesh Narayan, and Antonio Santos Villarreal. On the Mass Distribution and Birth Masses of Neutron Stars. *Astrophys. J.*, 757(1):55, September 2012. doi: 10.1088/0004-637X/757/1/55.

[248] Chris L. Fryer, Krzysztof Belczynski, Grzegorz Wiktorowicz, Michal Dominik, Vicky Kalogera, and Daniel E. Holz. Compact Remnant Mass Function: Dependence on

the Explosion Mechanism and Metallicity. *Astrophys. J.*, 749(1):91, April 2012. doi: 10.1088/0004-637X/749/1/91.

[249] Michael Zevin, Mario Spera, Christopher P L Berry, and Vicky Kalogera. Exploring the Lower Mass Gap and Unequal Mass Regime in Compact Binary Evolution. *arXiv e-prints*, art. arXiv:2006.14573, June 2020.

[250] Giacomo Fragione, Abraham Loeb, and Frederic A. Rasio. Merging Black Holes in the Low-mass and High-mass Gaps from 2 + 2 Quadruple Systems. *Astrophys. J. Lett.*, 895(1):L15, May 2020. doi: 10.3847/2041-8213/ab9093.

[251] Claire S. Ye, Wen-fai Fong, Kyle Kremer, Carl L. Rodriguez, Sourav Chatterjee, Giacomo Fragione, and Frederic A. Rasio. On the Rate of Neutron Star Binary Mergers from Globular Clusters. *Astrophys. J. Lett.*, 888(1):L10, January 2020. doi: 10.3847/2041-8213/ab5dc5.

[252] Tom Broadhurst, Jose M. Diego, and George F. Smoot. Interpreting ligo/virgo "mass-gap" events as lensed neutron star-black hole binaries, 2020.

[253] Mohammadtaher Safarzadeh and Abraham Loeb. Formation of mass-gap objects in highly asymmetric mergers. *arXiv e-prints*, art. arXiv:2007.00847, July 2020.

[254] Mohammadtaher Safarzadeh, Adrian S. Hamers, Abraham Loeb, and Edo Berger. Formation and Merging of Mass Gap Black Holes in Gravitational-wave Merger Events from Wide Hierarchical Quadruple Systems. *Astrophys. J. Lett.*, 888(1):L3, January 2020. doi: 10.3847/2041-8213/ab5dc8.

[255] Daniel A. Godzieba, David Radice, and Sebastiano Bernuzzi. On the maximum mass of neutron stars and gw190814, 2020.

[256] Yeunhwan Lim, Anirban Bhattacharya, Jeremy W. Holt, and Debdeep Pati. Revisiting constraints on the maximum neutron star mass in light of GW190814. *arXiv e-prints*, art. arXiv:2007.06526, July 2020.

[257] Antonios Tsokaros, Milton Ruiz, and Stuart L. Shapiro. GW190814: Spin and equation of state of a neutron star companion. *arXiv e-prints*, art. arXiv:2007.05526, July 2020.

[258] F. J. Fattoyev, C. J. Horowitz, J. Piekarewicz, and Brendan Reed. GW190814: Impact of a 2.6 solar mass neutron star on nucleonic equations of state. *arXiv e-prints*, art. arXiv:2007.03799, July 2020.

[259] Hung Tan, Jacquelyn Noronha-Hostler, and Nico Yunes. Kinky neutron stars in light of GW190814. *arXiv e-prints*, art. arXiv:2006.16296, June 2020.

[260] V. Dexheimer, R. O. Gomes, T. Klähn, S. Han, and M. Salinas. GW190814 as a massive rapidly-rotating neutron star with exotic degrees of freedom. *arXiv e-prints*, art. arXiv:2007.08493, July 2020.

[261] Piero Madau and Mark Dickinson. Cosmic star-formation history. *Annual Review of Astronomy and Astrophysics*, 52(1):415–486, 2014. doi: 10.1146/annurev-astro-081811-125615. URL https://doi.org/10.1146/annurev-astro-081811-125615.

[262] Edwin E. Salpeter. The Luminosity Function and Stellar Evolution. *Astrophys. J.*, 121:161, January 1955. doi: 10.1086/145971.

[263] Pavel Kroupa. On the variation of the initial mass function. *Mon. Not. R. Astron. Soc.*, 322(2):231–246, April 2001. doi: 10.1046/j.1365-8711.2001.04022.x.

[264] Kyle Kremer, Claire S. Ye, Nicholas Z. Rui, Newlin C. Weatherford, Sourav Chatterjee, Giacomo Fragione, Carl L. Rodriguez, Mario Spera, and Frederic A. Rasio. Modeling Dense Star Clusters in the Milky Way and Beyond with the CMC Cluster Catalog. *Astrophys. J. Suppl. Ser.*, 247(2):48, April 2020. doi: 10.3847/1538-4365/ab7919.